UNIVERSITA' DEGLI STUDI DI PADOVA

Dipartimento di Scienze del Farmaco

SCUOLA DI DOTTORATO DI RICERCA IN SCIENZE MOLECOLARI

INDIRIZZO SCIENZE FARMACEUTICHE

XXVI CICLO

PROTEINE DELLA COAGULAZIONE

IDENTIFICAZIONE DI NUOVE INTERAZIONI DELLA TROMBINA

Direttore della Scuola: Ch.mo Prof. Antonino Polimeno

Coordinatore d'indirizzo: Ch.mo Prof. Alessandro Dolmella

Supervisore:Ch.mo Prof. Vincenzo De Filippis

Dottorando: Laura Acquasaliente

UNIVERSITÀ
DEGLI STUDI
DI PADOVA

UNIVERSITY OF PADUA

Department of Pharmaceutical and Pharmacological Sciences

DOCTORAL SCHOOL IN MOLECULAR SCIENCE

PHARMACEUTICAL SCIENCES CURRICULUM

XXVI CYCLE

COAGULATION PROTEIN FACTORS

DISCOVERING NOVEL INTERACTIONS OF THROMBIN

School Director: Ch.mo Prof. Antonino Polimeno

Curriculum Coordinator: Ch.mo Prof. Alessandro Dolmella

Supervisor:Ch.mo Prof. Vincenzo De Filippis

PhD Candidate: Laura Acquasaliente

Life is an ordered sequence

of enzymatic reaction

R.Willstätter

Contents

RIASSUNTO

La trombina è una proteasi serinica appartenente, per omologia di sequenza, alla famiglia della chimotripsina dalla quale differisce per la presenza di numerosi *loop* d'inserzione, che le conferiscono una peculiare specificità di substrato. Essa si presenta come un ellissoide caratterizzato da due β-*barrels*, alla giunzione dei quali si colloca la cavità che ospita il sito attivo. Il riconoscimento molecolare dei diversi effettori, invece, è mediato da due regioni superficiali elettropositive, diametralmente opposte e circondanti la cavità catalitica. Queste sono definite, rispettivamente, esosito-I (*Anion Binding Exosite-I* o *Fibrinogen Recognition Site*) ed esosito-II (*Anion Binding Exosite-II* o *Heparin Binding Site*). L'esosito-I è coinvolto nel legame della trombina al fibrinogeno, al recettore piastrinico PAR-1, alla trombomodulina, e a inibitori endogeni, come il fattore eparinico II, ed esogeni come la coda C-terminale dell'irudina. L'esosito-II rappresenta il sito di legame per l'eparina, per il frammento F2 della pro-trombina e per inibitori fisiologici come l'antitrombina III e la nexina-I. A differenza della chimotrispsina, l'attività proteolitica della trombina è aumentata dal *binding* del Na^+ che stabilizza l'enzima in una conformazione più aperta e rigida.

La trombina è una proteasi multifunzionale: da una parte gioca un ruolo importante nella cascata coagulativa, dall'altra interviene in modo fondamentale nei processi infiammatori a carico del sistema nervoso centrale. Infatti, la trombina svolge un ruolo chiave all'interfaccia tra coagulazione, infiammazione, differenziamento cellulare, angiogenesi e malattie neurodegenartive, manifestando così effetti pleiotropici. Studi in vitro hanno evidenziato come tale proteina sia in grado di modulare la permeabilità vascolare, la formazione di neo-vasi e la ritrazione di neuriti su cellule di neuroblastoma; per di più sembra svolgere attività mitogena a carico di cellule muscolari ed endoteliali. Questi effetti si realizzano a basse concentrazioni (1-10nM), mentre concentrazioni maggiori (100nM) sembrano essere nocive e pro-infiammatorie a livello cerebrale. Allo stesso modo, elevate concentrazioni plasmatiche di trombina (100-500nM) portano alla formazione di un *clot* compatto di fibrina, non suscettibile a fibrinolisi. Alcuni studi hanno dimostrato come la maggior parte delle funzioni non emostatiche si manifestino mediante l'attivazione dei recettori piastrinici PAR (*Protease Activated Receptors*), recettori transmembrana accoppiati a proteine-G. Nel dettaglio, il dominio extracellulare del PAR-1, in seguito a proteolisi promossa dalla trombina, interagisce col corpo recettoriale favorendo la trasduzione del

segnale all'interno di piastrine e macrofagi. Il tutto si traduce in una risposta pro-aggregante e pro-infiammatoria. Questi dati suggeriscono la presenza di una stretta comunicazione biochimica tra i vari meccanismi che regolano i differenti effetti cellulari della trombina.

Alla luce di queste considerazioni, l'obiettivo saliente del mio Progetto di Dottorato è stato quello di identificare nuovi effettori della trombina, i cui meccanismi di interazione possono avere importanti ricadute nella definizione dei processi biochimici che regolano l'insorgenza e la progressione delle malattie cardiovascolari, neurodegenerative ed autoimmuni.

Durante il primo anno ho studiato l'effetto della beta2 glicoproteina I (β2GpI) sulle funzioni pro- e anti- coagulanti della trombina (Capitolo 2). La β2GpI, identificata come il principale antigene della sindrome da anticorpi antifosfolipidi (APS), è in grado di inibire le attività procoagulanti (generazione di fibrina ed aggregazione piastrinica) della trombina in vitro, senza compromettere l'unica sua funzione anticoagulante, ovvero la generazione di Proteina C attiva. I nostri esperimenti, condotti principalmente mediante *surface plasmon resonance* (SPR) hanno permesso inoltre di chiarire il *binding mode* di interazione delle due proteine: la β2GpI si lega agli esositi della trombina, il cui sito attivo rimane quindi accessibile al substrato.

Nel corso del secondo anno ho indagato l'interazione tra l'α-sinucleina (α-Sin) e la trombina umana (Capitolo 3). α-sin è una piccola proteina solubile presinaptica, implicata in diverse patologie neurodegenerative. Recentemente è stato dimostrato come l'α-Sin sia in grado di inibire l'attivazione e quindi l'aggregazione delle piastrine quando stimolate da trombina, limitando il rilascio degli α-granuli. Inoltre pazienti affetti dal morbo di Parkinson sono meno soggetti ad attacchi ischemici e presentano una velocità di aggregazione piastrinica significativamente ridotta. I risultati da noi ottenuti indicano che la porzione acida C-terminale dell'α-Sin è in grado di legarsi alla trombina con un'affinità nell'ordine del basso micromolare, coinvolgendo i due esositi. Quindi, il complesso [α-Sin - trombina] ostacola efficacemente l'aggregazione piastrinica, molto probabilmente in seguito all'ancoraggio del dominio N-terminale sulla superficie delle piastrine.

Infine, durante l'ultimo anno, è stata presa in considerazione la ceruloplasmina umana (CP), quale possibile *binder* della trombina (Capitolo 4). Elevati livelli di CP sono stati individuati in pazienti affetti da artrite reumatoide, malattia infiammatoria cronica autoimmunitaria a carico delle articolazioni sinoviali. Come osservato per la CP, i livelli di trombina sono notevolmente aumentati in tessuti infiammati e, in modo particolare, nel fluido

sinoviale di pazienti affetti da artrite reumatoide. Difatti, la trombina agisce come mediatore pro-infiammatorio e chemiotattico. In nostri dati indicano che la trombina è in grado di ostacolare, in seguito a proteolisi, l'attività antiossidante della ceruloplasmina. Queste evidenze sperimentali sono state confermate dal fatto che in presenza di irudina il *cleavage* della CP è inibito e l'infiammazione articolare nei soggetti con artrite reumatoide è ridotta.

ABSTRACT

Thrombin is a serine protease of the chymotrypsin family. Compared to chymotrypsin, thrombin displays several insertion loops, responsible for the unique substrate specificity of the enzyme. Two different insertions shape and narrow the access to the active site, while the interaction of binders involves allosteric sites, called exosite-I (Anion Binding Exosite-I or Fibrinogen Recognition Site) and exosite-II (Anion Binding Exosite-II or Heparin Binding Site). These contain electropositive amino acid residues and are localized at opposite poles of the active site, representing two potential exosites for the binding of macromolecular ligands. Exosite-I is involved in binding to fibrinogen, platelet receptor PAR-1, thrombomodulin, and to endogenous (i.e. heparin cofactor II) and exogenous (i.e. C-terminal tail of hirudin) inhibitors. Exosite-II interacts with heparin, F2 prothrombin fragment, and physiological inhibitors such us antithrombin III and protease nexin-I. Contrary to chymotrypsin, the proteolytic activity of thrombin is enhanced upon binding of Na^+, that stabilizes the enzyme into a more open and rigid conformation.

Thrombin is a multifunctional enzyme that plays a key role at interface between coagulation, inflammation and nervous system. The protease is involved in numerous physiological and pathological processes, including haemostasis and thrombosis, inflammation and chemotaxis, cellular proliferation and tumor growth, angiogenesis and neurodegenerative diseases, manifesting pleiotropic effects. For example, low concentrations of thrombin (i.e. 1-10nM) can influence glia cell mitosis and neuronal out-growth, acts as mitogen. Conversely, higher concentration of the enzyme (100nM) has been shown to induce apoptosis in motor neurons and to determine in the brain a pro-inflammatory state. Instead, i*n vivo*, the dynamic concentration of free thrombin during coagulation cascade reactions is estimated to vary from 1nM to over 100 – 500nM. Typically low concentration are associated with platelet activation and loosely organised fibrin strands susceptible to fibrinolysis; higher concentration produce tightly packet fibrin strands capable of forming a stable clot. Some of these effects are mediated by activation of Protease Activated Receptors (PARs). The general mechanism by which proteases activate PARs is the same: enzymes cleave at specific sites within the extracellular amino terminus of the receptors; this cleavage exposes a new amino terminus that serves as a tethered ligand domain, which binds to conserved regions in the second extracellular loop of the cleaved receptor, resulting in the initiation of signal

transduction. All these observations argue in favor of a biochemical communication between the different mechanisms regulating the cellular effects of thrombin.

The general aim of my PhD project was to identify novel effectors of thrombin, whose interaction may have important implications in defining the biochemical processes that regulate the onset and progression of cardiovascular diseases, neurodegenerative and autoimmune diseases.

During the first year, I studied the effect of beta2-glycoprotein I (β2GPI) on the procoagulant (i.e. fibrin generation and platelet aggregation) and anticoagulant (i.e. generation of activated protein C) functions of thrombin (Chapter 2). β2GPI, identified as the major antigen of antiphospholipid syndrome (APS), functions as a physiologic anticoagulant by inhibiting the key procoagulant activities of the protease, without affecting its unique anticoagulant function. Our experiments, conducted by surface plasmon resonance (SPR), clarify the binding mode of interaction: β2GPI binds to thrombin exosites, while the active site remains free and accessible for substrate binding.

In the second year of my PhD course, I have investigated the interaction between α-synuclein (α-Syn) and human thrombin (Chapter 3). α-Syn is a small soluble presynaptic protein implicated in different neurodegenerative disorders. Recent studies indicated that α-Syn is able to inhibit platelets degranulation, upon thrombin stimulation. In addition, clinical studies indicated that the incidence of ischemic stroke in patients with Parkinson disease is lower than in controls, and platelet aggregation is also significantly decreased. Our results suggest that the acidic C-terminal portion of α-Syn binds to thrombin exosites (Kd ~ μM). Consequently, we speculate that the complex [α-Syn – thrombin] effectively hinders platelet aggregation, due to the interaction of the N-terminal domain on the platelets surfaces.

During the last year, I studied human ceruloplasmin (CP) as a possible binder of thrombin (Chapter 4). The plasma level of CP is an important diagnostic indicator of inflammatory disease, such as Rheumatoid Arthritis (RA), a chronic systemic inflammatory autoimmune disorder. As observed with CP, thrombin concentration is markedly increased in inflamed tissues and specifically in the synovial fluid of RA patients. We conclude that the anti-inflammatory function of CP is regulated by thrombin: the enzyme, in fact, proteolytically hinders the antioxidant activity of CP. These results are confirmed in RA patients treated with hirudin that have clinical symptoms ameliorated. These data are unprecedented and set the basis for elucidating the biochemical mechanisms underlying the progression of inflammation in RA patients.

INTRODUCTION

CHAPTER 1.1

Human α-Thrombin

Human α-thrombin is a serine protease, described in 1982 by Alexander Schidmdt, and first identified by Buchanan in 1845 (1). The sequence of heavy chain of human thrombin is related to trypsin and chymotrypsin with 35 % sequence identity and 49 % sequence similarity; consequentently thrombin sequence numbering follows the numeration of chymotrypsynogen (Appendix B) (2). In vivo, thrombin is produced by the enzymatic cleavage of prothrombin, a vitamin K-dependent zymogen. Prothrombin (70 kDa), or coagulation factor II, is a glycoprotein with 579 aminoacid residues, produced in the liver parenchymal cells and secreted into the blood. In the penultimate step of the coagulation cascade, prothrombin is converted to thrombin by the prothrombinase complex comprising factor Xa and cofactor Va, assembled on the surface of platelets in the presence of calcium ions (3)

Molecular Structure of Human α-Thrombin: the Active Site

Human α-thrombin (36 kDa) is a heterodimer consisting of two polypeptides called chain A and B (2) (Fig. 1.1). The light chain A, consisting of 36 residues, is linked by a single disulfide bound to heavy chain B, 250 aminoacid residues, that contains three intra-chain disulfide bonds. The B chain carries the functional epitopes of the enzyme and has the typical fold of serine proteases, in which the catalytic triad for activity is representative by His57, Asp102 and Ser195. Briefly, the C atom is converted into a tetrahedral intermediate in the transition state, which is stabilized by hydrogen bonds between the charged carbonyl O atom of the peptide group of the scissile bond and the amide hydrogen atoms of Gly193 and Ser195 which form the oxyanion hole. The substrate is then acylated by the Oγ atom of Ser195 after transfer of a proton to His57 and its C-terminal fragment is released. A molecule of water, by nucleophilic attack, catalyses deacylation and releases the carboxylic acid product and the N-terminal fragment of the substrate. Subsequently, Asp102 anchors His57 in the correct orientation for proton transfer from and to Ser195, which compensates for the developing positive charge (4).

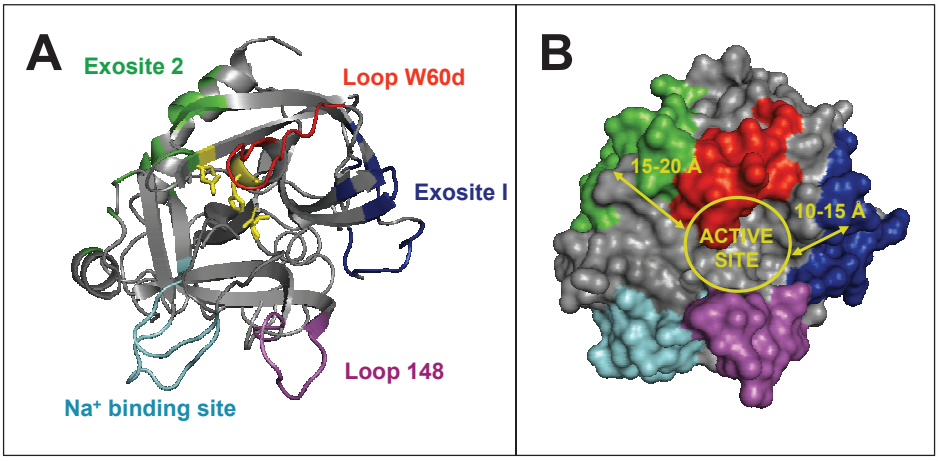

Figure 1.1 Crystallographic structure of thrombin. Thrombin (1PPB.pdb) structure is shown in the standard Bode orientation, in ribbon **(A)** and surface **(B)** mode. The active site containing the catalytic triad (H57, D102, and S195, yellow) is covered by the hydrophobic loop W60d (red) and by the hydrophilic loop 148 (magenta). Exosite 1 (blue) and 2 (green) are two electropositive patches that flank the active site and coordinate substrates/inhibitors recruitment. As for exosites, the Na^+-binding site (cyan) is located about 15-20 Å away from the catalytic triad, too.

Numerous insertions are present in thrombin, relative to trypsin and chymotrypsin, shaped as loops connecting β-strands in the B chain. Two different insertions shape and narrow the access to the active site. The Trp60d loop defines the upper rim of the active site and screens His57 and Ser195 from the solvent. The loop contains an insertion of nine residues, from Tyr60a to Ile60i, and protrudes into the solvent with the bulky side chain of Trp60d providing most of the steric hindrance (5). Opposite to the Trp60d loop, the autolysis 148-loop forms the lower rim of the active-site cleft. The 148-loop is strategically positioned in human α-thrombin (2)and is crucial for fibrinogen recognition (5).

In between the two insertion loops, the active-site residues are nestled in the centre of a narrow cleft framed. The trypsin-like specificity for basic residues at P1 (6) is conferred to thrombin by the presence of Asp189 at the S1 site occupying the bottom of the catalytic pocket. However, differently from trypsin pocket, thrombin increased flexibility allows accommodation of more hydrophobic or even uncharged P1 groups and confers a strong preference for P1-Arg over Lys residues (7). Relatively unique to thrombin is the acidic Glu192 residue positioned at the entrance to this pocket. The negatively charged of Glu192 is not compensated by hydrogen bonds or ion pair interactions with neighbour residues. The uncompensated charge plays an important role in discriminating against substrates carrying acidic groups near the scissile bond, like protein C and the platelet protease activated receptor 1 (PAR-1) (8). Based on the Trp215 indole moiety, a hydrophobic surface groove extends on top of the S1 pocket, which is partially delimited by the 60 loop. The conjunction of

hydrophobic residues together with the pavement of the active-site forms an apolar binding site, which is subdivided into the S2 cavity and the aryl binding site/S4 groove. This latter site hosts P4 side chain of all L-amino acids substrates, whereas the P3 side chain extends alongside Glu192, away from the active site. The S1' site of thrombin, positioned to the right of the active site, is limited in size by the Lys60f side chain, and therefore particularly suited to accommodate small polar P1' side chain. The S2' subsite is of medium size and mainly hydrophobic, so that bulky hydrophobic P2' residues are preferred. The S3' site, instead, is open and slightly acidic, so prefers basic P3' side chains (Table 1).

Table 1: Cleavage sequences of thrombin substrates or inhibitors around the scissile peptide bond and the reactive-centre loop, respectively.

	P4	P3	P2	P1	P1'	P2'	P3'	Ex- Cofactor
Fibrinogen A	Gly	Gly	Val	Arg	Gly	Pro	Arg	I
Fibrinogen B	Phe	Ser	Ala	Arg	Gly	His	Arg	I
FV (709)	Leu	Gly	Ile	Arg	Ser	Phe	Arg	I, II
FV (1018)	Leu	Ser	Pro	Arg	Thr	Phe	His	I, II
FV (1545)	Trp	Tyr	Leu	Arg	Ser	Asn	Asn	I, II
FVIII (372)	Ile	Gln	Ile	Arg	Ser	Val	Ala	I, II
FVIII (740)	Ile	Glu	Pro	Arg	Ser	Phe	Ser	I, II
FVIII (1689)	Gln	Ser	Pro	Arg	Ser	Phe	Gln	I, II
FXIII	Gly	Val	Pro	Arg	Gly	Val	Asn	None
PAR-1	Leu	Asp	Pro	Arg	Ser	Phe	Leu	I
PAR-4	Pro	Ala	Pro	Arg	Gly	Tyr	Pro	None
FXI	Ile	Lys	Pro	Arg	Ile	Val	Gly	I
PC	Val	Asp	Pro	Arg	Ile	Val	Gly	TM
TAFI	Val	Ser	Pro	Arg	Ala	Ser	Ala	TM
AT	Ile	Ala	Gly	Arg	Ser	Leu	Asn	Heparin
HCII	Phe	Met	Pro	Leu	Ser	Yhr	Gln	I, Heparin

AT, antithrombin; F, factor, HC, heparin cofactor, TAFI, thrombin-activable fibrinolysis inhibitor

On these bases, a P4 to P3' consensus sequence of an optimal thrombin polypeptide substrate should contain a P4-Phe/Leu, any P3 residue, a P2-Pro/Val, a P1-Arg, a P1'-Ser/Gly, a P2'-Phe, and a P3'-Arg residue. Although the majority of thrombin natural substrates follows the consensus scheme proposed, important exceptions are found with fibrinogen Aα (FAα), factor XIII, protein C, and heparin cofactor II (HCII) (5, 9). Consequently, the interaction of binders

to the active site of human α-thrombin also involves allosteric sites, called exosite I and exosite II. These contain electropositive amino acid residues and are localized at opposite poles of the active site, representing two potential exosites for the binding of macromolecular ligands.

Exosite-I or ABE-I

The prominent loop centred on Lys70 is called exosite-I and is homologous to the Ca^{2+} binding loop of the cognate proteases trypsin and chymotrypsin (10). Exosite-I is located about 10-15 Å away from the active site and is mainly placed on the Arg67 to Ile82 loop and bordered by the 37-loop and segment Lys109-Lys110. In this domain, four charged residues (Arg67, Lys70, Glu77 and Glu80) form a salt bridge cluster, which is buried well below the surface of the exosite, substantially contributing to the rigidity of the loop (2). Over this buried charged spot, several not compensated cationic residues (Arg73, Arg 75 and Arg 77a) form a strong electropositive field.

Electrostatic forces generated by the exosite-I charge have an important influence on the biomolecular association of thrombin with some ligands. In fact, exosite-I represents the recognition site for many macromolecular ligands, such as fibrin, fibrinogen (11), thrombomodulin (12), protease activated receptor-1 (PAR-1) (13), HCII, hirudin, coagulation factor V, VIII and XIII (14-16). It is hypothesized that the electrical field of exosite-I could pre-orient the enzyme for a productive interaction, so the hydrophobic stacking components can subsequently stabilized the various adducts.

In addition, exosite-I can communicate changes to the catalytic moiety of the enzyme. In fact, peptides derived from the physiological inhibitor HCII (17), PAR-1 (13) or hirudin C-terminal domain (18, 19) influence the active site of human α-thrombin allosterically.

Exosite-II or ABE-II

On the other side of the enzyme, opposite exosite-I, a prominent C-terminal helix hosts a number of positively charged residues that provide the anion binding exosite-II. Exosite-II is the template for interaction with polyanionic ligands such as heparin and glycosaminoglycans. At this surface, a small hydrophobic Leu234-based groove is delimited by basic residues Arg93, Arg101, Arg 165, Arg 233, Arg 126, Lys236, Lys235, Lys240 and His91 with most of their side chain charges not compensated by adjacent negative charges. This assignment was confirmed in the presence of exosite-II thrombin mutant, measuring the heparin-catalyzed

thrombin inhibition by anti-thrombin III (ATIII) (20). Exosite-II binds, also, to platelet receptor GpIbα (21) and to fibrinogen-elongated γ' chain (22).

Na^+ Binding Site and Allosteric Effect

Sodium ion has been found to be an important allosteric modulator of human α-thrombin. The binding of this monovalent cation to thrombin plays a relevant role in the allosteric control of the protease activities, as it causes a conformational transition from a Na^+-free form, referred to as slow, to a Na^+-bound form, referred to as fast. The slow and fast forms are significantly (2:3 ratio) populated under physiologic conditions because the Kd for Na^+ binding is 80-110mM at 37°C and physiologic NaCl concentration (140mM) is not sufficient for saturation (8, 23). The two forms exhibit different relative activities toward macromolecular substrates. The fast thrombin form cleaves fibrinogen and PAR-1 more efficiently and displays procoagulant, prothrombotic, and prosignaling properties. Notably, the slow form activates protein C with an efficiency similar to that of the fast form (Table 2).

Table 2. Effect of Na^+ on the catalytic activity of thrombin towards some relevant physiological substrates.

	k_{cat}/K_m (μM^{-1} s^{-1})		r
	Fast	**Slow**	
(D)FPR-pNA	88.9 ± 4	3.5 ± 0.5	26
Fibrinopeptide A release	35 ± 4	1.5 ± 0.1	23
Fibrinopeptide B release	17 ± 1	0.73 ± 0.03	23
PAR-1[a]	54 ± 2	1.4 ± 0.1	39
Protein C	0.21 ± 0.001	0.32 ± 0.01	0.7

All measures were performed in buffer that stabilized either the fast (0.2M NaCl) or the slow (0.2M ChCl) form. Kinetic constants were adapted from (5).

Na^+ binds 16–20 Å away from residues of the catalytic triad (His57, Asp102, Ser195) and within 5 Å from Asp189 in the primary specificity pocket, nestled between the 220- and 186-loops and coordinated octahedrally by the backbone O atoms of Arg221a and Lys224 and four buried water molecules anchored to the side chains of Asp189, Asp221 and the backbone atoms of Gly223 and Tyr184a. Na^+ binding to thrombin has been studied in great detail in terms of mutagenesis, structure, kinetics, and functional components (24). Currently available data suggest that Na^+-bound (fast) thrombin form is more stable and exhibits a more open accessible and rigid active site cleft, whereas the Na^+-free (slow) form possesses a more closed, flexible substrate binding region (8). In fact, Na^+ increases the catalytic activity of the

enzyme toward synthetic and physiological substrates, with the exception of the anticoagulant protein C (25). However, the affinity of Na^+ is strongly temperature dependent, with a large heat capacity change and enthalpy that cause the Kd to become comparable to the [Na^+] in the blood under physiological conditions (26).

Human α-Thrombin in the Vascular System

Human α-thrombin is the final protease generated in the coagulation cascade, in which plays a vital role encountering a large number of potential procoagulant and anticoagulant substrates (Fig. 1.2). The major procoagulant effect, the conversion of soluble fibrinogen to insoluble fibrin, is amplified by activation of factor XIII that covalently stabilises the fibrin clot (27, 28). Following this activation, factor XIII induces soluble fibrin monomers to interact end-to-end and side-to-side, causing it to become a soluble cross-linked fibrin monomer (29). Also, the inhibition of fibrinolysis *via* activation of thrombin-activable fibrinolysis inhibitor (TAFI) and the proteolytic activation of factors V, VIII and XI contribute to the procoagulant activity of thrombin (30, 31). In addition thrombin activates platelets through the cleavage of two protease platelet receptors, PAR-1 and PAR-4, promoting blood clotting (32).

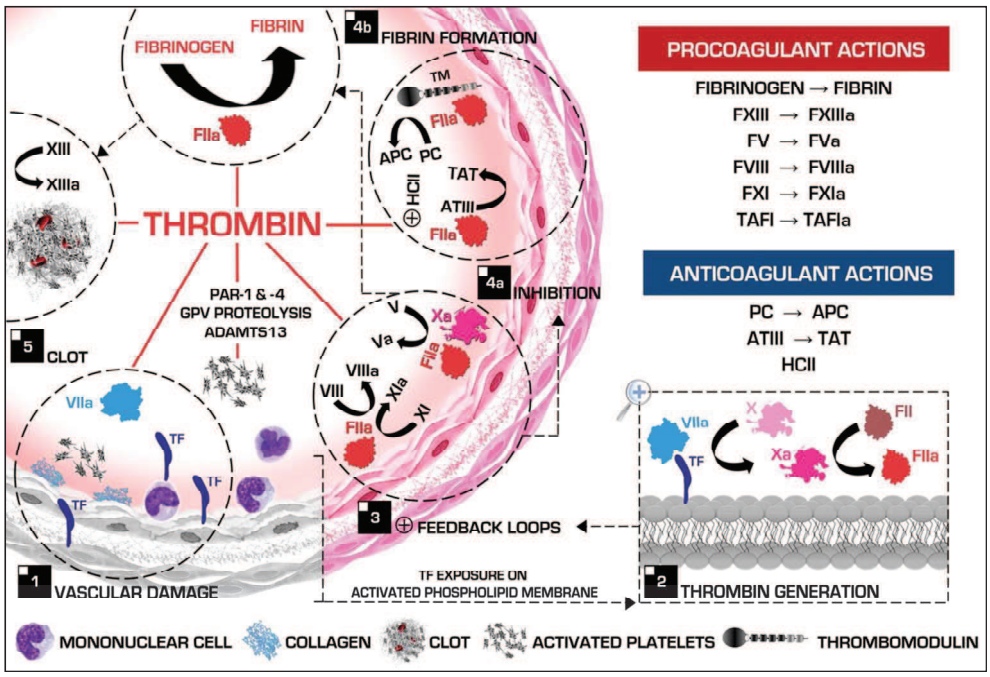

Figure 1.2 Antagonizing actions of thrombin in coagulation cascade. Thrombin is the final protease generated in the bloodstream, where it experts both procoagulant and anticoagulant functions. The figure was adapted from (66).

By contrast, regarding thrombin function as anticoagulant, activation of protein C (PC) is very important. The activation depends on the binding to thrombomodulin (TM), a member receptor on endothelia cells (14, 33, 34). The reaction is further enhanced by the presence of a specific endothelial cell protein C receptor (14). Activated protein C (aPC) cleaves and inactivates FVa and FVIIIa, essential for coagulation, and FXa and FIXa, required for thrombin generation, thereby down-regulating both the amplification and progression of the coagulation cascade. Notably, in the microcirculation the system thrombin-thrombomodulin-protein C constitutes the natural anticoagulant pathway that prevents massive intravascular conversion of fibrinogen into a soluble clot upon thrombin generation (14).

Efficient regulation of thrombin activity is essential to prevent excessive or improperly localized clot formation. The serine protease inhibitor (serpin) superfamily inhibits the catalytic activity of thrombin, reaction greatly accelerated in the presence of glycosamminoglycans such as heparin, heparan sulphate and dermatan sulphate (35). The most important serpins responsible for thrombin inhibition are antithrombin (originally called antithrombin III), heparin cofactor II (HCII) and protease nexin I (PNI) (36). Antithrombin is abundant in the blood (2.3 μM), inhibits a variety of serine proteases involved in blood coagulation and appears to be the main inhibitor limiting intravascular clot formation. In contrast, HCII is highly specific for thrombin and appears to regulate thrombin activity in extravascular tissues following vascular injury; whereas PNI is likely to inhibit thrombin at or near the surface of a variety of cell types but especially in the brain (36). In addition to these endogenous thrombin inhibitors, several potent thrombin inhibitors have been isolated from hematophagous organisms, including hirudin and haemadin from the leeches *Hirudo medicinalis* and *Haemadipsa sylvestris,* respectively (37).

Recent studies *in vitro* indicated that human α-thrombin modulates multiple processes in the vascular system including vascular permeability, vascular tone and neovessel formation (35). It was reported that thrombin activates angiogenesis and decreases the ability of endothelial cells to attach to basement membrane proteins *via* cyclic adenosime monophosphate (38). Thrombin also potentiates vascular endothelial grow factor (VEGF), by up-regulation of the expression of VEGF receptors (38). In addition, the enzyme increases vascular permeability, resulting in plasma protein leakage and the development of a proangiogenic matrix (39, 40).

In vivo, the dynamic concentration of free thrombin during coagulation cascade reactions is estimated to vary from 1nM (0.1 U/ml) to over 100 – 500nM, depending on detection methods and experimental conditions (41). Typically low concentration (< 10nM) are

associated with platelet activation and loosely organised fibrin strands susceptible to fibrinolysis; higher concentration produce tightly packet fibrin stands capable of a stable clot (28, 42). Furthermore, some studies *in vivo* indicate that thrombin administrated as a bolus causes microembolism, as well as the protein infused slowly at steady-state conditions (1.6 U/kg/min) leads to bleeds, but not to intravascular clotting. Beside, large quantity of thrombin infused at low rate (0.05 U/kg/min) increases the vascular permeability leading to tissue damage (35). Nevertheless, the true enzyme concentration in tissues is unknown; whether the serine protease can reach such an extraordinary concentration *in vivo* remains an un-answered question.

In conclusion, human α-thrombin is the central protease in the coagulation cascade and one of the most extensively studied of all enzyme. In addition to its essential role in the coagulation cascade and haemostasis, thrombin displays multiple pleiotropic effects through interaction with different targets localized at the level of platelets, endothelia, heart, neurons, leukocytes and tumor cells.

Human α-Thrombin in the Nervous System

Human α-thrombin is a promiscuous molecule that plays a key role at interface between coagulation, inflammation and nervous system. The serine protease dynamically modulates cell growth, development and response to injury in the central and peripheral nervous system, so this protein results important in the mediation of pain sensations (43). In fact, concentration of thrombin as low 1 -10nM can influence glia cell mitosis and neuronal out-growth (44), induces retraction of neuritis in neuroblastoma cells, acts as mitogen and provokes alteration in astrocytes morphology (45). All these effects seem to have a protective role in neurons and astrocytes and are mediated through activation of protease activating receptors (PARs) (45). Conversely, higher concentration of the enzyme (100nM) has been shown to induce apoptosis in motor neurons (46) and to determine in the brain a pro-inflammatory state (47). In addition, thrombin inhibits development neurite outgrowth from the dorsal root ganglion (DRG) *in vitro* (48).

Recent studies suggest that thrombin is also involved in neurodegenerative diseases. The protein accumulates in the brains of Alzheimer's diseases (AD) patients, both in vessel walls and senile plaques. In these regard, thrombin is directly toxic to neurons and can also potentiate neuronal injury indirectly *via* activation of neighboring microglia and astrocytes. Immunofluorescent analysis of the cerebrovasculature in AD mice demonstrates significant

increases in thrombin, interleukin-6 (IL-6), monocyte chemoattractant protein-1 (MCP-1), matrix metalloproteinases (MMPs) and reactive oxygen species (ROS) compared to controls (49). Furthermore, the serine protease is able to induce production of amyloid precursor protein (APP) and to hydrolyze APP, generating fragment of amyloid peptide similar to those found in fibrils of AD patients (50, 51). In Parkinson's disease (PD), instead, thrombin contributes directly to neuronal degeneration, by a toxic effect on dopaminergic neurons in the substantia nigra (52).

Numerous alterations in morphology and platelets aggregation have been found in AD and PD. Platelets degranulation induced by thrombin, thought PAR-mediated activation, is impaired by α-synuclein, an acid protein expressed in presynaptic neuron terminals and in a number of blood cells (53). α-Synuclein is also the major component of fibrillar deposits of AD and PD (54, 55). In fact, clinical studies have shown that PD patients are less susceptible to ischemic stroke and have reduced platelet aggregation (56).

Human α-Thrombin in the Inflammation Response

Inflammation and coagulation constitute two host defense systems with complementary roles in eliminating pathogens, limiting tissue damage and restoring homeostasis. Between these systems exists a reciprocal relationship: inflammation leads to activation of coagulation and coagulation considerably affects inflammatory activity (57). Thrombin has the ability to stimulate production and secretion of inflammatory cytokines like interleukin-1β (IL-1β), interleukin-6 (IL-6) and tumor necrosis factor (TNF-α), and this is primarily accomplished through nuclear factor kappa B (NF-κB) signaling pathways. With monocytes or monocyte-derived macrophages, thrombin enhances their adhesiveness and increases their production (58). The enzyme also stimulates production of platelet-activating factor (PAF) whose role is to attract neutrophils and contribute to their adhesion (59). As regards, several studies show the importance of IL-6 in the initiation of coagulation activation, and the role of IL-1β and TNF-α in the regulation of physiological anticoagulation (60).

Inflammation induced the activation of coagulation by dysfunction of the normal anticoagulant mechanisms, such as antithrombin and protein C systems (61), and by improve the tissue factor-mediated thrombin generation. Tissue factor (TF) plays a central role in the initiation of inflammation that promotes coagulation. Some data indicated that blocking TF activity completely inhibits inflammation-induced thrombin generation in models of

experimental endotoxaemia or bacteraemia (62). Inflammatory cells in atherosclerotic plaques produce abundant TF and upon plaque rupture there is extensive TF exposure to blood (63). In fact, in inflamed tissues thrombin concentration is markedly increased, especially in the synovial fluid of rheumatoid arthritis patients (64).

Summarizing, communication between inflammation and coagulation is bidirectional; coagulation proteases and protease inhibitors not only interact with coagulation protein zymogens, but also with specific cells receptors to induce signaling pathways. The pivotal mechanism by which thrombin modulates inflammation is binding to PARs, that are localized in the vasculature on endothelia cells, mononuclear cells, platelets, fibroblasts and smooth muscle cells (65).

REFERENCES

1. Gamgee, A., and Buchanan, A. (1879) On some Old and New Experiments on the Fibrin-Ferment. *J.Physiol.* 2, 145-163
2. Bode, W., and Huber, R. (1992) Natural protein proteinase inhibitors and their interaction with proteinases. *Eur.J.Biochem.* 204, 433-451
3. Pozzi, N., Chen, Z., Gohara, D.W., Niu, W., Heyduk, T., and Di Cera, E. (2013) Crystal structure of prothrombin reveals conformational flexibility and mechanism of activation. *J.Biol.Chem.* 288, 22734-22744
4. Warshel, A., Naray-Szabo, G., Sussman, F., and Hwang, J.K. (1989) How do serine proteases really work?. *Biochemistry.* 28, 3629-3637
5. Di Cera, E., Dang, Q.D., and Ayala, Y.M. (1997) Molecular mechanisms of thrombin function. *Cell Mol.Life Sci.* 53, 701-730
6. Schechter, I., and Berger, A. (1967) On the size of the active site in proteases. I. Papain. *Biochem.Biophys.Res.Commun.* 27, 157-162
7. Johnson, D.J., Adams, T.E., Li, W., and Huntington, J.A. (2005) Crystal structure of wild-type human thrombin in the Na+-free state. *Biochem.J.* 392, 21-28
8. De Filippis, V., De Dea, E., Lucatello, F., and Frasson, R. (2005) Effect of Na+ binding on the conformation, stability and molecular recognition properties of thrombin. *Biochem.J.* 390, 485-492
9. Di Cera, E. (2007) Thrombin as procoagulant and anticoagulant. *J.Thromb.Haemost.* 5 Suppl 1, 196-202

10. Bartunik, H.D., Summers, L.J., and Bartsch, H.H. (1989) Crystal structure of bovine beta-trypsin at 1.5 A resolution in a crystal form with low molecular packing density. Active site geometry, ion pairs and solvent structure. *J.Mol.Biol.* 210, 813-828
11. Stubbs, M.T., Oschkinat, H., Mayr, I., Huber, R., Angliker, H., Stone, S.R., and Bode, W. (1992) The interaction of thrombin with fibrinogen. A structural basis for its specificity. *Eur.J.Biochem.* 206, 187-195
12. Hall, S.W., Nagashima, M., Zhao, L., Morser, J., and Leung, L.L. (1999) Thrombin interacts with thrombomodulin, protein C, and thrombin-activatable fibrinolysis inhibitor via specific and distinct domains. *J.Biol.Chem.* 274, 25510-25516
13. Myles, T., Le Bonniec, B.F., and Stone, S.R. (2001) The dual role of thrombin's anion-binding exosite-I in the recognition and cleavage of the protease-activated receptor 1. *Eur.J.Biochem.* 268, 70-77
14. Esmon, C.T. (2003) The protein C pathway. *Chest.* 124, 26S-32S
15. Steen, M., and Dahlback, B. (2002) Thrombin-mediated proteolysis of factor V resulting in gradual B-domain release and exposure of the factor Xa-binding site. *J.Biol.Chem.* 277, 38424-38430
16. Sadasivan, C., and Yee, V.C. (2000) Interaction of the factor XIII activation peptide with alpha -thrombin. Crystal structure of its enzyme-substrate analog complex. *J.Biol.Chem.* 275, 36942-36948
17. Hortin, G.L., and Trimpe, B.L. (1991) Allosteric changes in thrombin's activity produced by peptides corresponding to segments of natural inhibitors and substrates. *J.Biol.Chem.* 266, 6866-6871
18. Liu, G., Mu, S.F., Yun, L.H., Ding, Z.K., and Sun, M.J. (1999) Systematic study of the substituted active C-terminus of hirudin. *J.Pept.Res.* 54, 480-490
19. De Filippis, V., De Boni, S., De Dea, E., Dalzoppo, D., Grandi, C., and Fontana, A. (2004) Incorporation of the fluorescent amino acid 7-azatryptophan into the core domain 1-47 of hirudin as a probe of hirudin folding and thrombin recognition. *Protein Sci.* 13, 1489-1502
20. Gan, Z.R., Li, Y., Chen, Z., Lewis, S.D., and Shafer, J.A. (1994) Identification of basic amino acid residues in thrombin essential for heparin-catalyzed inactivation by antithrombin III. *J.Biol.Chem.* 269, 1301-1305
21. De Cristofaro, R., and De Filippis, V. (2003) Interaction of the 268-282 region of glycoprotein Ibalpha with the heparin-binding site of thrombin inhibits the enzyme activation of factor VIII. *Biochem.J.* 373, 593-601

22. Lancellotti, S., Rutella, S., De Filippis, V., Pozzi, N., Rocca, B., and De Cristofaro, R. (2008) Fibrinogen-elongated gamma chain inhibits thrombin-induced platelet response, hindering the interaction with different receptors. *J.Biol.Chem.* 283, 30193-30204
23. Pozzi, N., Chen, R., Chen, Z., Bah, A., and Di Cera, E. (2011) Rigidification of the autolysis loop enhances Na(+) binding to thrombin. *Biophys.Chem.* 159, 6-13
24. Di Cera, E., Guinto, E.R., Vindigni, A., Dang, Q.D., Ayala, Y.M., Wuyi, M., and Tulinsky, A. (1995) The Na+ binding site of thrombin. *J.Biol.Chem.* 270, 22089-22092
25. Dang, Q.D., Guinto, E.R., and di Cera, E. (1997) Rational engineering of activity and specificity in a serine protease. *Nat.Biotechnol.* 15, 146-149
26. Prasad, S., Wright, K.J., Banerjee Roy, D., Bush, L.A., Cantwell, A.M., and Di Cera, E. (2003) Redesigning the monovalent cation specificity of an enzyme. *Proc.Natl.Acad.Sci.U.S.A.* 100, 13785-13790
27. Ratnoff, O.D. (1954) An accelerating property of plasma for the coagulation of fibrinogen by thrombin. *J.Clin.Invest.* 33, 1175-1182
28. Wolberg, A.S., and Aleman, M.M. (2010) Influence of cellular and plasma procoagulant activity on the fibrin network. *Thromb.Res.* 125 Suppl 1, S35-7
29. Komaromi, I., Bagoly, Z., and Muszbek, L. (2011) Factor XIII: novel structural and functional aspects. *J.Thromb.Haemost.* 9, 9-20
30. Anand, K., Pallares, I., Valnickova, Z., Christensen, T., Vendrell, J., Wendt, K.U., Schreuder, H.A., Enghild, J.J., and Aviles, F.X. (2008) The crystal structure of thrombin-activable fibrinolysis inhibitor (TAFI) provides the structural basis for its intrinsic activity and the short half-life of TAFIa. *J.Biol.Chem.* 283, 29416-29423
31. Walker, J.B., Binette, T.M., Mackova, M., Lambkin, G.R., Mitchell, L., and Bajzar, L. (2008) Proteolytic cleavage of carboxypeptidase N markedly increases its antifibrinolytic activity. *J.Thromb.Haemost.* 6, 848-855
32. Coughlin, S.R. (2005) Protease-activated receptors in hemostasis, thrombosis and vascular biology. *J.Thromb.Haemost.* 3, 1800-1814
33. Van Walderveen, M.C., Berry, L.R., Atkinson, H.M., and Chan, A.K. (2010) Covalent antithrombin-heparin effect on thrombin-thrombomodulin and activated protein C reaction with factor V/Va. *Thromb.Haemost.* 103, 910-919
34. Kim, P.Y., and Nesheim, M.E. (2010) Down regulation of prothrombinase by activated protein C during prothrombin activation. *Thromb.Haemost.* 104, 61-70

35. Siller-Matula, J.M., Schwameis, M., Blann, A., Mannhalter, C., and Jilma, B. (2011) Thrombin as a multi-functional enzyme. Focus on in vitro and in vivo effects. *Thromb.Haemost.* 106, 1020-1033
36. Arcone, R., Chinali, A., Pozzi, N., Parafati, M., Maset, F., Pietropaolo, C., and De Filippis, V. (2009) Conformational and biochemical characterization of a biologically active rat recombinant Protease Nexin-1 expressed in E. coli. *Biochim.Biophys.Acta.* 1794, 602-614
37. Corral-Rodriguez, M.A., Macedo-Ribeiro, S., Pereira, P.J., and Fuentes-Prior, P. (2010) Leech-derived thrombin inhibitors: from structures to mechanisms to clinical applications. *J.Med.Chem.* 53, 3847-3861
38. Tsopanoglou, N.E., and Maragoudakis, M.E. (2004) Role of thrombin in angiogenesis and tumor progression. *Semin.Thromb.Hemost.* 30, 63-69
39. Petaja, J. (2011) Inflammation and coagulation. An overview. *Thromb.Res.* 127 Suppl 2, S34-7
40. Kumar, P., Shen, Q., Pivetti, C.D., Lee, E.S., Wu, M.H., and Yuan, S.Y. (2009) Molecular mechanisms of endothelial hyperpermeability: implications in inflammation. *Expert Rev.Mol.Med.* 11, e19
41. Garcia, P.S., Gulati, A., and Levy, J.H. (2010) The role of thrombin and protease-activated receptors in pain mechanisms. *Thromb.Haemost.* 103, 1145-1151
42. Wolberg, A.S., and Campbell, R.A. (2008) Thrombin generation, fibrin clot formation and hemostasis. *Transfus.Apher.Sci.* 38, 15-23
43. Miller, R.J., Jung, H., Bhangoo, S.K., and White, F.A. (2009) Cytokine and chemokine regulation of sensory neuron function. *Handb.Exp.Pharmacol.* (194):417-49. doi, 417-449
44. Turgeon, V.L., Milligan, C.E., and Houenou, L.J. (1999) Activation of the protease-activated thrombin receptor (PAR)-1 induces motoneuron degeneration in the developing avian embryo. *J.Neuropathol.Exp.Neurol.* 58, 499-504
45. Vaughan, P.J., Pike, C.J., Cotman, C.W., and Cunningham, D.D. (1995) Thrombin receptor activation protects neurons and astrocytes from cell death produced by environmental insults. *J.Neurosci.* 15, 5389-5401
46. Smirnova, I.V., Zhang, S.X., Citron, B.A., Arnold, P.M., and Festoff, B.W. (1998) Thrombin is an extracellular signal that activates intracellular death protease pathways inducing apoptosis in model motor neurons. *J.Neurobiol.* 36, 64-80

47. Nishino, A., Suzuki, M., Ohtani, H., Motohashi, O., Umezawa, K., Nagura, H., and Yoshimoto, T. (1993) Thrombin may contribute to the pathophysiology of central nervous system injury. *J.Neurotrauma.* 10, 167-179
48. Faraut, B., Ravel-Chapuis, A., Bonavaud, S., Jandrot-Perrus, M., Verdiere-Sahuque, M., Schaeffer, L., Koenig, J., and Hantai, D. (2004) Thrombin reduces MuSK and acetylcholine receptor expression along with neuromuscular contact size in vitro. *Eur.J.Neurosci.* 19, 2099-2108
49. Tripathy, D., Sanchez, A., Yin, X., Luo, J., Martinez, J., and Grammas, P. (2013) Thrombin, a mediator of cerebrovascular inflammation in AD and hypoxia. *Front.Aging Neurosci.* 5, 19
50. Ciallella, J.R., Figueiredo, H., Smith-Swintosky, V., and McGillis, J.P. (1999) Thrombin induces surface and intracellular secretion of amyloid precursor protein from human endothelial cells. *Thromb.Haemost.* 81, 630-637
51. Igarashi, K., Murai, H., and Asaka, J. (1992) Proteolytic processing of amyloid beta protein precursor (APP) by thrombin. *Biochem.Biophys.Res.Commun.* 185, 1000-1004
52. Choi, S.H., Joe, E.H., Kim, S.U., and Jin, B.K. (2003) Thrombin-induced microglial activation produces degeneration of nigral dopaminergic neurons in vivo. *J.Neurosci.* 23, 5877-5886
53. Park, S.M., Jung, H.Y., Kim, H.O., Rhim, H., Paik, S.R., Chung, K.C., Park, J.H., and Kim, J. (2002) Evidence that alpha-synuclein functions as a negative regulator of Ca(++)-dependent alpha-granule release from human platelets. *Blood.* 100, 2506-2514
54. Bisaglia, M., Trolio, A., Tessari, I., Bubacco, L., Mammi, S., and Bergantino, E. (2005) Cloning, expression, purification, and spectroscopic analysis of the fragment 57-102 of human alpha-synuclein. *Protein Expr.Purif.* 39, 90-96
55. Bisaglia, M., Mammi, S., and Bubacco, L. (2009) Structural insights on physiological functions and pathological effects of alpha-synuclein. *FASEB J.* 23, 329-340
56. Sharma, P., Nag, D., Atam, V., Seth, P.K., and Khanna, V.K. (1991) Platelet aggregation in patients with Parkinson's disease. *Stroke.* 22, 1607-1608
57. O'Brien, M. (2012) The reciprocal relationship between inflammation and coagulation. *Top.Companion Anim.Med.* 27, 46-52
58. Kaplanski, G., Marin, V., Fabrigoule, M., Boulay, V., Benoliel, A.M., Bongrand, P., Kaplanski, S., and Farnarier, C. (1998) Thrombin-activated human endothelial cells support monocyte adhesion in vitro following expression of intercellular adhesion

molecule-1 (ICAM-1; CD54) and vascular cell adhesion molecule-1 (VCAM-1; CD106). *Blood.* 92, 1259-1267

59. Lorant, D.E., Patel, K.D., McIntyre, T.M., McEver, R.P., Prescott, S.M., and Zimmerman, G.A. (1991) Coexpression of GMP-140 and PAF by endothelium stimulated by histamine or thrombin: a juxtacrine system for adhesion and activation of neutrophils. *J.Cell Biol.* 115, 223-234
60. Levi, M. (2010) The coagulant response in sepsis and inflammation. *Hamostaseologie.* 30, 10-2, 14-6
61. Levi, M., Keller, T.T., van Gorp, E., and ten Cate, H. (2003) Infection and inflammation and the coagulation system. *Cardiovasc.Res.* 60, 26-39
62. Levi, M., van der Poll, T., and ten Cate, H. (2006) Tissue factor in infection and severe inflammation. *Semin.Thromb.Hemost.* 32, 33-39
63. Libby, P., and Aikawa, M. (2002) Stabilization of atherosclerotic plaques: new mechanisms and clinical targets. *Nat.Med.* 8, 1257-1262
64. Nakano, S., Ikata, T., Kinoshita, I., Kanematsu, J., and Yasuoka, S. (1999) Characteristics of the protease activity in synovial fluid from patients with rheumatoid arthritis and osteoarthritis. *Clin.Exp.Rheumatol.* 17, 161-170
65. Kastl, S.P., Speidl, W.S., Katsaros, K.M., Kaun, C., Rega, G., Assadian, A., Hagmueller, G.W., Hoeth, M., de Martin, R., Ma, Y., Maurer, G., Huber, K., and Wojta, J. (2009) Thrombin induces the expression of oncostatin M via AP-1 activation in human macrophages: a link between coagulation and inflammation. *Blood.* 114, 2812-2818
66. Borissoff, J.I., Spronk, H.M., Heeneman, S., and ten Cate, H. (2009) Is thrombin a key player in the coagulation-atherogenesis' maze?. Cardiovasc.Res. 82, 392-403

CHAPTER 1.2

Protease Activated Receptors

Proteolytic enzymes are estimated to comprise 2% of the human genome: proteases participate in different biological processes where, anchored to the plasma membrane or free in the extracellular fluid, can cleave ligands or receptors to either initiate or terminate signal transduction (1). The pivotal mechanism by which coagulation proteases modulate nervous system and inflammation is by binding to protease activated receptors (PARs). The PARs family (PAR-1, PAR-2, PAR-3 and PAR-4) consists of four members of G-protein coupled receptors found on endothelia cells, monuclear cells, platelets, fibroblasts and smooth muscle cells (2, 3).

The general mechanism by which proteases cleave and activate PARs is the same: enzymes cleave at specific sites within the extracellular amino terminus of the receptors; this cleavage expose a new amino terminus that serves as a tethered ligand domain, which binds to conserved regions in the second extracellular loop of the cleaved receptor, resulting in the initiation of signal transduction (1) (Fig. 1.3). PAR-1, PAR-3 and PAR-4 are thrombin receptors, and PAR-1 can also serve as receptor for the tissue factor-factor VIIa complex and factor Xa. PAR-2 cannot bind thrombin, but can be activated by the tissue factor-factor VIIa complex, factor Xa and by trypsin (4).

Structurally, PAR-1 is a protein of 425 amino acid residues with 7 hydrophobic domains. The deduced sequence of human PAR-1 contained an amino-terminal signal sequence, and extracellular amino-terminal domain of 75 residues and a potential cleavage site for thrombin within the amino-tail ($LDPR^{41}\downarrow S^{42}FLLRN$, where ↓ denotes cleavage). PAR-2 contains 395 residues with ~30% amino acid identity to human PAR-1. The extracellular amino terminus of 46 residues contained a putative trypsin cleavage site $SKGR^{34}\downarrow S^{35}LIGKV$. PAR-3 was found to share ~28% sequence homology to human PAR-1 and PAR-2. Like PAR-1 and PAR-2, PAR-3 has a thrombin cleavage site within the extracellular amino terminus at $LPIK^{38}\downarrow T^{39}FRGAP$, while PAR-4, 385 amino acid residues, presents a potential cleavage site for thrombin and trypsin in the extracellular amino-terminal domain: $PAPR^{47}\downarrow G^{48}YPGQV$ (1) (Fig. 1.4).

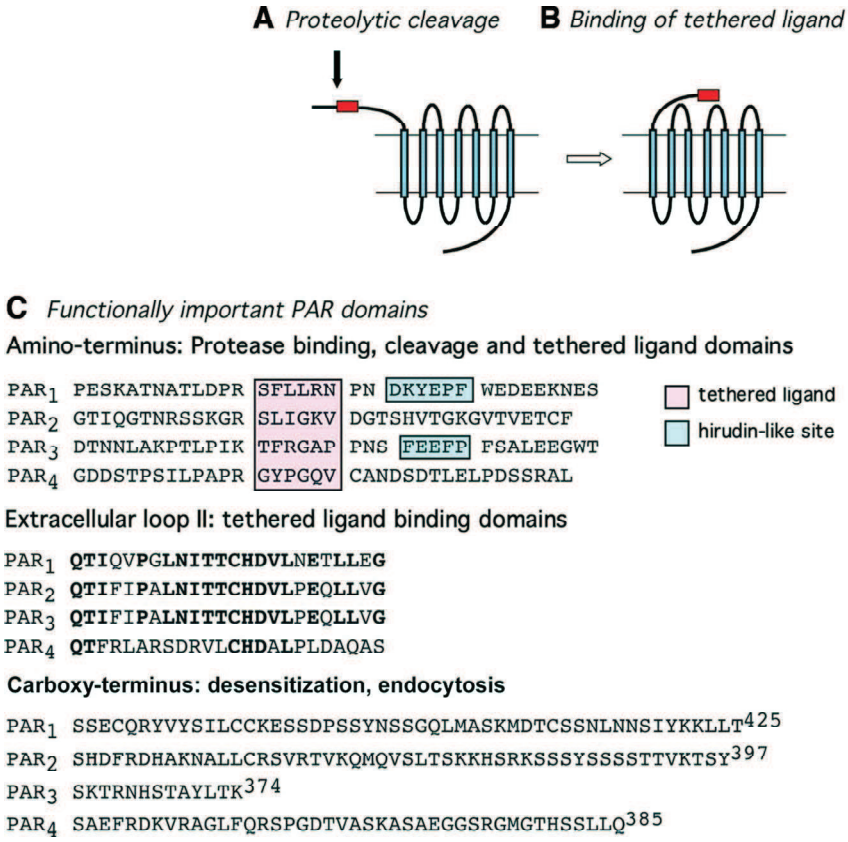

Figure 1.3 Structural and functional domains of PARs. The figure shows alignment of domains of human PAR-1, PAR-2, PAR-3 and PAR-4. **(A)** and **(B)**: mechanism of cleavage and interaction of the tethered ligand with extracellular binding domains. **(C)**: functionally important domains in the amino terminus, second extracellular loop, and carboxyl terminus. This figure was adapted from (1).

Protease Signaling in the Cardiovascular System

Serine proteases of the coagulation cascade are the most efficient activators of PARs (2, 5, 6). Human α-thrombin activates PAR-1, PAR-3 or PAR-4 at the surface of platelets, resulting in aggregation and granular secretion, which are essential for haemostasis. PAR-1 is the primary thrombin receptor on human platelets, while PAR-4 mediate the late phase of clotting activation (7). In addition, PAR-4 could act as a platelet receptor for other proteases, such as cathepsin G (8). Activation of PAR-1 by thrombin reduce vascular endothelial barrier function through signaling cascade that allow calcium influx, nitric oxide release and endothelia cell retraction (9). Moreover, proteolysis of PAR-1 stimulates proliferation of endothelial (10) and vascular smooth muscle cells (11) by up-regolaton of expression of vascular endothelial growth factor (VEGF). Similarly, thrombin activation of PAR-4 induces proliferation of vascular smooth muscle cells (12).

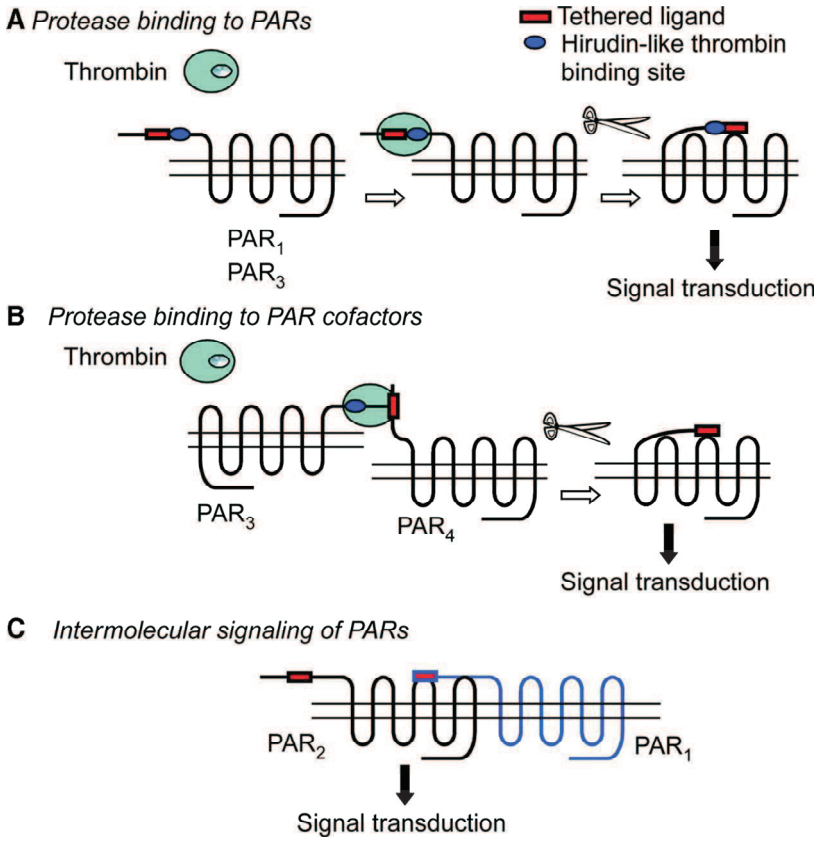

Figure 1.4 Mechanisms of activation and intermolecular cooperation of PARs. (A) Thrombin activates PAR-1 and PAR-3 in a two-step process. First, thrombin binds to a hirudin-like domain; second, thrombin cleaves to expose the tethered ligand, which binds and activates the cleaved receptor. **(B)** PAR-3 is a cofactor for PAR-4 in murine platelets. Thrombin binds to the hirudin site of PAR-3, but PAR-3 does not signal in mouse platelets. The PAR-3-bound thrombin then cleaves and activates PAR-4. **(C)** Intermolecular signalling of PAR-2 and PAR-1 in endothelial cells. The exposed tethered ligand domain of PAR-1 can bind and activate PAR-2, resulting in intermolecular signalling. This figure was adapted from (1).

The tissue factor-factor VIIa-factor Xa complex signals by cleaving PAR-1 and PAR-2 on a variety of cell types, including endothelia cells (13). Indeed it was reported that activation of PAR-2 can be stimulate proliferation of endothelial cells (14).

Protease Signaling in the Nervous System

The effects of thrombin on the nervous system are mediated through activation of PARs: these receptors have been linked to the development and regrowth of central nervous system pathway related to memory, neurodegenerative diseases and dopaminergic reward pathway. PAR-1 mRNA is expressed in the neocortex, cingulate/retrosplenial cortex, subiculum, nuclei within the hypothalamus and thalamus, and in discrete layers of the hippocampus, cerebellum, and olfactory bulb. PAR-1 is also expressed at low levels in glial

cells throughout the brain and by ependymal cells of the choroid plexus and ventricular lining; in addition, PAR-1 is present in the peripheral nervous system (15). PAR-2 expressed within the brain, at the level of neurons and glial cells of the hypothalamus (16); in the periphery, PAR-2 is expressed in primary spinal afferent neurons (17).

Activation of PARs by thrombin or other ligands has been associated with increased apoptosis of dopaminergic neurons in the substantia nigra and degeneration of hippocampal cells (18). The serine protease potentiates the activity of N-methyl-D-aspartate (NMDA) receptors in hippocampal cells through PAR-1, impacting synaptic and neuronal development and neuroprotection during early injury (19). Similarly, in the presence of thrombin, neuroexcitability and neuronal cells damage after injury are increased (20). In addition, both PAR-1 and PAR-2 have been implicated in neurogenic inflammation in the peripheral nervous system, whose clinical manifestations are vasodilatation, edema and pain responses (21). These receptors, in fact, exist on sensory afferent nerve endings in the peripheral nervous system. Their activation results in indirect release of substrate P and calcitonin peptide *in vivo*, two kinds of neuropeptides that mediate edema through loosening of the epithelial gap junctions (22).

Protease Signaling in the Inflammatory Response

Recent studies have shown that binding of tissue factor-factor VIIa to PAR-2 results in up-regulation of inflammatory mediators in endothelial cells (23). In this scenario the events that follow are production of reactive oxygen species, expression of major histocompatibility complex II (MHC II) and cell adhesion molecule, neutrophil infiltration and pro-inflammatory cytokine expression (4). The *in vivo* relevance of PARs has been confirmed in various experimental studies using PAR inhibitors or PAR-deficient mice. For example, observations on PAR-2 - deficient mice suggest a role for this receptor in inflammation of the airway, joints and kidney (1).

The role of PARs was investigated is some inflammatory disease, such as rheumatoid arthritis (RA). RA is a chronic inflammatory condition that is associated with inflammation of the synovium and hyperplasia. There is also elevated expression of tissue factor and thrombin in the synovium and the deposition of fibrin in the inflamed joint, indicating activation of the coagulation system (24). Immunization and subsequent challenge of mice with chicken collagen results in arthritis, and administration of the thrombin inhibitor hirudin reduces the severity of the inflammation, assessed by clinical scoring and measurement of expression of pro-inflammatory cytokines, providing direct evidence for the involvement of thrombin in the

inflammation (25). Evidence for a role of PAR-2 in arthritis has been provided from observations of PAR-2 - deficient animals, which are protected against arthritis induced by intra-articular and periarticular injection of adjuvant. This inflammation is accompanied by an up-regulation of PAR-2 expression, which is normally confined to the vasculature of the joints (26).

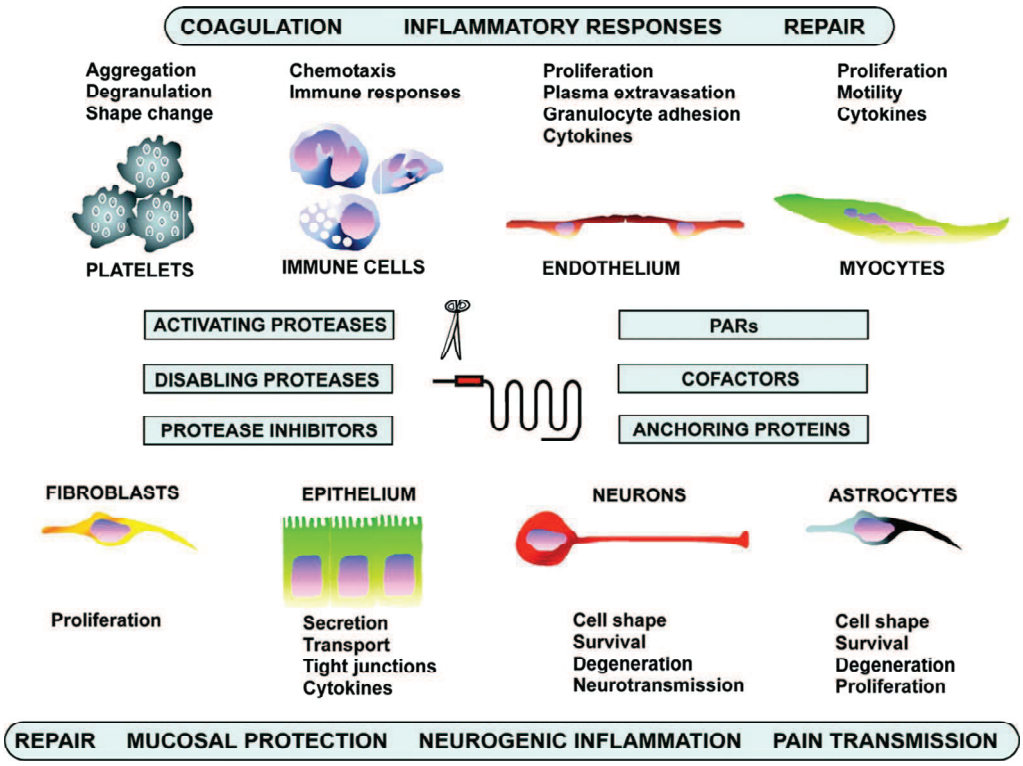

Figure 1.5 Summary of the potential physiological and pathophysiological roles of proteases and PARs in different cell types. This figure was adapted from (1).

REFERENCES

1. Ossovskaya, V.S., and Bunnett, N.W. (2004) Protease-activated receptors: contribution to physiology and disease. *Physiol.Rev.* 84, 579-621

2. Coughlin, S.R. (2000) Thrombin signalling and protease-activated receptors. *Nature.* 407, 258-264

3. Coughlin, S.R. (2005) Protease-activated receptors in hemostasis, thrombosis and vascular biology. *J.Thromb.Haemost.* 3, 1800-1814

4. Levi, M. (2010) The coagulant response in sepsis and inflammation. *Hamostaseologie.* 30, 10-2, 14-6

5. Grand, R.J., Turnell, A.S., and Grabham, P.W. (1996) Cellular consequences of thrombin-receptor activation. *Biochem.J.* 313 (Pt 2), 353-368

6. Riewald, M., and Ruf, W. (2003) Science review: role of coagulation protease cascades in sepsis. *Crit.Care.* 7, 123-129

7. Covic, L., Gresser, A.L., and Kuliopulos, A. (2000) Biphasic kinetics of activation and signaling for PAR1 and PAR4 thrombin receptors in platelets. *Biochemistry.* 39, 5458-5467

8. Sambrano, G.R., Huang, W., Faruqi, T., Mahrus, S., Craik, C., and Coughlin, S.R. (2000) Cathepsin G activates protease-activated receptor-4 in human platelets. *J.Biol.Chem.* 275, 6819-6823

9. Kumar, P., Shen, Q., Pivetti, C.D., Lee, E.S., Wu, M.H., and Yuan, S.Y. (2009) Molecular mechanisms of endothelial hyperpermeability: implications in inflammation. *Expert Rev.Mol.Med.* 11, e19

10. Mirza, H., Yatsula, V., and Bahou, W.F. (1996) The proteinase activated receptor-2 (PAR-2) mediates mitogenic responses in human vascular endothelial cells. *J.Clin.Invest.* 97, 1705-1714

11. McNamara, C.A., Sarembock, I.J., Gimple, L.W., Fenton, J.W.,2nd, Coughlin, S.R., and Owens, G.K. (1993) Thrombin stimulates proliferation of cultured rat aortic smooth muscle cells by a proteolytically activated receptor. *J.Clin.Invest.* 91, 94-98

12. Bretschneider, E., Kaufmann, R., Braun, M., Nowak, G., Glusa, E., and Schror, K. (2001) Evidence for functionally active protease-activated receptor-4 (PAR-4) in human vascular smooth muscle cells. *Br.J.Pharmacol.* 132, 1441-1446

13. Riewald, M., and Ruf, W. (2001) Mechanistic coupling of protease signaling and initiation of coagulation by tissue factor. *Proc.Natl.Acad.Sci.U.S.A.* 98, 7742-7747

14. Mirza, H., Yatsula, V., and Bahou, W.F. (1996) The proteinase activated receptor-2 (PAR-2) mediates mitogenic responses in human vascular endothelial cells. *J.Clin.Invest.* 97, 1705-1714

15. Weinstein, J.R., Gold, S.J., Cunningham, D.D., and Gall, C.M. (1995) Cellular localization of thrombin receptor mRNA in rat brain: expression by mesencephalic dopaminergic neurons and codistribution with prothrombin mRNA. *J.Neurosci.* 15, 2906-2919

16. Smith-Swintosky, V.L., Cheo-Isaacs, C.T., D'Andrea, M.R., Santulli, R.J., Darrow, A.L., and Andrade-Gordon, P. (1997) Protease-activated receptor-2 (PAR-2) is present in the rat hippocampus and is associated with neurodegeneration. *J.Neurochem.* 69, 1890-1896

17. Steinhoff, M., Vergnolle, N., Young, S.H., Tognetto, M., Amadesi, S., Ennes, H.S., Trevisani, M., Hollenberg, M.D., Wallace, J.L., Caughey, G.H., Mitchell, S.E., Williams, L.M., Geppetti, P., Mayer, E.A., and Bunnett, N.W. (2000) Agonists of proteinase-activated receptor 2 induce inflammation by a neurogenic mechanism. *Nat.Med.* 6, 151-158
18. Choi, S.H., Lee, D.Y., Kim, S.U., and Jin, B.K. (2005) Thrombin-induced oxidative stress contributes to the death of hippocampal neurons in vivo: role of microglial NADPH oxidase. *J.Neurosci.* 25, 4082-4090
19. Gingrich, M.B., Junge, C.E., Lyuboslavsky, P., and Traynelis, S.F. (2000) Potentiation of NMDA receptor function by the serine protease thrombin. *J.Neurosci.* 20, 4582-4595
20. Zeng, F., Yu, S.Z., and Zeng, Q.X. (2005) Enhancement of NMDA receptor sensitivity by thrombin and its relationship with tissue transglutaminase. *Zhonghua Nei Ke Za Zhi.* 44, 668-671
21. Vergnolle, N., Wallace, J.L., Bunnett, N.W., and Hollenberg, M.D. (2001) Protease-activated receptors in inflammation, neuronal signaling and pain. *Trends Pharmacol.Sci.* 22, 146-152
22. Garcia, P.S., Gulati, A., and Levy, J.H. (2010) The role of thrombin and protease-activated receptors in pain mechanisms. *Thromb.Haemost.* 103, 1145-1151
23. Rothmeier, A.S., and Ruf, W. (2012) Protease-activated receptor 2 signaling in inflammation. *Semin.Immunopathol.* 34, 133-149
24. Nakano, S., Ikata, T., Kinoshita, I., Kanematsu, J., and Yasuoka, S. (1999) Characteristics of the protease activity in synovial fluid from patients with rheumatoid arthritis and osteoarthritis. *Clin.Exp.Rheumatol.* 17, 161-170
25. Marty, I., Peclat, V., Kirdaite, G., Salvi, R., So, A., and Busso, N. (2001) Amelioration of collagen-induced arthritis by thrombin inhibition. *J.Clin.Invest.* 107, 631-640
26. Ferrell, W.R., Lockhart, J.C., Kelso, E.B., Dunning, L., Plevin, R., Meek, S.E., Smith, A.J., Hunter, G.D., McLean, J.S., McGarry, F., Ramage, R., Jiang, L., Kanke, T., and Kawagoe, J. (2003) Essential role for proteinase-activated receptor-2 in arthritis. *J.Clin.Invest.* 111, 35-41

RESULTS

CHAPTER 2.1

β2-Glycoprotein I

β2-Glycoprotein I (β2GpI), or apolipoprotein H (ApoH), is a 50 kDa protein, synthesized in the liver and placenta, abundantly present in human plasma (50–500 μg/ml) second only to fibrinogen, among the plasma proteins involved in clotting (1, 2). The plasma level of the protein may be increased in chronic infections, hyperlipidaemia, smoking, male gender and increasing age (3). β2GpI is highly conserved in all mammals: human, bovine, canine and mouse proteins have 60-80% amino acid sequence homology (4).

Molecular Structure of β2-Glycoprotein I: Different Conformations

The mature sequence of human β2GpI is heavily glycosylated and consists of 326 amino acids arranged into four repeating units (domains I-IV) and a distinctly folded C-terminal domain V, which is responsible for the binding to phospholipids membrane (5) (Fig. 2.1). Domains I to IV belong to the Complement Control Protein (CCP) family and contains about 60 amino acids each, sharing a common elliptically β-sandwich structure, stabilized by two conserved disulfide bonds (2, 6). These domains are also characterized by the presence of high proline content (i.e. 8-15%), a conserved Cys-Pro peptide bond in the N-terminal region of each domain and a single Trp-residue stacked against the disulfide bond connecting the first and third cysteine. Conversely, domain V is aberrant because it contains 82 amino acids that fold into a central β-spiral structure flanked by two small helices. In addition, it contains three disulfide bonds, has a relatively low proline content (i.e. 3.5%) and the single Trp-residue is not structurally conserved. Besides, the fifth domain contains a conserved positively charged (multiple lysine) region between cysteine 281 and 288 (Fig. 2.1) that is critical for phospholipid binding (7). Many of the positively charged side chains are located in a particular surface region of domain V, consisting of three loops (8). To the phospholipid binding region in domain V, a secondary interaction between domain I and phospholipid has also been suggested, which occurs only at low ionic strengths (9). Thus, β2GpI binding to anionic phospholipids could result either from the combined interaction of the lysine-rich region with the hydrophobic loop or from a two step process involving domains V and I. In summary, the structure of β2GpI suggests a lipid membrane insertion area on the fifth

domain, two domains (III and IV) protected from proteolysis by glycosylation and two further domains (I and II) projecting away from the lipid surface into the extracellular space, and thus able to interact with other proteins and/or antibodies. Hence, both hydrophobic and electrostatic interactions appear necessary for β2GpI binding to anionic phospholipids (4).

The crystallographic structure of human β2GpI (Fig. 2.2A) show that the five domains are arranged like beads on a string to form an elongated J-shaped molecule (10), whereas small-angle X-ray scattering analysis (Fig. 2.2B) indicates that β2GpI in solution assumes a predominantly S-shaped conformation, resulting from a tilt between domain II and III (11). Recent electron microscopy data (Fig. 2.2C), instead, show that β2GpI can assume either a closed circular or an open conformation, similar to the crystallographic structure (2, 12). In these case, plasma purified β2GpI assumes a circular conformation whereby domain I interacts with domain V and after interaction with anionic surface (i.e. phospholipids membranes and lipopolysaccharides) the protein elongates in a J-shaped open conformation. In addition, the interaction of domain V with lipopolysaccharides (LPS), the major constituents of the outer membrane of Gram-negative bacteria, results in a conformational change from the closed to the open conformation (12).

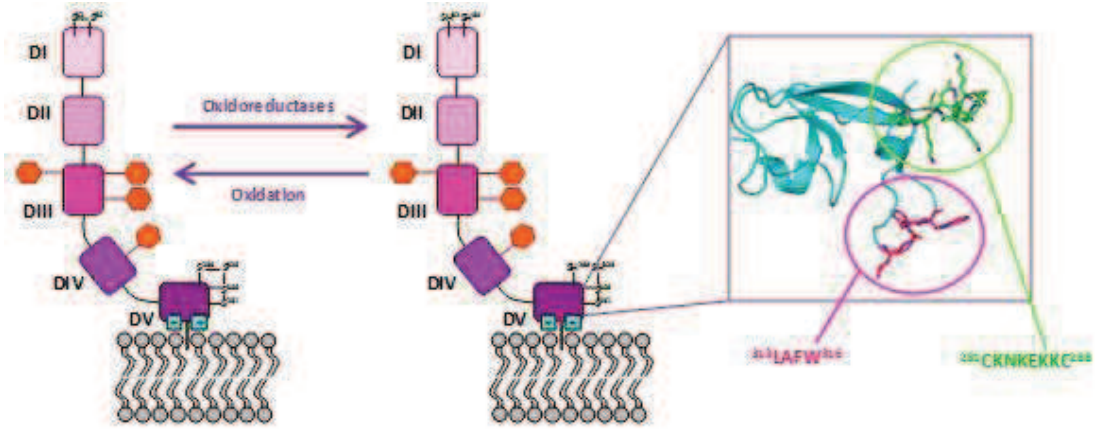

Figure 2.1 Schematic representation of the interaction of β2GpI with phospholipid membranes. The four glycosylation sites in domain III and IV (i.e. Asn143, Asn164, Asn174, Asn243) are indicated by orange hexagons. Zooming on domain five shows the stereoview structures of the phospholipid binding domain (1QUB.pdb). In pink the C-terminal hydrophobic loop (i.e. 313LAFW316) is indicated, while in green is shown the multiple lysine sequence (281CKNKEKKC288). Under oxidative conditions, the carboxyl-terminal amino acid, Cys326, forms a disulfide (S-S) bridge with Cys288 in domain V, while Cys32 in domain I binds to Cys60. In this manner it forms the oxidized-immunogenic species present in APS Patients (31).

β2-Glycoprotein I in the Coagulation Cascade

β2GpI has been shown to interact with a number of steps of the coagulation and fibrinolytic pathways, in fact both pro-coagulant and anti-coagulant activities in vitro have been reported for these protein over the last 30 years (2, 4). Few data show that β2GpI hinders the contact activation in the intrinsic blood coagulation pathway and impairs platelet aggregation by inhibiting the effect of adenosinephospate (13). More recent results indicate that β2GpI binds with low affinity to the A1 domain of vWF and reduce the ability of the co-factor to promote platelet adhesion and agglutination (14). In the presence of dextran sulfate, β2GpI binds to zymogen factor XI and inhibits its activation by thrombin and factor XII, with a resulting down-regulation of factor Xa and thrombin generation (15). β2GpI has also been shown to bind platelet factor 4, a small protein released from platelet α-granules, displaying both pro- and anti- coagulant functions (16). Contrasting data has been reported for the effect of β2GpI on the activation of the zymogen protein C (PC) and on the inhibition of activated PC (aPC) (17-19). Finally, the protein might also exert pro-coagulant functions by protecting thrombin from inactivation by heparin cofactor II (20).

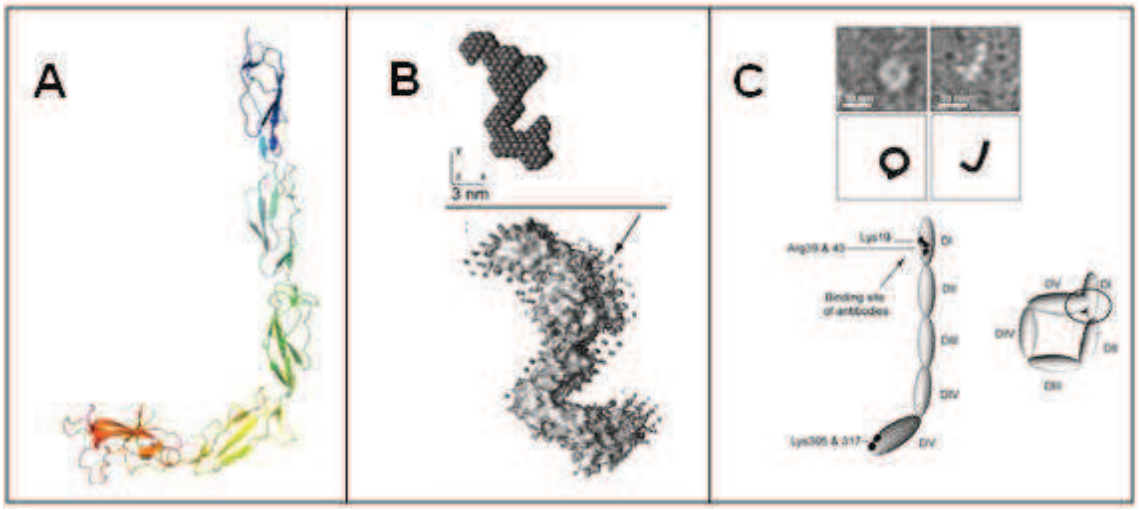

Figure 2.2 Different proposed conformation of β2GpI. (A) Elongated J-shaped form obtained from crystallographic structure (1QUB.pdb). **(B)** S-shaped conformation resulting by small-angle X-ray scattering analysis in solution. **(C)** Dynamic equilibria between closed circular and open conformation, suggest by electron microscopy data. In this case, plasma purified β2GpI assumes a circular conformation whereby domain I interacts with domain V and only after interaction with anionic surface the protein elongates in a J-shaped open conformation.

Recently, mice lacking β2GpI have been produced by gene targeting. Plasma from these knockout mice exhibited impaired thrombin generation in vitro. In heterozygous mice, thrombin generation was not as impaired as in the knockouts. This suggests a correlation between thrombin generation and β2GPI levels (21, 22). In fact, it was reported that in vitro β2GpI in circular-native conformation does not affect the biochemical parameter of thrombin generation. Preincubation with phospholipids, thereby inducing a conformational change from its native to an open J-shaped conformation revealed anticoagulant properties for the protein to thrombin generation (23). Nevertheless, the exact role of β_2GpI in the clotting cascade is not fully elucidated.

The Antiphospholipid Syndrome

β2GpI has been identified as the major antigen in the antiphospholipid syndrome (APS), a severe thrombotic autoimmune disease that can affect both the venous and arterial circulations (2, 4, 24). Clinical features of APS mainly include recurrent thrombosis, thrombocytopenia, recurrent spontaneous miscarriages and various neurological syndromes. The syndrome may occur alone (primary APS) or in association with systemic lupus erythematosus (SLE), other autoimmune diseases, and rarely with infections and drugs (secondary APS). In addition, the catastrophic antiphospholipid syndrome is characterized by clots in multiple small vascular beds and leads to multi-organ failure with high mortality, is generally developed in a small subgroup of patients (24, 25). The other major clinical manifestations of the APS are obstetrical. They include the unexplained death of fetuses at or beyond the 10^{th} week of gestation, the premature birth of neonates before the 34^{th} week of gestation and the spontaneous abortions before the 10^{th} week of gestation (26).

The antiphospholipid syndrome is associated with the presence of antiphospholipid antibodies (aPLAb) (26, 27). These antibodies are directed against either anionic phospholipids or phospholipid-binding protein epitopes localized, for example, at the level of β2GpI. In fact, it was demonstrated that β2GpI binds to anionic phospholipid membranes using positively charged patches in domain V (Fig. 2.1) (28), while it interacts with pathogenic aPLAb by the N-terminal domain I (DmI) (1, 29). Of note, high plasma levels of aPLAb recognizing DmI strongly correlate with thrombosis, whereas aPLAb recognizing other different regions of β2GpI do not seem to be pathogenic. Mutagenesis studies indicate that the antigenic epitope of β2GpI in DmI is discontinuous in nature and comprises amino acid residues Asp8 and Asp9 and the Arg39-Arg43 segment (2). It is possible that aPLAb

directly bind to the constitutive epitope in DmI or, alternatively, to the cryptic epitope that becomes exposed in DmI only after β2GpI binds to negatively charged surfaces. Summarizing, the increase in affinity of β2GpI for anionic phospholipid upon antibody binding further supports the pathogenetic role of this molecule in disorders caused by aPLAb, maybe through interference with phospholipid-dependent steps in coagulation (30). However, the exact mechanism of β2GpI–phospholipid interaction in antibody binding is still unresolved.

In addition, oxidative stress plays a direct role in the structure and function of β2GpI in patients with the antiphospholipid syndrome (24). In healthy persons, the free thiol -non immunogenic- form of β2GpI predominates in the plasma (i.e. Cys32, Cys60, Cys288 and Cys326). Under conditions of oxidative stress, disulfide bonds form at these sites, in correspondence of DmI (Cys32-Cys60) and DmV (Cys288-Cys326) (31). It was demonstrated that in patients with APS the major species of β2GpI is the oxidized -immunogenic- form (Fig. 2.1). In fact, these patients have decreased levels of plasma nitrite, as compared with controls (32). They also have impaired endothelium-dependent vascular responses, which suggest that the activity of endothelial nitric oxide synthase is abnormal (21). In a murine model, aPLAb decreased bioavailable nitric oxide by antagonizing the activity of endothelial nitric oxide synthase, which led to monocyte adhesion to the endothelium (33).

As regards to the fetal mortality in patients with APS, the exact role of aPLAb is not yet fully clarified. One hypothesis suggests that they prevent implantation in vivo, by the binding of aPLAb to the trophectoderm of preimplantation embryos (34). Another suggested a mechanism in which the placental prostaglandin synthesis is impaired, due to the interaction of aPLAb with the β2GpI-mediated activity of lipoprotein lipase on maternal membrane phospholipids (35). It has also been suggest that there is an increased macrophage uptake of oxidised LDL, secondary to aPLAb binding, inducing placental atherogenesis (36).

The Role of β2-Glycoprotein I in the Thrombotic Events of APS

The interference of the physiological interaction between β2GpI and coagulation factors by aPLAb could be a possible pathogenic mechanism correlated with thrombosis in APS patients. The inhibition of FXa generation on activated platelets by β2GpI has been shown to be counteracted by aPLAb, leading to an increased, unopposed FXa generation (37). Another mechanism by which aPLAb may predispose an individual with APS to thrombosis is by interfering with the fibrinolytic mechanism. It was proposed that the competitive

interaction of the complex aPLAb- β2GpI for anionic phospholipid binding sites could hinder the protein S - activated protein C (APC) proteolytic system (4). Indeed, the proteolytic degradation of both FVa and FVIIIa is mediated by the APC complex and the activation of protein C is greatly enhanced by phospholipids (38).

The effect of aPLAb in the pathogenesis of APS-associated thrombosis may also be considered in relation to protein Z (PZ). PZ is a vitamin-K-dependent plasma protein that serves as a cofactor for the inactivation of FXa by protein-Z-dependent protease inhibitor (ZPI). Recent studies suggested that β2GpI modestly delayed the FXa inactivation by PZ/ZPI and aPLAb were found to further increase the inhibitory potential of β_2GPI on PZ/ZPI activity (39). So PZ/ZPI system is commonly impaired in APS patients thus probably increasing the thrombotic risk.

Finally, aPLAb have been shown to exert direct anti-endothelial cell activity in APS patients. The binding of aPLAb to β_2GPI on the endothelial cell (EC) surface, through the specific cell surface receptor annexin II, results in EC activation via the up-regulation of adhesion molecules and cytokines. This induces a proinflammatory and procoagulant phenotype in endothelial cells. This effect also implies that aPLAb, in the presence of β_2GPI, may well bind to healthy EC without anionic phospholipid involvement (40).

REFERENCES

1. Pozzi, N., Banzato, A., Bettin, S., Bison, E., Pengo, V., and De Filippis, V. (2010) Chemical synthesis and characterization of wild-type and biotinylated N-terminal domain 1-64 of beta2-glycoprotein I. *Protein Sci.* 19, 1065-1078
2. de Groot, P.G., and Meijers, J.C. (2011) beta(2) -Glycoprotein I: evolution, structure and function. *J.Thromb.Haemost.* 9, 1275-1284
3. Propert, D.N. (1978) The relation of sex, smoking status, birth rank, and parental age to beta2-glycoprotein I levels and phenotypes in a sample of Australian Caucasian adults. *Hum.Genet.* 43, 281-288
4. Miyakis, S., Giannakopoulos, B., and Krilis, S.A. (2004) Beta 2 glycoprotein I--function in health and disease. *Thromb.Res.* 114, 335-346
5. Bendixen, E., Halkier, T., Magnusson, S., Sottrup-Jensen, L., and Kristensen, T. (1992) Complete primary structure of bovine beta 2-glycoprotein I: localization of the disulfide bridges. *Biochemistry.* 31, 3611-3617

6. Bork, P., Downing, A.K., Kieffer, B., and Campbell, I.D. (1996) Structure and distribution of modules in extracellular proteins. *Q.Rev.Biophys.* 29, 119-167

7. Sheng, Y., Sali, A., Herzog, H., Lahnstein, J., and Krilis, S.A. (1996) Site-directed mutagenesis of recombinant human beta 2-glycoprotein I identifies a cluster of lysine residues that are critical for phospholipid binding and anti-cardiolipin antibody activity. *J.Immunol.* 157, 3744-3751

8. Hoshino, M., Hagihara, Y., Nishii, I., Yamazaki, T., Kato, H., and Goto, Y. (2000) Identification of the phospholipid-binding site of human beta(2)-glycoprotein I domain V by heteronuclear magnetic resonance. *J.Mol.Biol.* 304, 927-939

9. Lee, A.T., Balasubramanian, K., and Schroit, A.J. (2000) beta(2)-glycoprotein I-dependent alterations in membrane properties. *Biochim.Biophys.Acta.* 1509, 475-484

10. Schwarzenbacher, R., Zeth, K., Diederichs, K., Gries, A., Kostner, G.M., Laggner, P., and Prassl, R. (1999) Crystal structure of human beta2-glycoprotein I: implications for phospholipid binding and the antiphospholipid syndrome. *EMBO J.* 18, 6228-6239

11. Hammel, M., Kriechbaum, M., Gries, A., Kostner, G.M., Laggner, P., and Prassl, R. (2002) Solution structure of human and bovine beta(2)-glycoprotein I revealed by small-angle X-ray scattering. *J.Mol.Biol.* 321, 85-97

12. Agar, C., van Os, G.M., Morgelin, M., Sprenger, R.R., Marquart, J.A., Urbanus, R.T., Derksen, R.H., Meijers, J.C., and de Groot, P.G. (2010) Beta2-glycoprotein I can exist in 2 conformations: implications for our understanding of the antiphospholipid syndrome. *Blood.* 116, 1336-1343

13. Nimpf, J., Wurm, H., and Kostner, G.M. (1985) Interaction of beta 2-glycoprotein-I with human blood platelets: influence upon the ADP-induced aggregation. *Thromb.Haemost.* 54, 397-401

14. Hulstein, J.J., Lenting, P.J., de Laat, B., Derksen, R.H., Fijnheer, R., and de Groot, P.G. (2007) beta2-Glycoprotein I inhibits von Willebrand factor dependent platelet adhesion and aggregation. *Blood.* 110, 1483-1491

15. Shi, T., Iverson, G.M., Qi, J.C., Cockerill, K.A., Linnik, M.D., Konecny, P., and Krilis, S.A. (2004) Beta 2-Glycoprotein I binds factor XI and inhibits its activation by thrombin and factor XIIa: loss of inhibition by clipped beta 2-glycoprotein I. *Proc.Natl.Acad.Sci.U.S.A.* 101, 3939-3944

16. Sikara, M.P., Routsias, J.G., Samiotaki, M., Panayotou, G., Moutsopoulos, H.M., and Vlachoyiannopoulos, P.G. (2010) {beta}2 Glycoprotein I ({beta}2GPI) binds platelet

factor 4 (PF4): implications for the pathogenesis of antiphospholipid syndrome. *Blood.* 115, 713-723

17. Oosting, J.D., Derksen, R.H., Hackeng, T.M., van Vliet, M., Preissner, K.T., Bouma, B.N., and de Groot, P.G. (1991) In vitro studies of antiphospholipid antibodies and its cofactor, beta 2-glycoprotein I, show negligible effects on endothelial cell mediated protein C activation. *Thromb.Haemost.* 66, 666-671
18. Mori, T., Takeya, H., Nishioka, J., Gabazza, E.C., and Suzuki, K. (1996) beta 2-Glycoprotein I modulates the anticoagulant activity of activated protein C on the phospholipid surface. *Thromb.Haemost.* 75, 49-55
19. Keeling, D.M., Wilson, A.J., Mackie, I.J., Isenberg, D.A., and Machin, S.J. (1993) Role of beta 2-glycoprotein I and anti-phospholipid antibodies in activation of protein C in vitro. *J.Clin.Pathol.* 46, 908-911
20. Rahgozar, S., Giannakopoulos, B., Yan, X., Wei, J., Cheng Qi, J., Gemmell, R., and Krilis, S.A. (2008) Beta2-glycoprotein I protects thrombin from inhibition by heparin cofactor II: potentiation of this effect in the presence of anti-beta2-glycoprotein I autoantibodies. *Arthritis Rheum.* 58, 1146-1155
21. Miyakis, S., Robertson, S.A., and Krilis, S.A. (2004) Beta-2 glycoprotein I and its role in antiphospholipid syndrome-lessons from knockout mice. *Clin.Immunol.* 112, 136-143
22. Sheng, Y., Reddel, S.W., Herzog, H., Wang, Y.X., Brighton, T., France, M.P., Robertson, S.A., and Krilis, S.A. (2001) Impaired thrombin generation in beta 2-glycoprotein I null mice. *J.Biol.Chem.* 276, 13817-13821
23. Ninivaggi, M., Kelchtermans, H., Lindhout, T., and de Laat, B. (2012) Conformation of beta2glycoprotein I and its effect on coagulation. *Thromb.Res.* 130 Suppl 1, S33-6
24. Giannakopoulos, B., and Krilis, S.A. (2013) The pathogenesis of the antiphospholipid syndrome. *N.Engl.J.Med.* 368, 1033-1044
25. Cervera, R., Bucciarelli, S., Plasin, M.A., Gomez-Puerta, J.A., Plaza, J., Pons-Estel, G., Shoenfeld, Y., Ingelmo, M., Espinos, G., and Catastrophic Antiphospholipid Syndrome (CAPS) Registry Project Group (European Forum On Antiphospholipid Antibodies) (2009) Catastrophic antiphospholipid syndrome (CAPS): descriptive analysis of a series of 280 patients from the "CAPS Registry". *J.Autoimmun.* 32, 240-245
26. Miyakis, S., Lockshin, M.D., Atsumi, T., Branch, D.W., Brey, R.L., Cervera, R., Derksen, R.H., DE Groot, P.G., Koike, T., Meroni, P.L., Reber, G., Shoenfeld, Y., Tincani, A., Vlachoyiannopoulos, P.G., and Krilis, S.A. (2006) International consensus statement on

an update of the classification criteria for definite antiphospholipid syndrome (APS). *J.Thromb.Haemost.* 4, 295-306

27. Kandiah, D.A., Sali, A., Sheng, Y., Victoria, E.J., Marquis, D.M., Coutts, S.M., and Krilis, S.A. (1998) Current insights into the "antiphospholipid" syndrome: clinical, immunological, and molecular aspects. *Adv.Immunol.* 70, 507-563
28. Hunt, J.E., Simpson, R.J., and Krilis, S.A. (1993) Identification of a region of beta 2-glycoprotein I critical for lipid binding and anti-cardiolipin antibody cofactor activity. *Proc.Natl.Acad.Sci.U.S.A.* 90, 2141-2145
29. Banzato, A., Frasson, R., Acquasaliente, L., Bison, E., Bracco, A., Denas, G., Cuffaro, S., Hoxha, A., Ruffatti, A., Iliceto, S., De Filippis, V., and Pengo, V. (2012) Circulating beta2 glycoprotein I-IgG anti-beta2 glycoprotein I immunocomplexes in patients with definite Antiphospholipid Syndrome. *Lupus.* 21, 784-786
30. Takeya, H., Mori, T., Gabazza, E.C., Kuroda, K., Deguchi, H., Matsuura, E., Ichikawa, K., Koike, T., and Suzuki, K. (1997) Anti-beta2-glycoprotein I (beta2GPI) monoclonal antibodies with lupus anticoagulant-like activity enhance the beta2GPI binding to phospholipids. *J.Clin.Invest.* 99, 2260-2268
31. Ioannou, Y., Zhang, J.Y., Qi, M., Gao, L., Qi, J.C., Yu, D.M., Lau, H., Sturgess, A.D., Vlachoyiannopoulos, P.G., Moutsopoulos, H.M., Rahman, A., Pericleous, C., Atsumi, T., Koike, T., Heritier, S., Giannakopoulos, B., and Krilis, S.A. (2011) Novel assays of thrombogenic pathogenicity in the antiphospholipid syndrome based on the detection of molecular oxidative modification of the major autoantigen beta2-glycoprotein I. *Arthritis Rheum.* 63, 2774-2782
32. Ames, P.R., Batuca, J.R., Ciampa, A., Iannaccone, L., and Delgado Alves, J. (2010) Clinical relevance of nitric oxide metabolites and nitrative stress in thrombotic primary antiphospholipid syndrome. *J.Rheumatol.* 37, 2523-2530
33. Ramesh, S., Morrell, C.N., Tarango, C., Thomas, G.D., Yuhanna, I.S., Girardi, G., Herz, J., Urbanus, R.T., de Groot, P.G., Thorpe, P.E., Salmon, J.E., Shaul, P.W., and Mineo, C. (2011) Antiphospholipid antibodies promote leukocyte-endothelial cell adhesion and thrombosis in mice by antagonizing eNOS via beta2GPI and apoER2. *J.Clin.Invest.* 121, 120-131
34. Sthoeger, Z.M., Mozes, E., and Tartakovsky, B. (1993) Anti-cardiolipin antibodies induce pregnancy failure by impairing embryonic implantation. *Proc.Natl.Acad.Sci.U.S.A.* 90, 6464-6467

35. Miyakis, S., Giannakopoulos, B., and Krilis, S.A. (2004) Beta 2 glycoprotein I-function in health and disease. *Thromb.Res.* 114, 335-346

36. Hasunuma, Y., Matsuura, E., Makita, Z., Katahira, T., Nishi, S., and Koike, T. (1997) Involvement of beta 2-glycoprotein I and anticardiolipin antibodies in oxidatively modified low-density lipoprotein uptake by macrophages. *Clin.Exp.Immunol.* 107, 569-573

37. Shi, W., Chong, B.H., Hogg, P.J., and Chesterman, C.N. (1993) Anticardiolipin antibodies block the inhibition by beta 2-glycoprotein I of the factor Xa generating activity of platelets. *Thromb.Haemost.* 70, 342-345

38. Freyssinet, J.M., Gauchy, J., and Cazenave, J.P. (1986) The effect of phospholipids on the activation of protein C by the human thrombin-thrombomodulin complex. *Biochem.J.* 238, 151-157

39. Forastiero, R.R., Martinuzzo, M.E., Lu, L., and Broze, G.J. (2003) Autoimmune antiphospholipid antibodies impair the inhibition of activated factor X by protein Z/protein Z-dependent protease inhibitor. *Journal of Thrombosis and Haemostasis.* 1, 1764-1770

40. Riboldi, P., Gerosa, M., Raschi, E., Testoni, C., and Meroni, P.L. (2003) Endothelium as a target for antiphospholipid antibodies. *Immunobiology.* 207, 29-36

CHAPTER 2.2

β2-Glycoprotein I Binds to Thrombin and Selectively Inhibits the Enzyme Procoagulant Functions

INTRODUCTION

β2-Glycoprotein (β2GpI)I is abundantly present in human plasma (50–500 μg/ml) and highly conserved in all mammals (1). β2GpI has been identified as the major antigen in the antiphospholipid syndrome (APS), a severe thrombotic autoimmune disease (2). Despite its importance in the pathogenesis of APS, the physiological role of β2GpI is still elusive. In fact, both pro-coagulant and anti-coagulant activities in vitro have been reported for β2GpI over the last 30 years (1, 3).

The crystallography structure of β2GpI shows that it composed of five domains, arranged like beads on a string to form an elongated J-shaped molecule (4), whereas small-angle X-ray scattering analysis indicates that β2GpI in solution assumes a predominantly S-shaped conformation (5). Recent electron microscopy data have shown that β2GpI can assume either a closed circular and an open conformation, similar to the crystallographic structure (6). In these case, plasma purified β2GpI assumes a circular conformation whereby domain I interacts with domain V and after interaction with anionic surface (phospholipids membranes and lipopolysaccharides) the protein elongates in a J-shaped open conformation.

Thrombin is the final effector protease in the coagulation cascade (7) and exerts both procoagulant and anticoagulant functions in haemostasis. The procoagulant functions mainly entail conversion of fibrinogen into fibrin and activation of platelets through cleavage of type 1 protease activated receptor (PAR-1) (8), whereas the anticoagulant functions of thrombin are essentially related to its ability to proteolytically activate the anticoagulant protein C in the presence of thrombomodulin (TM) (9). Thrombin has a chymotrypsin-like fold and accomplishes most of its activities through the hydrolytic active site, located in a deep crevice at the interface between two β-barrels (7). For macromolecular substrate targeting, thrombin also exploits two positively charged exosites (exosite-1 and exosite-2) which are located at opposite sides from the catalytic cleft (10). In particular, exosite-1 binds fibrinogen, PAR1 and TM, while exosite-2 binds to the prothrombin F2 fragment, heparin and the elongated γ′-chain of fibrinogen. Furthermore, thrombin uses exosite-2 for interacting with its platelet

receptor glycoprotein-Ibα (GpIbα) and to properly localize on the platelet surface for cleaving PAR1 (11, 12). Thrombin functions are also regulated by sodium ion that binds to a specific site on the protease and enhances its hydrolytic efficiency (8).

Previous qualitative results from Krilis and co-workers, obtained by immobilizing β2GpI onto plastic plates after prolonged exposure to high pH, seemed to indicate that β2GpI binds to both thrombin exosites (13). However, neither biochemical nor functional data pertaining to the proposed β2GpI-thrombin interaction have been reported so far (13). To fill this gap, here we have investigated the effect of physiological concentrations of β2GpI on the procoagulant (fibrin generation and platelet aggregation) and anticoagulant (generation of active protein C) functions of thrombin.

MATERIALS AND METHODS

Materials

Human α-thrombin, PPACK (D-Phe-Pro-Arg-chloromethyl ketone)-inhibited thrombin, protein-C, prothrombin, fibrinogen, activated factor-Xa, and thrombomodulin were purchased from Haematologyic Technologies (Essex Junction, VT, USA); HD1 and HD22 aptamers were obtained from Primm (Milan, Italy); p-aminobenzamidine (PABA); Nα-(2-naphthyl-sulphonyl-glycyl)-D,L-p-amidinophenylalanyl-piperidine (NAPAP), lypopolysaccharide (LPS) and ecarin were from Sigma (St. Louis, USA); hirugen(54-65) peptide, fibrinogen γ′-chain peptide(408-427), hirudin N-terminal domain Hir(1-47), and PAR1(38-60) were chemically synthesized (14, 15).

Purification and Characterization of β2GpI

Natural β2GpI was purified from normal human plasma according to the perchloric acid precipitation method (16), followed by affinity chromatography on a heparin-sepharose column and cation exchange chromatography on a Mono-S column (GE-Healthcare, Piscataway, NJ, USA). The homogeneity and chemical identity of β2GpI preparations (ε_{280}=47$mM^{-1}\cdot cm^{-1}$) was established by SDS-PAGE (4-12% acrylamide), RP-HPLC, and mass spectrometry on a 4800 Plus Maldi-Tof instrument (AB-Sciex, Framingham, MA). β2GpI purified from three different preparations was used.

Production and Characterization of Recombinant Thrombin

Recombinant wild-type thrombin was expressed and refolded as previously described (17). Briefly, pET23(+) plasmid vector containing the cDNA corresponding to wild-type human prethrombin-2 (preThb-2) sequence (Dr. J. Huntington, University of Cambridge, UK) was used to transform E. coli strain BL21(DE3)pLysS cells. After inducing preThb-2 expression with isopropyl β-D-thiogalactoside (IPTG), harvested cells were sonicated and inclusion bodies recovered by centrifugation. Refolding of preThb-2 chain was carried out by diluting drop wise solubilized inclusion bodies (in 6M Gdn-HCl) into the renaturing solution: 20mM Tris-HCl buffer pH 8.5, 0.6M L-arginine hydrochloride, 0.5M NaCl, 1mM EDTA, 10% glycerol, 0.2% Brij-58, and1mM L-cysteine. After dialysis and centrifugation, correctly folded pThb-2 was purified on a heparin-sepharose column followed by treatment with ecarin to generate active thrombin, which was purified on a heparin-sepharose column. Mutations in the preThb2 cDNA were introduced by the oligonucleotide-directed mutagenesis method, using the QuickChange mutagenesis kit (Stratagene, La Jolla, CA). The purity of thrombin preparations (~98%) was established by SDS/PAGE (12% acrylamide gel) and RP-HPLC on a C4 analytical column (4.6 x 150 mm, 5 μm particle size, 300 Å porosity) from Grace-Vydac (Hesperia, CA, U.S.A.). The column was equilibrated with 0.1% (v/v) aqueous TFA and eluted with a linear 0.1% (w/w)-TFA-acetonitrile gradient at a flow rate of 0.8 ml/min. The absorbance of the effluent was recorded at 226 nm. The chemical identity of the purified proteins was established by ESI-TOF mass spectrometry on a Mariner instrument from Perseptive Biosystems (Stafford, TX, U.S.A.). Mutants of human thrombin (i.e. K36A, L65A, K81A, K110A, R165A, K169A, D178A, and K235A) were a generous gift of Dr. N. Pozzi (Dep. of Biochemistry and Molecular Biology, St. Louis University, USA) and were expressed in baby hamster kidney cells, refolded, and purified to homogeneity as previously described (18).

Binding Measurements

Surface Plasmon resonance (SPR) measurements were carried out on a Biacore X100 instrument (GE-Healthcare, Piscataway, NJ, USA). Purified β2GpI (50 μg/ml) in 10mM ammonium acetate buffer pH 4.5, was injected for 10 min at a flow rate of 5 μl/min and covalently immobilized on a carboxymethylated dextran chip (CM5) using the amine coupling chemistry, according to the manufacturer's instructions. The sensor chip was first activated with an equimolar (0.2M) mixture of N-ethyl-N′-dimethylaminipropylcarbodiimide (EDC) and N-hydroxysuccinimide (NHS) and then reacted with a solution of β2GpI (i.e. the ligand). Unreacted carboxymethyl-groups on the sensor chip were blocked by reaction with

1M ethanolamine at pH 8.5. Final immobilization levels of 11100 resonance units (RU) were obtained, corresponding to approximately 11.1 ng of bound β2GpI/mm^2. To avoid autoproteolysis, the inactive thrombin mutant S195A was used. When active human or thrombin mutants at exosite-I and exosite-II were used, the catalytic site was inhibited after incubation with 5-fold molar excess of NAPAP. In competition experiments exosite-I (i.e. HD1 and hirugen) and exosite-II (i.e. HD22 and γ′-peptide) binders were first incubated with thrombin and then injected over the β2GpI-coated sensor chip. All measurements were carried out at 25°C in Hepes-EP+ (10mM Hepes pH 7.4, 150mM NaCl, 3mM EDTA, 0.005% Tween20 polyoxyethylene sorbitan) at a flow rate of 30 μl/min. Each SPR trace was subtracted for unspecific binding (<2% of Rmax) of thrombin. The response units (RU) at the steady state were plotted as a function of [thrombin] and fitted to the Langmuir equation (eq.1) to yield the dissociation constant, Kd, of thrombin-β2GpI interaction:

$$R_{eq} = C \cdot R_{max}/(C + K_d) \qquad \text{(eq.1)}$$

where R_{max} is the value in RU at complex saturation and R_{eq} is the change in RU at each given concentration C after reaching equilibrium.

Studies of the ionic strength dependence of the interaction thrombin- β2GpI were carried out by SPR at different concentration of NaCl (i.e. 0.1M, 0.15M, 0.2M, 0.3M, 0.35M, 0.4M, 0.5M) in Hepes-EP+ buffer at 25°C. The thrombin samples that were injected were prepared in each different buffer so that the flowing buffer and the thrombin sample buffer were always identical. A total of six different [thrombin] were injected for every salt concentration. The data plotted as ln Kd versus ln [salt] were fitted to a straight line according to the following expression (eq.2):

$$-\ln Kd = A_0 + \Gamma_{salt} \ln [salt] \qquad \text{(eq.2)}$$

where Kd is a dissociation constant, the slope Γ_{salt} represents a thermodynamic measure of the effect of salt concentration on binding equilibria (19) and provides the minimum number of ionic interaction involved, and A_0 is the true Kd for the interaction from the intercept at 1M [salt] (20).

Binding of PABA (ε_{293nm} = 15mM$^{-1}\cdot$cm^{-1}) and Hir(1-47) (ε_{280nm}=2560M$^{-1}\cdot$cm^{-1}) to thrombin was performed by fluorescence measurements (21, 22) in the absence or presence of 4μM β2GpI. Measurements were carried out at 37±0.1°C on a Jasco (Tokyo, Japan) FP-6500 fluorimeter in Hepes-buffered-saline (HBS, 10mM Hepes pH 7.4, 0.15M NaCl, 0.1% PEG_{6000}). For the binding of PABA, the data were corrected for inner filter effect. For PABA binding, thrombin samples were excited at 336 nm and the fluorescence intensity was

recorded at 375 nm. The data were corrected for inner filter effect (eq.3) (23) and fitted with the Langmuir equation (eq.4) using the program Origin 7.5 (MicroCal, Inc.):

$$F_{corr} = F_{obs} \cdot 10^{-(Aex \cdot d/2)} \quad \text{(eq.3)}$$

where A_{ex} is the solution absorbance at the excitation wavelengths and d is the cuvette path-length.

$$F_{corr} = F_0 + \{(F_{max} \cdot [I])/(Kd+[I])\} \quad \text{(eq.4)}$$

where F_0 and F_{max} are the intensities of PABA fluorescence in the thrombin-free or thrombin-bound state, respectively, and Kd is the dissociation constant of thrombin-PABA complex.

For Hir (1-47) binding, thrombin samples were excited at 295nm and the fluorescence recorded at 334nm as a function of inhibitor concentration. The data were analyzed within the framework of the tight binding model (eq.5) using the program Origin 7.5 (MicroCal, Inc.):

$$\Delta F = \{(\Delta F_{max}+[I]+Kd) - \{(\Delta F_{max}+[I]+Kd)^2 - 4 \cdot \Delta F_{max}\,[I]\}^{1/2}\}/2 \quad \text{(eq.5)}$$

where Kd is the dissociation constant of the inhibitor-thrombin complex and ΔF_{max} is maximal fluorescence change at saturating [I], such as Hir(1-47).

Clotting Assays

The turbidity (i.e. absorbance at 350 nm) of a desalted fibrinogen solution was measured after addition of thrombin (0.5 - 4 nM) at 37±0.1°C in HBS on a Jasco V-630 spectrophotometer (Tokyo, Japan), in the absence or presence of 4μM β2GpI (21). The rate of thrombin-induced platelet aggregation was determined by turbidimetric measurements at 350 nm at 37±0.1°C on a PACKS-4 aggregometer (Helena Laboratories, Sunderland, UK) (14). Platelets from normal donors were obtained by gel filtration of platelet-rich plasma onto a (1×25cm) Sepharose 2B column equilibrated with 10mM Hepes buffer pH 7.4, 135mM NaCl, 5mM KCl, 5mM glucose, 0.1% BSA. Gel-filtered platelets (220000/μl) were activated with human thrombin (1nM) and the velocity (v) of platelets aggregation was estimated as $v = \Delta A_{350}/\Delta t$, where ΔA_{350} is the increase in absorbance at 350 nm and Δt (i.e. 4 min) is the time range in which A_{350} is a linear function of time The IC_{50} value was estimated by fitting the data points of %vi versus [β2GpI] to a logistic equation (eq.6) using the program Origin 7.5 (MicroCal, Inc.):

$$v = v_{max} + \{(v_{min}-v_{max})/1+([\beta 2GpI]/IC_{50})^p\} \quad \text{(eq.6)}$$

where v_{min} and v_{max} are the asymptotic values that assumes v in the absence or in the presence of saturating [β2GpI], p is the slope factor, and IC_{50} is the concentration of β2GpI inhibiting by 50% thrombin-induced platelet aggregation.

The effect of β2GpI on the thrombin-induced clotting in whole blood was determined at 37°C by Multiple Electrode Aggregometry (MEA) using a Multiplate analyzer (Dynabyte, Munich, Germany). The Area Under the aggregating Curve (AUC) was calculated over 6-min reaction (24). Citrate-treated blood samples were taken from three healthy donors, two males and one female, 23-28 years of age, and non-smokers. The donors gave written informed consent for participation to this study, approved by the institutional ethics committee. Ecarin clotting time (ECT) and thrombin clotting time (TCT) assays were carried out at 25°C with normal and β2GpI-deficient plasma (Affinity Biologicals, Ancaster, Canada) using an ACL-Top300 coagulometer (Instrumentation Laboratory, Milan, Italy) according to the manufacturer's procedures.

PAR-1 Hydrolysis and PC Activation

Measurement of thrombin-mediated PAR-1 hydrolysis on gel-filtered platelets was carried out by immunocytofluorimetry on FACScan flow-cytometer (Becton Dickinson, Mountain View, CA) (11, 14), using a SPAN-12 mAb recognizing intact PAR-1. Briefly, gel-filtered platelets (10000/μl) were activated at 37±0.1°C with human thrombin (0.2nM) in the presence of β_2GpI (0-2μM). The presence of intact PAR-1 molecules on the platelet membrane after thrombin stimulation was measured by adding saturating concentrations (2 μg) of SPAN12 monoclonal antibody (mAb) (Immunotech, Monrovia, CA, USA), a phycoerythrin (PE)-conjugated anti-PAR-1 mAb recognizing the N-terminal portion of PAR-1 segment 35–46 ^{35}NATLDPR↓SFLLR^{46}, exclusively in the intact, uncleaved form. Data points were fitted to a logistic equation (eq.7) to obtain the IC_{50} value, using the program Origin 7.5 (MicroCal, Inc.):

$$F = F_0 + \{(F_1-F_0)/1 + ([\beta 2GpI]/IC_{50})^p\} \quad \text{(eq.7)}$$

where F_0 and F_1 are the fluorescence of PE-conjugated anti-PAR-1 mAb at [β_2GpI] = 0 and 2μM, respectively, p is the slope factor, and IC_{50} is the concentration of β2GpI inhibiting by 50% thrombin-mediated cleavage of PAR-1 on platelets. Fluorescence data are expressed as the per cent of the maximum emission recorded by incubating platelets with SPAN12 mAb.

Hydrolysis of PAR-1(38-60) peptide (1μM) by thrombin (0.1nM) was carried out at 25°C in Tris-buffered-saline (TBS) and monitored by RP-HPLC (14). The peptide PAR-1(38-60) ^{38}LDPR↓SFLLRNPNDKYEPFWEDEE^{60} was synthesized in our laboratory by solid phase techniques, using the fluorenylmethyloxycarbonyl chemistry, purified to homogeneity by RP-HPLC, and its chemical identity established by MS. The effect of β2GpI (1μM) was

investigated by pre-incubating the enzyme with the protein. At time intervals, aliquots of the reaction mixture was blocked with aqueous formic acid (10%) and the time course of PAR-1 (42-60) release was monitored by RP-HPLC, onto a (4.6x150mm) Vydac C18 column eluted (0.8 ml/min) with a linear acetonitrile-0.1% TFA gradient from 5 to 45% in 45 min, by recording the absorbance of the effluent at 214 nm. When substrate concentrations are lower than Km values of thrombin (E) for PAR-1 (>10μM) (25) the concentration of product [P] [i.e. PAR-1(42-60)] can be measured as a function of time (t) according to the pseudo first-order kinetic equation (eq.8), using the program Origin 7.5 (MicroCal, Inc.):

$$[P] = [P] \infty [1 - \exp(-t \cdot k_{obs})] \quad \text{(eq.8)}$$

where $[P]\infty$ is the concentration of the product at $t=\infty$ and k_{obs} is the observed kinetic constant given by kobs = [E]s, in which [E] is the enzyme concentration and s is the specificity constant kcat/Km. The s values were analyzed as a function of the inhibitor concentration, [I] (i.e. β2GpI) using the linkage equation (25).

Protein C (PC) activation by thrombin alone or in the presence of 4μM β2GpI was monitored with or without thrombomodulin at 37°±0.1C in TBS, containing 5mM $CaCl_2$, according to the quenching method described elsewhere (24). At time intervals, aliquots of the reaction mixture were added to a TBS solution containing the aPC substrate S2366 (200μM) (Chromogenix, Milan, Italy), and hirudin HM2 (1μM) to selectively inhibit thrombin. The initial velocity, vi, of S2366 hydrolysis was determined by measuring the release of p-nitroanilide at 405 nm, using a Victor3 plate reader (Perkin-Elmer, Norwalk, CA) and 96-well polystyrene plates (Sigma, St. Louis, MO, USA). At each time point, the concentration of the newly generated aPC was determined from a standard curve of vi versus [aPC], obtained with aPC solutions of known concentration. The kcat/Km. value of PC hydrolysis was obtained from the time-course of aPC generation, using the pseudo first-order kinetic model (eq.8).

Modelling

Docking was performed with Ultrafast-FFT GPU-based HEX 6.3 software (26), run on nVidia GeForce GTX680, starting from the structures of β2GpI (1C1Z.pdb) (4) and inhibitor-free thrombin (1PPB-pdb) (7). Simulations were run using default parameters, without introducing any geometric/energetic constrain. One hundred poses were generated and ranked according to the HEX scoring function (26). The top three poses were almost identical and selected for data analysis.

RESULTS

Chemical Characterization of Purified β2GpI

Natural β2GpI was purified from normal human plasma by means of perchloric acid precipitation. This procedure yields highly homogenous (> 95%) β2GpI preparations, as obtained from RP-HPLC and SDS-PAGE (Fig. 2.3).Under reducing conditions, β2GpI migrates as a single band at ~53 kDa, in agreement with the known lower electrophoretic mobility of glycosylated proteins. Malti-tof mass spectrometry analysis of purified β2GpI yields an average molecular mass of 44957 ± 20 a.m.u.

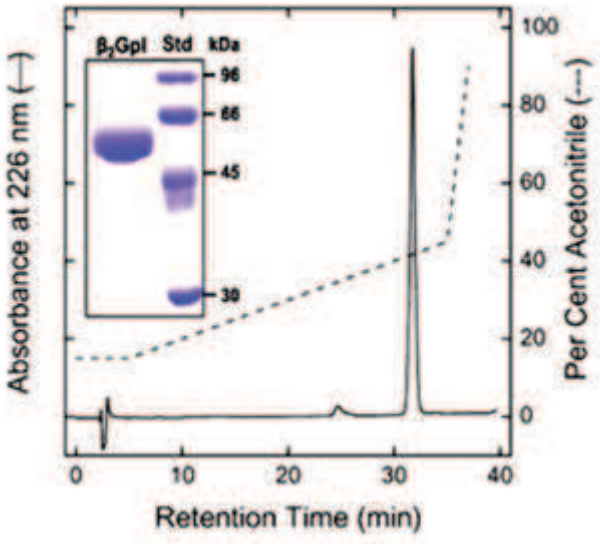

Figure 2.3 Analytical characterization of purified β2GpI (30 μg) by RP-HPLC. The material eluted in correspondence of the major chromatographic peak was collected, lyophilized and analyzed by Maldi-tof mass spectrometry. **Inset:** SDS-PAGE (4-12% acrylamide) analysis of β2GpI under reducing conditions. Lane 1, purified β2GpI (4 μg); lane 2 molecular weight protein standards (Std).

β2GpI-Thrombin Interaction Probed by SPR

Increasing concentrations of the inactive mutant S195A (Fig. 2.4A) or recombinant wild-type α-thrombin (Fig. 2.4B), pre-treated with the active-site inhibitor NAPAP (Kd = 7nM), were injected over a CM5 sensor chip loaded with purified β2GpI up to 11´100 resonance units (RU). Our data (Fig. 2.4A) show that S195A and the NAPAP-inhibited wild-type thrombin bind to immobilized β2GpI with the same affinity (Kd = 37nM and 34nM, respectively), suggesting that the active-site of thrombin is not (or only loosely) involved in β2GpI interaction. This conclusion was further supported by the lack of any significant effect of β2GpI on the affinity of thrombin for structurally different active-site inhibitors, like PABA

(Fig. 2.4D) and Hir (1-47) (Fig. 2.4E). While PABA is a small molecule interacting with the primary specificity site of trypsin-like proteases (27), Hir (1-47) is a globular polypeptide encompassing the N-terminal domain of hirudin and extensively penetrating into the enzyme subsites (15). Interestingly, β2GpI does not reduce and even slightly enhances the affinity of the inhibitors for thrombin (Fig. 2.4). Control experiments, carried out with unmodified CM5 sensor chip, unequivocally demonstrate that β2GpI does not interact with the negative surface of the carboxymethyldextran-coated sensor chip, either in the absence of soluble carboxymethyldextran (1 mg/ml).

Mapping β2GpI-Thrombin Interaction Sites

The role of thrombin exosites in β2GpI binding was assessed by:

1. competition experiments with ligands specific for exosite-I (hirugen, HD1 aptamer and TM) or exosite-II (fibrinogen γ′-peptide and HD22 aptamer);
2. binding with thrombin mutants having exosite-I or exosite-II partially compromised by point mutations;
3. binding with thrombin zymogens prothrombin (ProT) and prethrombin-2 (Pre2) and nicked thrombin (β_T-thrombin) having one or both exosites variably compromised.

In competition experiments (Fig. 2.5A, 2.5B, 2.5C) exosite-I or exosite-II were blocked with saturating concentrations of ligands specific for either one of the two exosites. The resulting thrombin-ligand solutions were injected over the β2GpI-immobilized sensor chip and the decrease in the SPR signal was interpreted as an indication that the blocked exosite was involved in the interaction with β2GpI. SPR analyses indicate that blockage of either exosite-I or exosite-II results in 40-60% decrease of RU, while the simultaneous blockage of both exosites with hirugen and γ′-peptide completely abrogates binding. In addition, linkage-experiments with increase concentration of inhibitors (0-2μM for hirugen and 0-160 μM for fibrinogen γ′-peptide) confirm that both exosites are involved in the interaction: Kd, in the presence of saturating concentration of exosite-I or exosite-II binders, increases of 3-5 fold.

Perturbations of thrombin exosites by point mutations indicate that Ala-shaving of R73 in exosite-I or R101 in exosite-II slightly reduces affinity for β2GpI (Fig. 2.5D). Data obtained with a small library of mutant of human thrombin (Exosite-I: K36A, L65A, K81A, K110A; Exosite-II: R165A, K169A, D178A, K235A) suggest that the ionic interaction plays

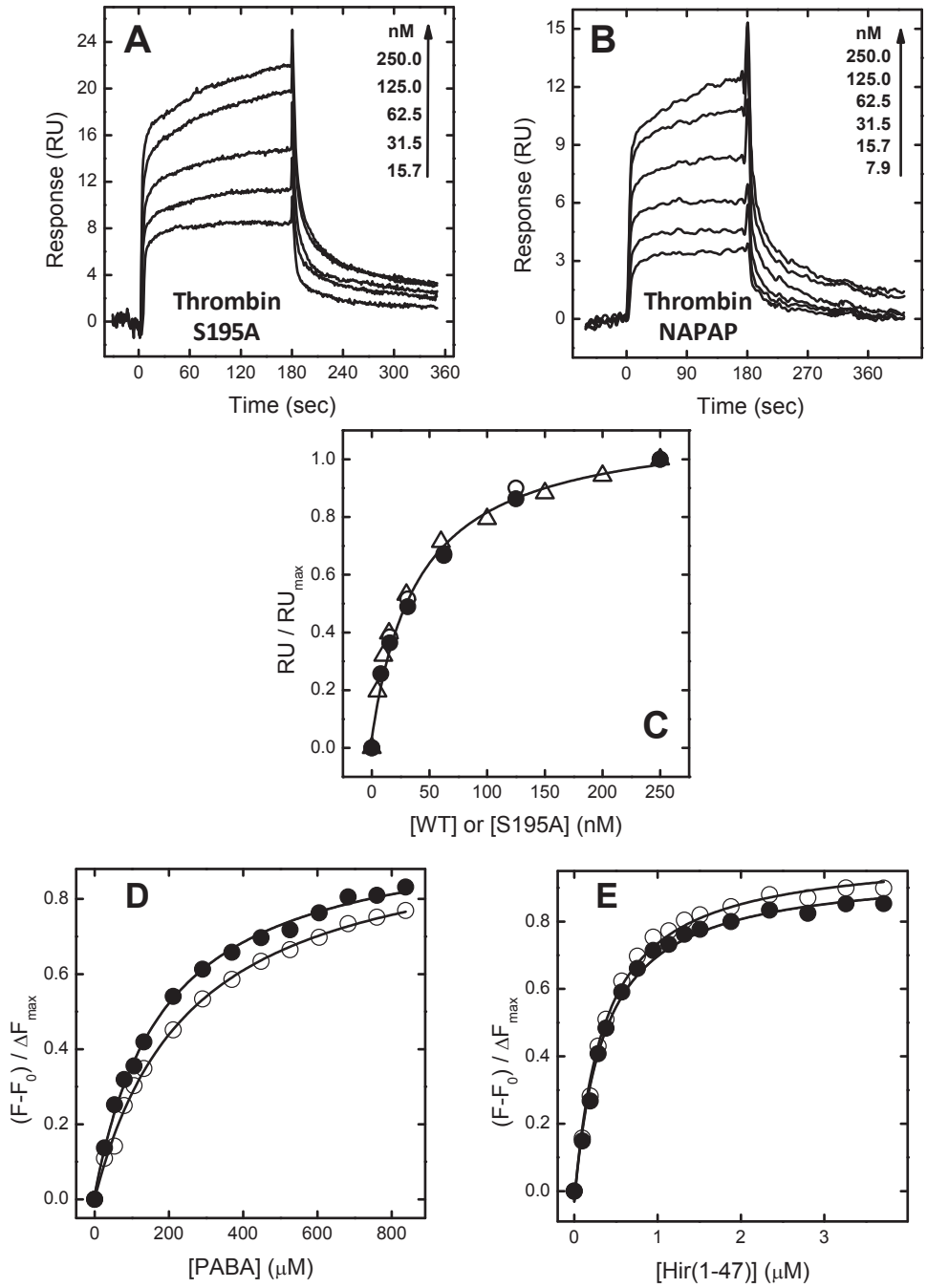

Figure 2.4 Surface plasmon resonance analysis of β2GpI-thrombin interaction. (A) Binding of the inactive recombinant S195A thrombin mutant. **(B)** Binding of wild-type thrombin inhibited with NAPAP (1μM). **(C)** Plot of RU/RU$_{max}$ ratio as a function of [Thrombin], where RU$_{max}$ is the RU value extrapolated at [Thrombin]→∞. Data fitting yields a Kd = 37 ± 4 nM for S195A mutant (○,Δ) and Kd = 34 ± 4 nM for NAPAP-inhibited wild-type thrombin (●).

Effect of β2GpI on the affinity of active-site inhibitors for thrombin. (**A**) PABA binding: thrombin samples (25nM) in the absence (○) and presence (●) of 4μM β2GpI were excited at 336 nm and the fluorescence of PABA was recorded at 375 nm. Kd for PABA binding was calculated as 256 ± 6μM and 187 ± 9μM in the absence or in the presence of β2GpI. (**B**) Hir(1-47) binding: thrombin samples (50nM) in the absence (○) and presence (●) of 4 μM β2GpI were excited at 295 nm and the fluorescence was recorded at 334 nm. Kd values for Hir(1-47) binding were calculated as 151 ± 8nM and 145 ± 7nM in the absence or in the presence of β2GpI. The error on fluorescence measurements was <5%.

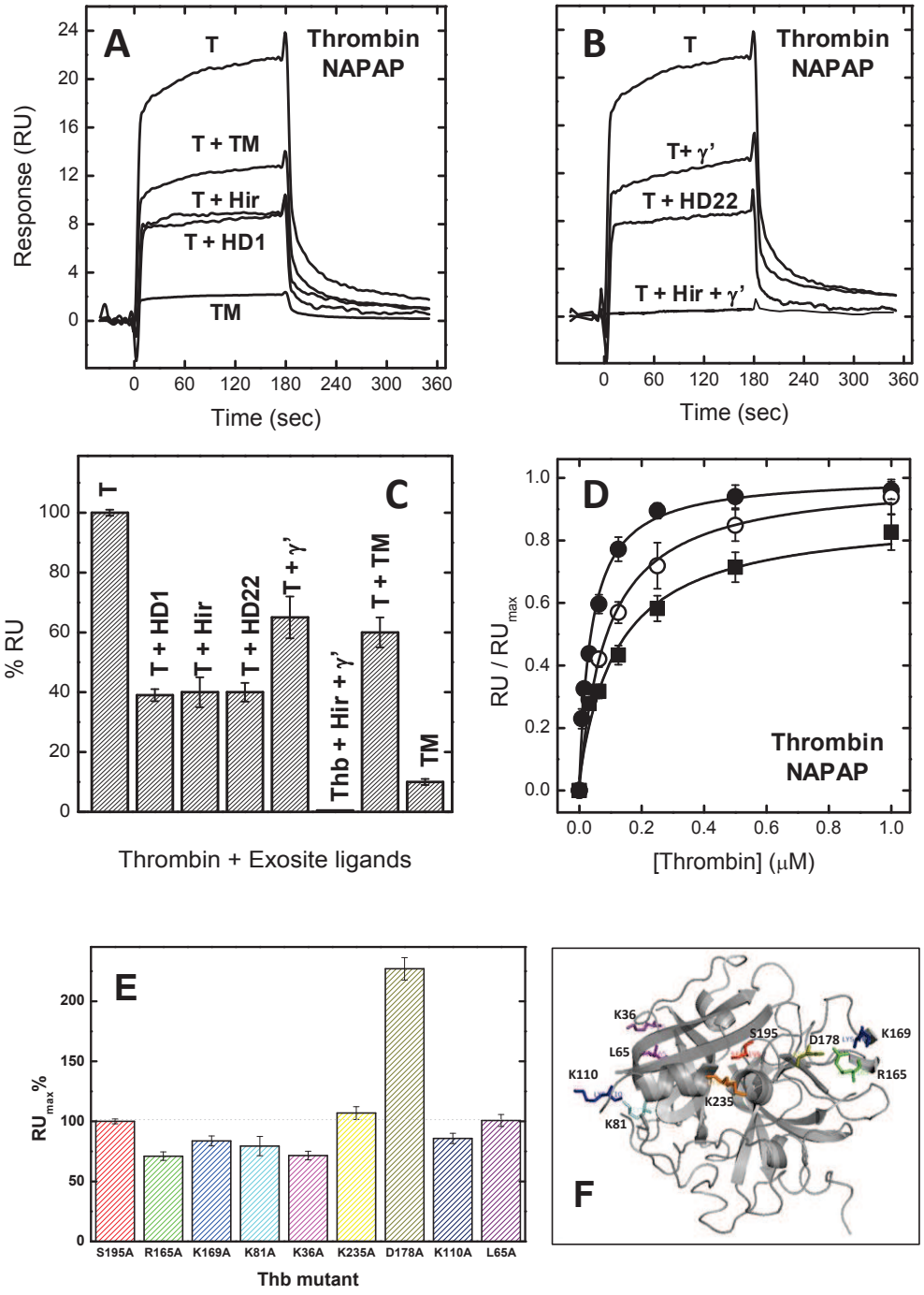

Figure 2.5 Surface plasmon resonance analysis of β2GpI binding to thrombin exosites. (A) Exosite-I: thrombin (T, 250nM) inhibited with NAPAP (5μM) was incubated for 5 min with 1μM HD1 or 20μM hirugen (Hir) and the resulting complex injected over the bound β2GpI. In the case of TM, the cofactor alone (10nM) or an equimolar (10nM) TM-thrombin solution was loaded. **(B)** Exosite-II: NAPAP-inhibited thrombin (250nM) were separately incubated with 1μM HD22 and 270μM fibrinogen γ'-peptide or with a solution of 20μM hirugen+200μM γ'-peptide. **(C)** %RU measured for the binding of thrombin to immobilized β2GpI in the presence of exosite binders, as obtained in **A** and **B**. **(D)** Interaction of recombinant wild-type (●) and mutant thrombins R73A (○) and R101A (■) to bound β2GpI. Data fitting yields Kd value of 72 ± 8 nM for R73A, 91 ± 10 nM for R101A, and 45 ± 4 for wild-type. **(E)** Interaction of mutant human thrombin to bound β2GpI; D178A displays incremental of affinity by 4 fold. **(F)** Localization of amino acid residue substituted by point mutations in the thrombin structure (1PPB.pdb).

a relevant role in the binding. In fact, all the above mutations did not significantly influence the affinity for β2GpI immobilized on sensor chip; the only exception is D178A (Fig.2.5E). In this case, the substitution on negative charge of Asp residue with Ala residue comport an incremental of affinity by 4 fold.

Binding measurements with thrombin zymogens (Fig. 2.6A) show that full-length ProT does not significantly bind to β2GpI, whereas the shorter zymogen intermediate Pre2 interacts with β2GpI with an affinity 7-8 fold lower than that of mature α-thrombin, Kd = 264 ± 15 nM (Fig.2.6A, 2.6B). These results can be rationalized considering that in ProT both exosites are heavily compromised, whereas in Pre2 only exosite-1 is perturbed while exosite-2 is still functional. Consistently with these findings, the affinity of β_T-thrombin (17) is dramatically reduced (Fig. 2.6A), as a result of tryptic cleavage of Arg77a-Asn78 bond, causing disruption of exosite-I and perturbation of exosite-II (28). Conversely to thrombin, immobilized β2GpI does not bind to activated factor X (FXa) (Fig. 2.6B), the serine protease immediately upstream to thrombin in the coagulation cascade.

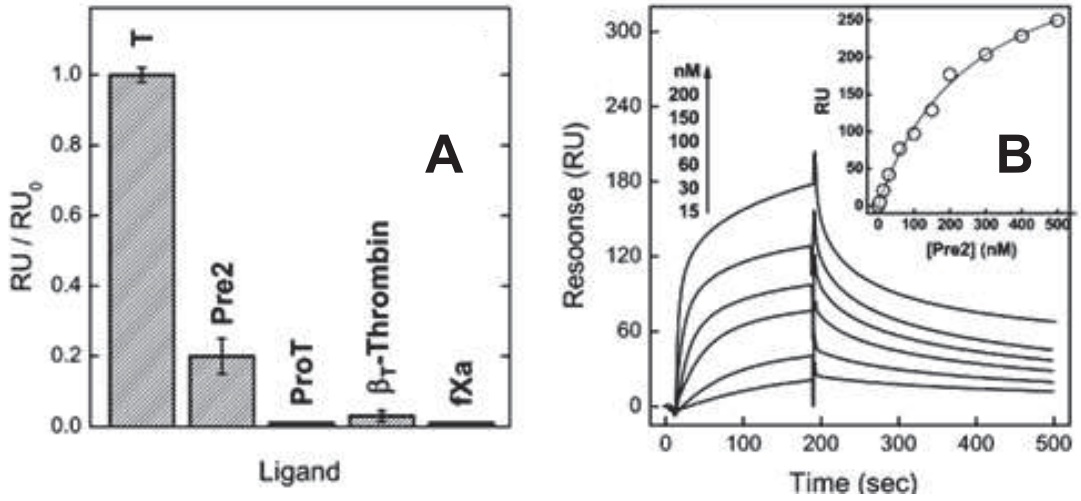

Figure 2.6 Surface plasmon resonance analysis of β2GpI binding to thrombin zymogens. (A) RU/RU_0 ratio measured for the binding of Pre2 (10nM) and ProT (1μM), β-thrombin (10nM) and FXa (10nM) to bound β2GpI. RU_0 is the signal obtained with thrombin S195A alone (10nM). **(B)** SPR analysis of the interaction of Pre2 to immobilized β2GpI. After data fitting (**Inset**), a Kd = 264 ± 15 nM was obtained.

Electrostatic Steering of β2GpI-Thrombin Interaction

The effect of the salt (i.e. 0.1M, 0.15M, 0.2M, 0.3M, 0.35M, 0.4M, 0.5M Na^+) in the interaction of β2GpI with thrombin (Fig.2.7A) can be further quantified by plotting the data as ln Kd, at different concentration of NaCl, verses ln [salt] on a straight line according to eq. 2. The value of Γ_{salt} for this interaction was calculated from the slope of the line as -2.36 ± 0.15 (Fig. 2.7B). The value of Γ_{salt} for β2GpI-thrombin interaction is compared with the Γ_{salt} values calculated for the enzyme and other exosite-I and exosite-II ligands obtained from the literature (19). Thrombin ligands that bind at its exosite-I (i.e. fibrinogen and hirudin) have little salt dependence and values of Γ_{salt} around 1.0, whereas known exosite-II binders (i.e. heparin and thrombomodulin) are characterized by Γ_{salt} values around 4-5 (19). In this respect, β2GpI is behaving as a thrombin exosite-I – exosite-II binding ligand. In addition, if the association between β2GpI and thrombin is solely due to an electrostatic association, the values of Γ_{salt} will also indicated the minimum number of ionic bound involved in the binding (20). Thus, it might be expected that a minimum of two-three ionic bonds contribute to this interaction.

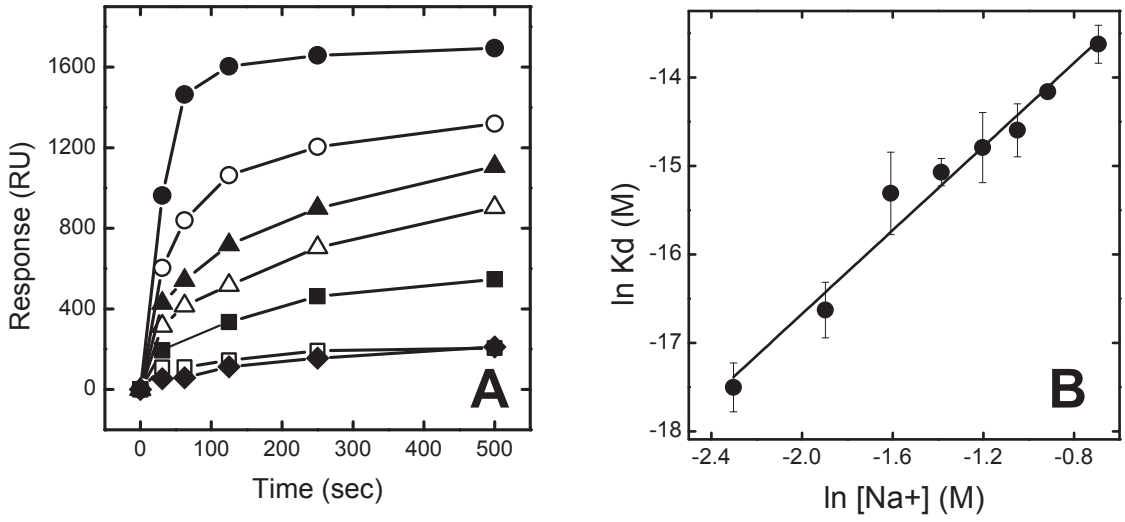

Figure 2.7 Salt dependence of β2GpI-thrombin interaction. (A) Interaction of thrombin to immobilized β2GpI at different concentration of NaCl: 0.1M ●●, 0.15M ○○, 0.2M ▲▲, 0.3M ΔΔ, 0.35M ■■, 0.4M □□, 0.5M ♦♦. **(B)** The dissociation constant, Kd, for the β2GpI-thrombin interaction derived from the curves in **A** were plotted as a function of the respective Na^+ ion concentration on a ln-ln scale, and fitted by linear regression according to eq.2. After data fitting a Γ_{salt} = -2.36 ± 0.15 was obtained.

β2GpI Prolongs the Clotting Time in Fibrin Generation Assays

Fibrin generation was started by addition of thrombin to a solution of purified human fibrinogen at increasing [β2GpI] and monitored by turbidimetry at 350nm. The resulting clotting curves were analyzed to extract the values of ΔA_{max}, t_{max}, t_c, and $\Delta t_c = t_c - t_\infty$, where ΔA_{max} is the maximum slope of the clotting curve, t_{max} is the time needed to reach ΔA_{max}, t_c (i.e. the clotting time) is the lag-time and t_∞ is the value that assumes t_c at [Thrombin]→∞ (21). The value of t_∞ was calculated as 33 ± 4 sec and found identical to that previously determined, t_∞ = 32.5 ± 1.4sec (18). Of note, t_{max} and t_c are correlated quantities: $t_{max} = 26.4 + 1.11 \cdot t_c$ (21).

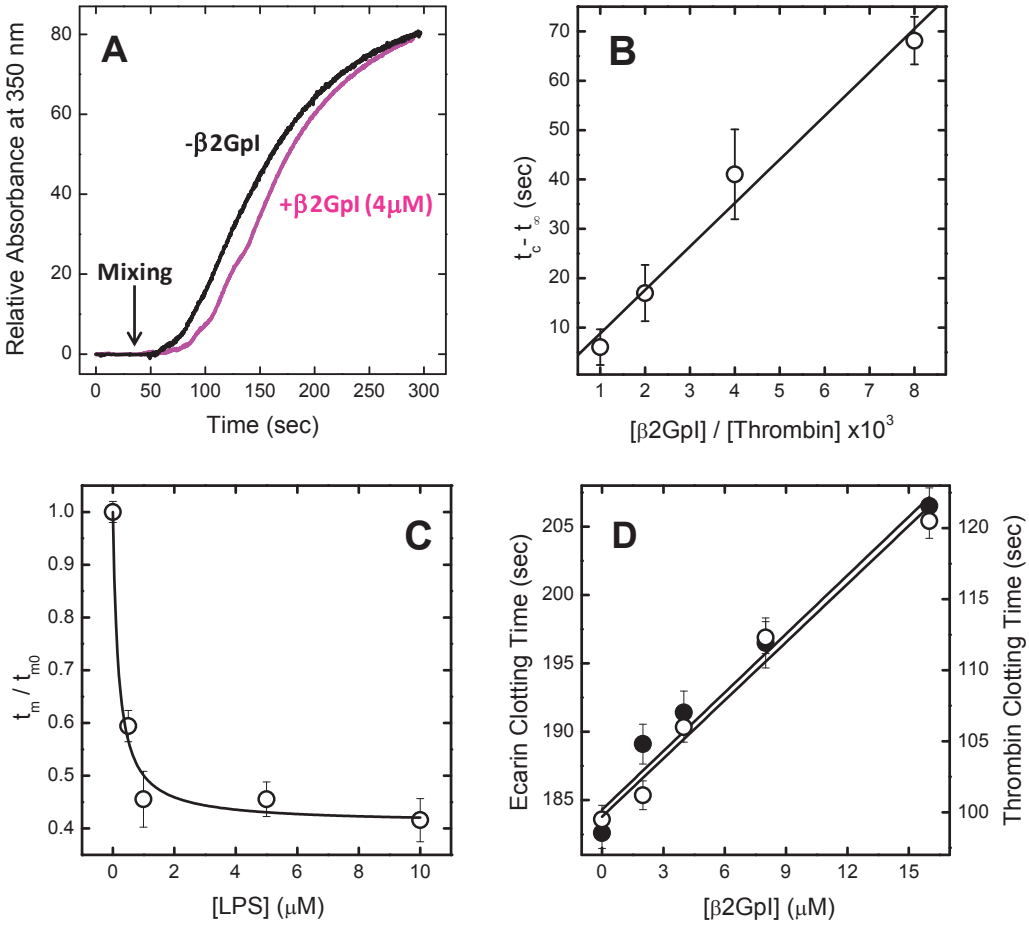

Figure 2.8 Effect of β2GpI on fibrin generation (A) Representative clotting curves for the generation of fibrin in the absence and presence of β2GpI. To a human fibrinogen solution (0.44μM) in HBS at 37°C was added plasma thrombin (1nM), with or without β2GpI (4μM) and the increase in turbidity ($Abs_{350\ nm}$) was recorded over time. **(B)** Plot of $\Delta t = t_c - t_\infty$ as a function of [β2GpI]/[thrombin] ratio. The concentration of β2GpI is kept constant at 4μM while thrombin concentration is varied in the 0.5-4nM range. **(C)** Effect of [LPS] on fibrin generation. Reaction was started by addition of thrombin (1nM) in the presence of β2GpI (4μM). The t_{max}/t^0_{max} ratio is plotted as a function of [LPS], where t^0_{max} is the value of t_{max} at [LPS] = 0. **(D)** Effect of β2GpI on ECT (●) and TCT (○) in β2GpI-deficient plasma. Increasing concentrations of β2GpI were added to diluted (1:1 in TBS) β2GpI-deficient plasma samples (100μl) and the clotting time was determined by measuring the absorbance at 671 nm from the addition of ecarin (0.25 EU/ml) or human thrombin (0.5 NIH units/ml).

Our data show that addition of a physiological concentration of β_2GpI to the clotting reaction significantly prolonged t_c (Fig. 2.8A), compared to thrombin alone, and that Δt_c increases linearly by increasing the [β_2GpI]/[thrombin] ratio (Fig. 2.8B). Interestingly, the data in Fig. 2.8C indicate that bacterial LPS dose-dependently opposed the effect of β_2GpI by reducing t_{max} by 60%. Finally, the data obtained with isolated fibrinogen favourably correlate with ecarin (ECT) and thrombin clotting time (TCT) measurements carried out on β_2GpI-deficient plasma (Fig. 2.8D).

β2GpI Hinders Thrombin-Induced Platelet Aggregation by Inhibiting PAR-1 Hydrolysis

Turbidimetric measurements (Fig. 2.9A, 2.9B) indicate that β2GpI inhibits aggregation of gel-filtered platelets with $IC_{50} = 0.36 \pm 0.1\mu M$. A similar IC_{50} value of $0.32 \pm 0.1\mu M$ was obtained by immunocytofluorimetric determination of PAR-1 cleavage on gel-filtered platelets (Fig. 2.9C).

The effect of β2GpI on platelet aggregation was also determined on whole blood, by Multiple Electrode Aggregometry (MEA) (29) (Fig. 2.9D). MEA exploits the increase of electric impedance measured in the measure cell and proportional to the amount of platelets sticking on the electrodes. Our data indicate that β_2GpI dose-dependently inhibits platelet aggregation in whole blood and that this effect is partially opposed by LPS. Notably, IC_{50} values estimated from MEA curves on whole blood are approximately ten-fold lower than those obtained with gel-filtered platelets. Likely, this is predominantly caused by the intrinsic higher sensitivity of platelets in whole blood (29) and to a minor extent by the contribution of fibrin generation to the increase of the measured electric impedance. In the presence of 80μM LPS (Fig. 2.9E) the inhibitory effect of β2GpI on platelet aggregation was partially reversed. This finding is consistent with recent results showing that LPS binds β2GpI domain V (6) and therefore can impair the β2GpI-thrombin interaction.

Finally, the inhibitory effect of β2GpI on PAR-1 cleavage was explored with the synthetic peptide PAR-1(38-60), chemically synthesized by solid phase techniques. With 1 μM β2GpI, a concentration four-fold lower than that found *in vivo* (1, 2), the efficiency of PAR-1(38-60) hydrolysis is almost halved (Fig. 2.9F).

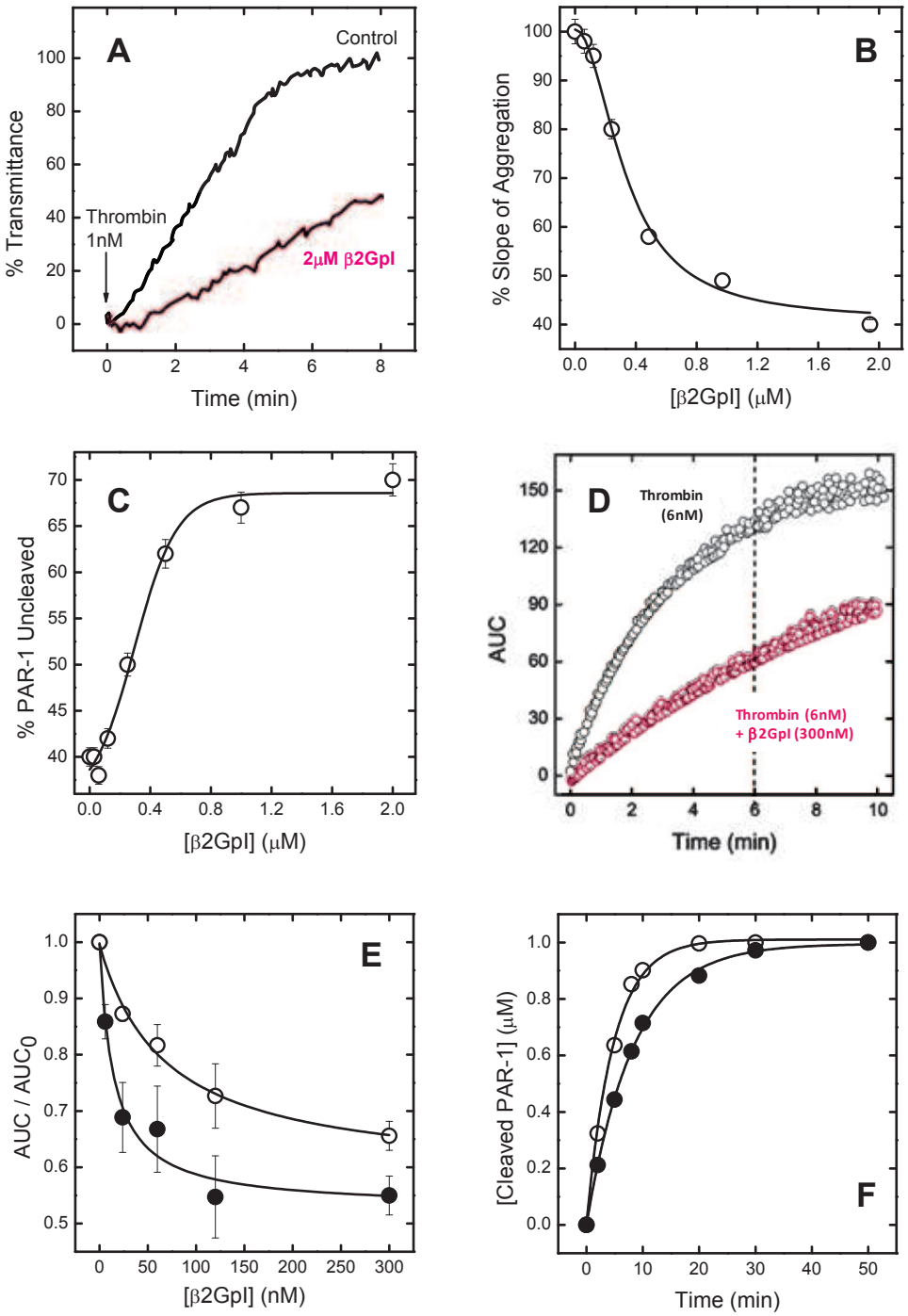

Figure 2.9 Inhibition of thrombin-induced platelet aggregation and PAR-1 hydrolysis by β2GpI
(A-B) Gel-filtered platelets (220000/μl) in HBS were activated at 37°C with human thrombin (1nM) and the change in transmittance at 350 nm with time **(A)** was recorded to determine the rate (v) of platelet aggregation **(B)** Data fitting yields IC_{50} = 0.36 ± 0.1μM. **(C)** Inhibition of thrombin-induced PAR-1 hydrolysis by β2GpI on intact platelets. Gel-filtered platelets (10000/μl) were activated at 37°C with human thrombin (0.2nM) in the presence of β_2GpI. Uncleaved PAR-1 was quantified by immuno-cytofluorometry, adding saturating amounts (2 μg) of SPAN12 mAb which selectively recognizes intact PAR-1. Data fitting yields IC_{50} = 0.32 ± 0.1μM. **(D-E)** Effect of β2GpI on platelet aggregation on whole blood **(D)**, induced by addition of thrombin (6nM), in the presence (○) or in the absence (●) of LPS (80μM) **(E)**. The data are expressed as the AUC/AUC_0 ratio, where AUC_0 is the Area Under the aggregation Curve at [β2GpI]=0. **(F)** Time-course cleavage of PAR-1(38-60) peptide by thrombin(0.1nM) in the absence (●) and in the presence (○) of β2GpI (1μM) at 25°C. The release of PAR-1(42-60) was quantified by RP-HPLC. The data were analyzed with the pseudo-first order kinetic model and the values of k_{cat}/K_m were calculated as 35.8 ± 0.1 and 19.7 ± 0.1 μM^{-1} s^{-1} in the absence and presence of 1μM β2GpI, respectively. The error on the quantification of cleaved PAR1 was <5%.

β2GpI Does Not Influence PC Activation by Thrombin

The effect of physiological concentrations of β2GpI on activated PC (aPC) generation was investigated in the absence or presence of TM (Fig. 2.10). Without TM, β2GpI does not alter, or even slightly enhances (by 3-fold) the efficiency with which thrombin hydrolyses PC. With TM, the efficiency of aPC generation is dramatically increased, as expected (9), but in the presence of the cofactor the effect of β2GpI is negligible. The slight increase of k_{cat}/K_m observed with β2GpI likely reflects the widening of thrombin active site that might be induced allosterically by interaction of β2GpI with exosite-I, as already observed with other exosite-I binders (7, 30). With TM, this enhancing effect is masked by the overwhelming affinity of the co-factor for thrombin, compared to that of β2GpI.

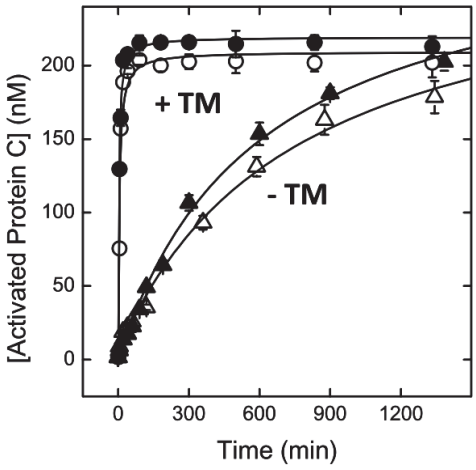

Figure 2.10 Effect of β2GpI on the generation of aPC by thrombin in the presence or absence of thrombomodulin. Effect of β_2GpI on PC activation with (○,●) or without (Δ,▲) TM. To a solution of PC (200nM) was added human thrombin (5nM) in the absence (Δ) or in the presence (▲) of β2GpI (4μM) at 37°C. Under conditions of pseudo-first reaction, the values of k_{cat}/K_m and $[aPC]_\infty$ were determined as follows: -β2GpI, $k_{cat}/K_m = 0.30 \pm 0.2\ mM^{-1}\cdot s^{-1}$ and $[aPC]_\infty = 194 \pm 9$ nM; +β2GpI, $k_{cat}/K_m = 1.00 \pm 0.2\ mM^{-1}\cdot s^{-1}$ and $[aPC]_\infty = 213 \pm$ 2n M. The effect of β2GpI on PC activation in the presence of 50nM TM (○,●) was determined as above, with [thrombin] = 10nM: -β2GpI, $k_{cat}/K_m = 215 \pm 1\ mM^{-1}\cdot s^{-1}$ and $[aPC]_\infty = 202 \pm 3$nM; +β2GpI, $k_{cat}/K_m = 280 \pm 3mM^{-1}\cdot s^{-1}$ and $[aPC]_\infty = 212 \pm 5$nM.

DISCUSSION

β2GpI Function as an Anticoagulant Protein

β2GpI was described for the first time about 50 years ago and since that time no clear physiological function has been identified for this protein (1, 3). The results of these study provide experimental evidence that β2GpI may function as an anticoagulant protein. In fact, it inhibits key procoagulant activities of thrombin *in vitro*, such as fibrin generation (Fig. 2.8) and platelet aggregation either (Fig. 2.9), without affecting its unique anticoagulant function,

i.e. PC activation (Fig. 2.10). In particular, β2GpI dose-depend impairs thrombin-mediated generation of fibrin from purified fibrinogen (Fig. 2.8A, 2.8B) or from β2GpI-deficient plasma, as shown by the significant prolongation of the clotting time observed after the addition of fully active thrombin in the TCT assay or the direct prothrombin activator ecarin in the ECT assay (Fig. 2.8D) Likewise, β2GpI inhibits the thrombin-induced aggregation of platelets, by impairing thrombin cleavage of PAR-1 (Fig. 2.9C, 2.9F), either when they are isolated from blood by gel filtration (Fig. 2.9B) or when they are in the complex matrix of whole blood (Fig. 2.9E). It is noteworthy that β2GpI binding is specific for the newly generated active thrombin, and does not involve the inactive zymogene ProT or FXa, the protease immediately upstream in the coagulation cascade (Fig. 2.6A).

Mechanism of B2GpI-Thrombin Interaction

Using several different molecular probes, we have demonstrated that β2GpI affects thrombin functions by binding to protease exosites, while leaving the active site accessible (Fig. 2.4, 2.5, 2.6). The picture of β2GpI-thrombin interaction derived from experimental data is fully compatible with the theoretical model of the β2GpI-thrombin complex shown in Fig. 2.11. The model shows a clear geometric and electrostatic complementarity between the positively charged exosites of thrombin and the large negatively charged surface distributed over the concave face of β2GpI, within domains DIII, DIV and DV (15 Asp+Glu). Notably, DV has an asymmetric charge distribution, with a negative region (6 Asp+Glu) on the upper face pointing towards thrombin exosite-I and a positive region (9 Lys+Arg) on the lower face, amenable to interact with negatively charged surfaces (phospholipid membranes and LPS) (1, 6). Importantly, the model shows that thrombin active site is fully accessible for substrate/ligand binding after β2GpI binding.

In addition, the binding of β2GpI to thrombin appears to be in part salt-dependent (Fig. 2.7). The value of Γ_{salt} (i.e. -2.36 ± 0.15) exceeds the values reported for fibrinogen and hirudin (19) and signals a electrostatic contribution to the binding of β2GpI to thrombin. Moreover, it is likely that a minimum of two-three ionic bonds are involved in this interaction.

SPR data show that ligand saturation of a specific thrombin exosite does not completely abolish binding of β2GpI, with a significant residual signal being still measurable (Fig. 2.5A, 2.5B, 2.5C). Nevertheless, the concomitant saturation of both exosites with hirugen and γ′-peptide completely abrogates binding (Fig. 2.5B). Likewise, structural perturbation of exosite-I in Pre2 (31) results in a 7-8 fold decrease in affinity (Fig. 2.6A,

2.6B), whereas inactivation of both exosites, as in ProT (7) and β_T-thrombin (17, 28), almost completely abrogates interaction (Fig. 2.6A). These results can be interpreted according to a dynamic binding model in which the conformationally flexible β2GpI molecule (1, 4-6) exploits different sites on DIII, DIV and DV domains to interact with exosite-I and -II on thrombin surface (Fig. 2.11) and suggest that the strong affinity measured for β2GpI binding to thrombin (K_d = 34nM; ΔG_b= -10.6 kcal/mol) is distributed over several different interacting sites and it is fully expressed only when both thrombin exosites are available for binding. According to the model, in fact, when one of the two exosites is already occupied by a given ligand present in solution, β2GpI can still interact with thrombin, albeit with lower affinity, at the other exosite available on the protease surface to form a ternary complex. Hence, the binding properties of β2GpI can be dynamically regulated by the specificity and affinity of the ligand that can contact thrombin at either one of the two exosites. This simple model explains why β2GpI hinders binding of ligands displaying moderate affinity for exosite-I like fibrinogen (Kd = 1.1μM) (30) (Fig. 2.8), whereas it is not able to compete with a much stronger exosite-I binder like TM (Kd = 0.5nM) (9) (Fig. 2.8).

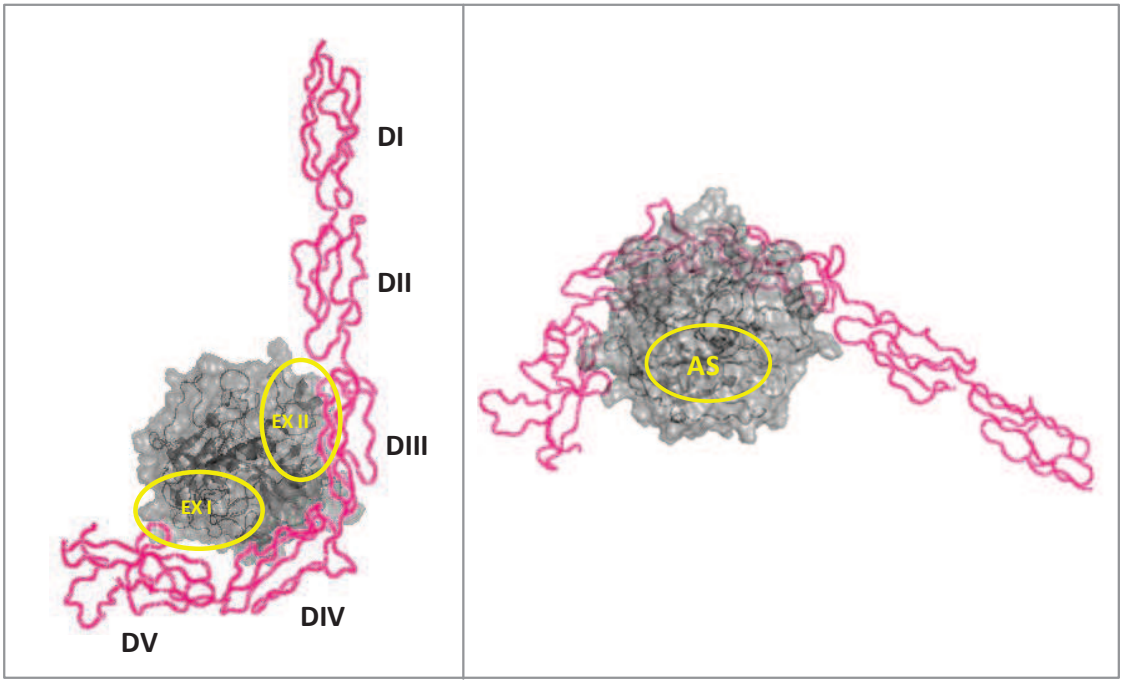

Figure 2.11 Theoretical Model of β2GpI-thrombin interaction. The docking model was obtained using the HEX software, starting from the coordinates of isolated β_2GpI (1C1Z.pdb) and thrombin (1PPB.pdb). β_2GpI is shown as a ribbon drawing (pink) while thrombin is shown as an surface (grey). The approximate position of active site, exosite-I and -II on thrombin surface is indicated in yellow.

In this study a collection of thrombin mutants was used to provide a structural mapping of the key residues involved in the thrombin-β2GpI binding. Our results indicated that the point mutations at exosite-I or exosite-II, involving positive charged amino acid residue (Arg→Ala, Lys→Ala), are not sufficient for hinder the interaction. However, if a negatively charged amino acid is replaced (Asp→Ala) the affinity changes drastically (Fig. 2.5E). Perhaps, the loss of the negative charge Asp178 is more significant than the deficiently of a positive charge residue, because thrombin has an extensive electropositive surface area (200 $Å^2$) whose residues are well exposed to the solvent. So, the lack of Arg or Lys can be compensated by other positively charged residues, localized principally at the level of exosites. This may be in agreement with the demonstrated salt-dependency in the formation of thrombin-β2GpI complex.

Effect of β2GpI on Coagulation

As expected from the involvement of exosite-I in thrombin-β2GpI interaction (Fig. 2.5) β2GpI inhibits hydrolysis of those procoagulant substrates, like fibrinogen (Fig. 2.6) and PAR-1 (Fig. 2.9C, 2.9F), that use exosite-I as a hot spot for binding to thrombin (30). Likewise, participation of exosite-II in β2GpI binding (Fig. 2.5) highlights the possibility that β2GpI hinders exosite-II mediated anchoring of thrombin on its platelet receptor GpIbα (11, 12) with a resulting inhibition of platelet aggregation, as shown in Fig. 2.9. Notably, the data also indicate that β2GpI does not fully impair platelet aggregation, even at the highest concentrations tested. Probably this effect arises from the presence on platelet surface of PAR-4 a receptor that, contrary to PAR-1, is cleaved by thrombin independently of exosite binding (30). Importantly, both experimental and theoretical data herein reported seem to indicate that β2GpI binds to thrombin without covering the catalytic site. This distinctive feature of β2GpI-thrombin interaction is fully consistent with the observation that β2GpI does not alter the efficiency with which thrombin hydrolyses PC (Fig. 2.10), a zymogen which is known to interact with the thrombin exclusively at its active site (32).

Our data show that β2GpI is quite specific for active α-thrombin and does not bind neither to ProT nor to FXa (Fig. 2.6A), the serine protease immediately upstream to thrombin in the coagulation cascade. This effect likely arises from the markedly different distribution of surface charges in the two enzymes (28). Like thrombin, FXa has a positively charged exosite-II, although more dispersed than the corresponding patch on thrombin. Conversely, the region on FXa topologically equivalent to exosite-I on thrombin, is highly negative and

this might cause electrostatic repulsion with the negative surface on β2GpI. Additional results indicate that bacterial LPS seem to oppose the inhibitory effects of β2GpI on fibrin generation (Fig. 2.8C) and platelet aggregation on whole blood (Fig. 2.9E). β2GpI has been recently shown to act as a scavenger of LPS, which tightly binds (Kd = 62nM) to β2GpI domain V (6). Hence, we speculate that the effect of LPS on β2GpI function results from masking/alteration of β2GpI binding sites for thrombin.

To address the possible role of β2GpI in the regulation of haemostasis *in vivo*, one should consider that the haemostatic process is the result of a delicate equilibrium between opposing procoagulant and anticoagulant systems, variably operating in different vascular compartments (e.g. large vessels and capillaries). Down-regulation of blood coagulation is accomplished mainly on the vascular endothelium by tissue factor pathway inhibitor (TFPI), heparin-like proteoglycans (HP), and TM. TFPI acts in the initiation phase, whereas HP and TM function in the attenuation-phase of blood coagulation (33). In the macrovasculature, where the concentration of TM is too low (0.2nM) for efficient PC activation, thrombin inhibition is mainly exerted by the HP-antithrombin III system. In the microvasculature, instead, where the concentration of TM increases up to 300nM, due to the higher surface/volume ratio of the capillaries compared to large vessels (34), the major anticoagulant function is accomplished by TM. Endothelial cell-bound TM interacts with thrombin exosite-I and shifts the substrate specificity of the protease by preventing binding of fibrinogen and PAR-1. In addition, TM dramatically enhances thrombin activation of PC by bringing thrombin and PC close together and inducing conformational changes both in the protease and substrate (9, 33). Intriguingly, while present on most endothelial cells, TM is absent in the vasculature of human brain (35).

All these considerations and the high plasma concentration of β2GpI (up to 10μM ~ 0.5 mg/ml) (1) allow us to speculate that under physiological conditions β2GpI may function as a plasma-soluble anticoagulant protein acting in those vascular compartments where the more potent TM-thrombin pathway poorly functions, as in the large vessels, or is even absent, as in the brain vasculature. Further, indirect support to our proposal is given by clinical studies showing that significantly reduced β2GpI levels are found in patients with stroke and in elderly patients with thrombotic disorders (36), whereas high circulating levels of β2GpI appear to be associated with a reduced risk of myocardial infarction (37). In addition, there is a positive correlation between the presence of auto-antibodies against β2GpI and thrombotic manifestations in APS patients (1, 3).

In conclusion, the results herein reported highlight the unique anticoagulant properties of β2GpI, selectively inhibiting the procoagulant functions of thrombin without altering its anticoagulant activity. These findings are unprecedented and pave the way to the discovery of a novel physiological anticoagulant pathway.

REFERENCES

1. de Groot, P.G., and Meijers, J.C. (2011) beta(2) -Glycoprotein I: evolution, structure and function. *J.Thromb.Haemost.* 9, 1275-1284
2. McNally, T., Cotterell, S.E., Mackie, I.J., Isenberg, D.A., and Machin, S.J. (1994) The interaction of beta 2 glycoprotein-I and heparin and its effect on beta 2 glycoprotein-I antiphospholipid antibody cofactor function in plasma. *Thromb.Haemost.* 72, 578-581
3. Miyakis, S., Robertson, S.A., and Krilis, S.A. (2004) Beta-2 glycoprotein I and its role in antiphospholipid syndrome-lessons from knockout mice. *Clin.Immunol.* 112, 136-143
4. Schwarzenbacher, R., Zeth, K., Diederichs, K., Gries, A., Kostner, G.M., Laggner, P., and Prassl, R. (1999) Crystal structure of human beta2-glycoprotein I: implications for phospholipid binding and the antiphospholipid syndrome. *EMBO J.* 18, 6228-6239
5. Hammel, M., Kriechbaum, M., Gries, A., Kostner, G.M., Laggner, P., and Prassl, R. (2002) Solution structure of human and bovine beta(2)-glycoprotein I revealed by small-angle X-ray scattering. *J.Mol.Biol.* 321, 85-97
6. Agar, C., van Os, G.M., Morgelin, M., Sprenger, R.R., Marquart, J.A., Urbanus, R.T., Derksen, R.H., Meijers, J.C., and de Groot, P.G. (2010) Beta2-glycoprotein I can exist in 2 conformations: implications for our understanding of the antiphospholipid syndrome. *Blood.* 116, 1336-1343
7. Bode, W., and Huber, R. (1992) Natural protein proteinase inhibitors and their interaction with proteinases. *Eur.J.Biochem.* 204, 433-451
8. Di Cera, E. (2007) Thrombin as procoagulant and anticoagulant. *J.Thromb.Haemost.* 5 Suppl 1, 196-202
9. Esmon, C.T. (2003) The protein C pathway. *Chest.* 124, 26S-32S
10. Huntington, J.A. (2005) Molecular recognition mechanisms of thrombin. *J.Thromb.Haemost.* 3, 1861-1872
11. De Candia, E., Hall, S.W., Rutella, S., Landolfi, R., Andrews, R.K., and De Cristofaro, R. (2001) Binding of thrombin to glycoprotein Ib accelerates the hydrolysis of Par-1 on intact platelets. *J.Biol.Chem.* 276, 4692-4698

12. De Cristofaro, R., and De Filippis, V. (2003) Interaction of the 268-282 region of glycoprotein Ibalpha with the heparin-binding site of thrombin inhibits the enzyme activation of factor VIII. *Biochem.J.* 373, 593-601
13. Rahgozar, S., Giannakopoulos, B., Yan, X., Wei, J., Cheng Qi, J., Gemmell, R., and Krilis, S.A. (2008) Beta2-glycoprotein I protects thrombin from inhibition by heparin cofactor II: potentiation of this effect in the presence of anti-beta2-glycoprotein I autoantibodies. *Arthritis Rheum.* 58, 1146-1155
14. Lancellotti, S., Rutella, S., De Filippis, V., Pozzi, N., Rocca, B., and De Cristofaro, R. (2008) Fibrinogen-elongated gamma chain inhibits thrombin-induced platelet response, hindering the interaction with different receptors. *J.Biol.Chem.* 283, 30193-30204
15. De Filippis, V., Vindigni, A., Altichieri, L., and Fontana, A. (1995) Core domain of hirudin from the leech Hirudinaria manillensis: chemical synthesis, purification, and characterization of a Trp3 analog of fragment 1-47. *Biochemistry.* 34, 9552-9564
16. Pozzi, N., Banzato, A., Bettin, S., Bison, E., Pengo, V., and De Filippis, V. (2010) Chemical synthesis and characterization of wild-type and biotinylated N-terminal domain 1-64 of beta2-glycoprotein I. *Protein Sci.* 19, 1065-1078
17. Hofsteenge, J., Braun, P.J., and Stone, S.R. (1988) Enzymatic properties of proteolytic derivatives of human alpha-thrombin. *Biochemistry.* 27, 2144-2151
18. Marino, F., Pelc, L.A., Vogt, A., Gandhi, P.S., and Di Cera, E. (2010) Engineering thrombin for selective specificity toward protein C and PAR1. *J.Biol.Chem.* 285, 19145-19152
19. Li, C.Q., Vindigni, A., Sadler, J.E., and Wardell, M.R. (2001) Platelet glycoprotein Ib alpha binds to thrombin anion-binding exosite II inducing allosteric changes in the activity of thrombin. *J.Biol.Chem.* 276, 6161-6168
20. Olson, S.T., Halvorson, H.R., and Bjork, I. (1991) Quantitative characterization of the thrombin-heparin interaction. Discrimination between specific and nonspecific binding models. *J.Biol.Chem.* 266, 6342-6352
21. De Cristofaro, R., and Di Cera, E. (1991) Phenomenological analysis of the clotting curve. *J.Protein Chem.* 10, 455-468
22. De Filippis, V., De Dea, E., Lucatello, F., and Frasson, R. (2005) Effect of Na+ binding on the conformation, stability and molecular recognition properties of thrombin. *Biochem.J.* 390, 485-492

23. Birdsall, B., King, R.W., Wheeler, M.R., Lewis, C.A.,Jr, Goode, S.R., Dunlap, R.B., and Roberts, G.C. (1983) Correction for light absorption in fluorescence studies of protein-ligand interactions. *Anal.Biochem.* 132, 353-361
24. Pozzi, N., Barranco-Medina, S., Chen, Z., and Di Cera, E. (2012) Exposure of R169 controls protein C activation and autoactivation. *Blood.* 120, 664-670
25. Arosio, D., Ayala, Y.M., and Di Cera, E. (2000) Mutation of W215 compromises thrombin cleavage of fibrinogen, but not of PAR-1 or protein C. *Biochemistry.* 39, 8095-8101
26. Ritchie, D.W., and Venkatraman, V. (2010) Ultra-fast FFT protein docking on graphics processors. *Bioinformatics.* 26, 2398-2405
27. Evans, S.A., Olson, S.T., and Shore, J.D. (1982) p-Aminobenzamidine as a fluorescent probe for the active site of serine proteases. *J.Biol.Chem.* 257, 3014-3017
28. Bianchini, E.P., Pike, R.N., and Le Bonniec, B.F. (2004) The elusive role of the potential factor X cation-binding exosite-1 in substrate and inhibitor interactions. *J.Biol.Chem.* 279, 3671-3679
29. Toth, O., Calatzis, A., Penz, S., Losonczy, H., and Siess, W. (2006) Multiple electrode aggregometry: a new device to measure platelet aggregation in whole blood. *Thromb.Haemost.* 96, 781-788
30. Huntington, J.A. (2005) Molecular recognition mechanisms of thrombin. *J.Thromb.Haemost.* 3, 1861-1872
31. Pozzi, N., Chen, Z., Zapata, F., Pelc, L.A., Barranco-Medina, S., and Di Cera, E. (2011) Crystal structures of prethrombin-2 reveal alternative conformations under identical solution conditions and the mechanism of zymogen activation. *Biochemistry.* 50, 10195-10202
32. Pozzi, N., Chen, R., Chen, Z., Bah, A., and Di Cera, E. (2011) Rigidification of the autolysis loop enhances Na(+) binding to thrombin. *Biophys.Chem.* 159, 6-13
33. Hoffman, M., and Monroe, D.M. (2007) Coagulation 2006: a modern view of hemostasis. *Hematol.Oncol.Clin.North Am.* 21, 1-11
34. Esmon, C.T., and Esmon, N.L. (2011) The link between vascular features and thrombosis. *Annu.Rev.Physiol.* 73, 503-514
35. Ishii, H., Salem, H.H., Bell, C.E., Laposata, E.A., and Majerus, P.W. (1986) Thrombomodulin, an endothelial anticoagulant protein, is absent from the human brain. *Blood.* 67, 362-365

36. Lin, F., Murphy, R., White, B., Kelly, J., Feighery, C., Doyle, R., Pittock, S., Moroney, J., Smith, O., Livingstone, W., Keenan, C., and Jackson, J. (2006) Circulating levels of beta2-glycoprotein I in thrombotic disorders and in inflammation. *Lupus.* 15, 87-93
37. de Laat, B., Pengo, V., Pabinger, I., Musial, J., Voskuyl, A.E., Bultink, I.E., Ruffatti, A., Rozman, B., Kveder, T., de Moerloose, P., Boehlen, F., Rand, J., Ulcova-Gallova, Z., Mertens, K., and de Groot, P.G. (2009) The association between circulating antibodies against domain I of beta2-glycoprotein I and thrombosis: an international multicenter study. *J.Thromb.Haemost.* 7, 1767-1773

This chapter was adapted from: Pozzi, N., **Acquasaliente, L.***, Frasson, R., Cristiani, A., Moro, S., Banzato, A., Pengo, V., Scaglione, G.L., Arcovito, A., De Cristofaro, R., and De Filippis, V. (2013) beta2-Glycoprotein I Binds Thrombin and Selectively Inhibits the Enzyme Procoagulant Functions. J.Thromb.Haemost. 11, 1093-1102.*

CHAPTER 3.1

α-Synuclein

α-synuclein (α-Syn) is a small (14.5 kDa, 140 amino acids) soluble presynaptic protein that is highly conserved in vertebrates and has been implicated in different neurodegenerative disorders, called "synucleinopathies". These disorders include, among others, Parkinson's disease (PD) and Alzheimer's disease (AD). PD is the most common movement disorder, whereas AD is the most common form of dementia (1). PD is characterized by eosinophilic cytoplasmatic inclusion, called Lewy bodies (LB), found in dopaminergic neurons of the substantia nigra and composed of α-Syn extensively ubiquitinylated (2). AD is characterized by intracellular neurofibrillary tangles that are composed of the hyperphosphorylated protein τ and extracellular β-amyloid plaques (3). It was reported that the central region of α-Syn, known as the non Aβ component of amyloid plaques, seems to be responsible for its aggregation process in the neurodegenerative status. In fact, the term "synucleinopathies" was introduced after found filamentous α-syn deposits (4).

Structure and Conformational Properties of α-Synuclein: a Protein Chameleon

α-synuclein is a small highly acidic natively unfolded protein that is abundantly expressed in the brain, where it is concentrated in presynaptic nerve terminals (5). Its primary sequence can be divided into three regions (Fig. 3.1). The N-terminal region (residues 1–60) includes 7 imperfect 11-residues repeats, each containing a highly conserved hexameric motif (KTKEGV) necessary to form amphipathic α-helices, typical of the lipid-binding domain of apolipoproteins (6). The central region (residues 61–95) comprises the non Aβ component of amyloid (NAC) sequence that seems to be responsible for the ability of α-Syn to form a single cylindrical β-sheet and to form Aβ-like protofibrils and fibrils (1, 5). The C-terminal region (residues 96–140), instead, is extremely enriched in acidic residues and prolines.

α-Syn is a typical intrinsically disordered (or natively unfolded) protein, which possesses little or no ordered structure under physiological conditions *in vitro* (7). These proteins have recently been recognized as a new protein class, due to their capacity to perform numerous biological functions although the lack of unique structure. In fact, intrinsically

disordered proteins exist as dynamic and highly flexible ensembles that undergo a number of distinct inter conversions on different timescales. Recent studies, obtained by small angle X-ray scattering, shown that α-Syn has a radius of gyration of ~40 Å, larger than that predicted for a folded globular protein of 140 residues (i.e. 15Å), but significantly smaller than that for a fully unfolded random coil (i.e. 52 Å). In fact, a high-resolution NMR analysis reveled that α-Syn is largely unfolded in aqueous solutions, but exhibits a region between residues 6 and 37 (N-terminal lipid - binding domain) with a preference for helical conformation (8, 9).

Nevertheless the structure of α-Syn is extremely sensitive to its environment and can be easily modulated by a change in conditions. α-Syn can acquire a pre-molten globule state in several conditions such as low pH, high temperature and presence of metal ions (4, 7). In organic solvent the protein forms α-helical species (10), as well as in the presence of synthetic lipid vesicles and detergent micelles (11). Upon binding to negatively charged surface, the N-terminal domains adopts a highly helical structure (extended-helix state), instead the micelle-bound form of α-Syn consists of two non-contacting antiparallel helices in the N-terminal region, with a short-break around residues 38-44 and a flexible conformation in the C-terminal domain (broken-helix state) (Fig. 3.2) (12). α-Syn can form several morphologically different types of aggregates, including dimers, oligomeric protofibrillar species and insoluble amorphous aggregates. Hence, the conformational/functional properties of the protein are highly environment-dependent and therefore α-synuclein is now regarded as a protein-chameleon (4).

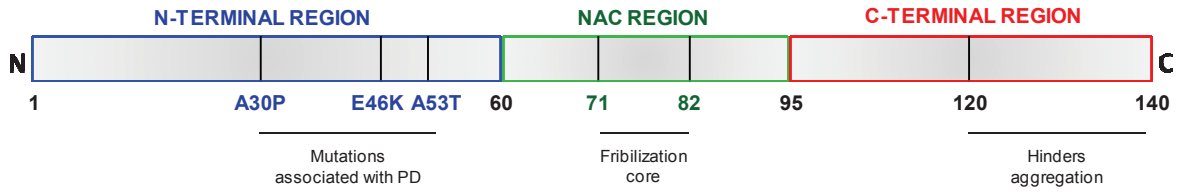

Figure 3.1 Schematic representation of the primary structure of α-Syn. The three different regions that compose the protein are indicated. The N-terminal amphipathic region (in blue) contains most of the repeats and the three point mutations linked to autosomal dominant early-onset PD. The central region (NAC) (in green), which encompasses the most hydrophobic residues, promotes aggregation, while the acidic C-terminal portion (in red) of the protein tends to decrease protein aggregation.

Physiological Functions of α-Synuclein

Presently the normal function of α-synuclein remains poorly understood, although numerous biological roles and possible interactions have been proposed for this protein. α-

Syn has been estimated to account for as much as 1% of total protein in soluble cytosolic brain fractions and has been linked with synaptic plasticity (13), learning (14) and maintenance of synaptic vesicle pools (15). Indeed, the protein is involved in the vesicular transport: α-Syn knockout mice exhibit enhanced dopaminergic release at nigro striatal terminals only in response to paired electrical stimuli, suggesting that it is an activity-dependent, negative regulator of dopaminergic neurotransmission (16). In addition, some studies reveal that α-Syn regulates catecholamine release from the synaptic vesicles, and its over-expression inhibits a vesicle 'priming' step that occurs after secretory vesicle trafficking to 'docking' sites but before calcium-dependent vesicle membrane fusion (17).

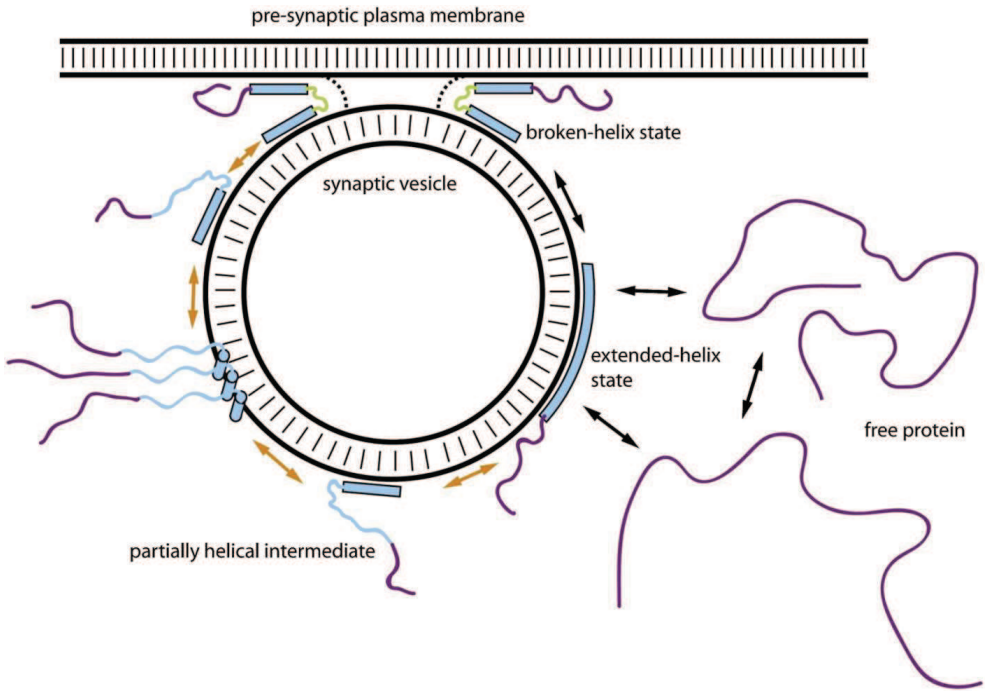

Figure 3.2 Different tridimensional organization of α-synuclein. Structured protein regions are depicted as solid lines (in violet), while helical regions are depicted as filled bars or cylinders (in light blue). Membrane bilayers are indicated as double black lines with hashes. The unbound, intrinsically disordered state of α-Syn is depicted as existing in equilibrium between less compact and more compact conformations, which are also in equilibrium with the vesicle-bound extended-helix state. The latter can convert to the broken-helix state upon approach of the vesicle to another membrane, such as the pre-synaptic plasma membrane. Transitions between these conformations are indicated by black double arrows. The potential activity of the broken helix state in modulating membrane properties during membrane fusion is indicate by the green color of the linker region and the dotted lines between the vesicle and plasma membranes. Either the extended- or broken-helix states may be able to convert to a membrane-bound partially helical intermediate by the release of the C-terminal region of the lipid-binding domain from the membrane surface. Intermolecular association of these intermediates, driven by the membrane-associated N-terminal helices, may bring the disordered regions into close proximity, facilitating intermolecular β-sheet formation leading to amyloid oligomer and fibril formation. These transitions, which are considered to occur as part of the pathological behavior of α-Syn, are indicated by orange double arrows. This figure was adapted from (12).

Other studies have proposed a putative function of α-Syn as a chaperone protein, based on its abundance in the cytosol, its natively unfolded structure, and its prevention of protein aggregation induced by heat shock or chemical treatment (18). *In vivo* the protein can protect the nerve terminals against injury via cooperation with cysteine string protein α (CSPα) and soluble N-ethylmaleimide sensitive factor (NSF) attachment receptor proteins on the presynaptic membrane interface (19).

α-Syn interacts stably with synthetic phospholipid vesicles containing negatively charged groups, phospholipid membrane, fatty acid and detergent micelles (4). It is proposed that α-Syn plays a role in modulating the organization of membrane lipid components: the protein, in the presence of negatively charged membrane of multilamellar vesicles, has a profound effect on the integrity of these bilayers, causing the formation of non-bilayer or small vesicular structures (20). Finally, it has been found that monomeric α-Syn bound to lipid membrane can prevent lipid oxidation (21).

α-Syn has been shown to interact with at least 50 proteins and other ligands (21, 22). The protein acts as a high affinity inhibitor of phospholipase D2, which catalyzes the hydrolysis of phosphatidylcholine to phosphatidic acid (23). These results suggest that α-Syn influences the membrane remodeling processes involved in vesicle fusion or budding. At last, α-Syn interacts whit several polyvalent metal cations including Fe^{2+}, Al^{3+}, Zn^{2+}, Cu^{2+}, Mg^{2+} and Ca^{2+} (4).

α-Synuclein in the Cardiovascular System

α-synuclein was ubiquitously expressed in various hematopoietic cells including T cells, B cells, NK cells and monocytes (24). Recent studies identify red blood cells as the major source of α-Syn (25). Almost all (> 99%) of the protein in blood is present in red blood cells; only minor amount were measured in peripheral blood mononuclear cells (0.05%) and platelets (0.2%) as well as in the plasma (0.1%). Nevertheless, if the amount of synuclein is normalized to the amount of cellular protein, platelets have the highest amount of α-Syn (i.e. 264 ± 36 α-syn/protein ng/ml for platelets, 131 ± 23 α-syn/protein ng/ml for red blood cells) (26). In addition immune-gold electron microscopy of platelets showed that α-syn is loosely associated with the plasma membrane, the endomembrane system and, occasionally, with the membrane of secretory α-granules. These findings suggest that the protein may play a critical role during hematopoietic cell differentiation and vesicle release (27). In this context, the hematopoietic system may be regarded as exceptional populations since expression of α-Syn

in adult stage has been demonstrated in some lineages, including lymphocytes and platelets (28).

It was reported that α-Syn functions as a negative regulator of Ca^{2+}-dependent α-granule release from human platelets (29), and that the protein can be able to penetrate in platelet only in the presence of NAC region, as well as in neuronal cells (30). Moreover, α-Syn play a role as a negative regulator in Weibel-Palade body exocytosis in endothelia cells (31). Clinical studies indicated that the incidence of ischemic stroke in patients with PD is lower than in controls, and platelet aggregation is also significantly decreased (32). In fact, it seems that the platelets from PD patients have defect in their secretory pathways: the intracytoplasmatic vacuoles are larger and contain numerous granular molecules around the open canalicular system (33). All these results suggest that α-synuclein functions might not be restricted to neurons.

REFERNCES

1. Bisaglia, M., Trolio, A., Tessari, I., Bubacco, L., Mammi, S., and Bergantino, E. (2005) Cloning, expression, purification, and spectroscopic analysis of the fragment 57-102 of human alpha-synuclein. *Protein Expr.Purif.* 39, 90-96
2. Goedert, M. (2001) Alpha-synuclein and neurodegenerative diseases. *Nat.Rev.Neurosci.* 2, 492-501
3. Selkoe, D.J. (2001) Alzheimer's disease: genes, proteins, and therapy. *Physiol.Rev.* 81, 741-766
4. Uversky, V.N. (2007) Neuropathology, biochemistry, and biophysics of alpha-synuclein aggregation. *J.Neurochem.* 103, 17-37
5. Ueda, K., Fukushima, H., Masliah, E., Xia, Y., Iwai, A., Yoshimoto, M., Otero, D.A., Kondo, J., Ihara, Y., and Saitoh, T. (1993) Molecular cloning of cDNA encoding an unrecognized component of amyloid in Alzheimer disease. *Proc.Natl.Acad.Sci.U.S.A.* 90, 11282-11286
6. Clayton, D.F., and George, J.M. (1998) The synucleins: a family of proteins involved in synaptic function, plasticity, neurodegeneration and disease. *Trends Neurosci.* 21, 249-254
7. Uversky, V.N., Li, J., and Fink, A.L. (2001) Evidence for a partially folded intermediate in alpha-synuclein fibril formation. *J.Biol.Chem.* 276, 10737-10744

8. Syme, C.D., Blanch, E.W., Holt, C., Jakes, R., Goedert, M., Hecht, L., and Barron, L.D. (2002) A Raman optical activity study of rheomorphism in caseins, synucleins and tau. New insight into the structure and behaviour of natively unfolded proteins. *Eur.J.Biochem.* 269, 148-156

9. Bertoncini, C.W., Jung, Y.S., Fernandez, C.O., Hoyer, W., Griesinger, C., Jovin, T.M., and Zweckstetter, M. (2005) Release of long-range tertiary interactions potentiates aggregation of natively unstructured alpha-synuclein. *Proc.Natl.Acad.Sci.U.S.A.* 102, 1430-1435

10. Munishkina, L.A., Phelan, C., Uversky, V.N., and Fink, A.L. (2003) Conformational behavior and aggregation of alpha-synuclein in organic solvents: modeling the effects of membranes. *Biochemistry.* 42, 2720-2730

11. Eliezer, D., Kutluay, E., Bussell, R.,Jr, and Browne, G. (2001) Conformational properties of alpha-synuclein in its free and lipid-associated states. *J.Mol.Biol.* 307, 1061-1073

12. Dikiy, I., and Eliezer, D. (2011) Folding and misfolding of alpha-synuclein on membranes. *Biochim.Biophys.Acta.*

13. Watson, J.B., Hatami, A., David, H., Masliah, E., Roberts, K., Evans, C.E., and Levine, M.S. (2009) Alterations in corticostriatal synaptic plasticity in mice overexpressing human alpha-synuclein. *Neuroscience.* 159, 501-513

14. George, J.M., Jin, H., Woods, W.S., and Clayton, D.F. (1995) Characterization of a novel protein regulated during the critical period for song learning in the zebra finch. *Neuron.* 15, 361-372

15. Murphy, D.D., Rueter, S.M., Trojanowski, J.Q., and Lee, V.M. (2000) Synucleins are developmentally expressed, and alpha-synuclein regulates the size of the presynaptic vesicular pool in primary hippocampal neurons. *J.Neurosci.* 20, 3214-3220

16. Abeliovich, A., Schmitz, Y., Farinas, I., Choi-Lundberg, D., Ho, W.H., Castillo, P.E., Shinsky, N., Verdugo, J.M., Armanini, M., Ryan, A., Hynes, M., Phillips, H., Sulzer, D., and Rosenthal, A. (2000) Mice lacking alpha-synuclein display functional deficits in the nigrostriatal dopamine system. *Neuron.* 25, 239-252

17. Larsen, K.E., Schmitz, Y., Troyer, M.D., Mosharov, E., Dietrich, P., Quazi, A.Z., Savalle, M., Nemani, V., Chaudhry, F.A., Edwards, R.H., Stefanis, L., and Sulzer, D. (2006) Alpha-synuclein overexpression in PC12 and chromaffin cells impairs catecholamine release by interfering with a late step in exocytosis. *J.Neurosci.* 26, 11915-11922

18. Souza, J.M., Giasson, B.I., Lee, V.M., and Ischiropoulos, H. (2000) Chaperone-like activity of synucleins. *FEBS Lett.* 474, 116-119

19. Chandra, S., Gallardo, G., Fernandez-Chacon, R., Schluter, O.M., and Sudhof, T.C. (2005) Alpha-synuclein cooperates with CSPalpha in preventing neurodegeneration. *Cell.* 123, 383-396
20. Madine, J., Doig, A.J., and Middleton, D.A. (2006) A study of the regional effects of alpha-synuclein on the organization and stability of phospholipid bilayers. *Biochemistry.* 45, 5783-5792
21. Zhu, M., Qin, Z.J., Hu, D., Munishkina, L.A., and Fink, A.L. (2006) Alpha-synuclein can function as an antioxidant preventing oxidation of unsaturated lipid in vesicles. *Biochemistry.* 45, 8135-8142
22. Dev, K.K., Hofele, K., Barbieri, S., Buchman, V.L., and van der Putten, H. (2003) Part II: alpha-synuclein and its molecular pathophysiological role in neurodegenerative disease. *Neuropharmacology.* 45, 14-44
23. Jenco, J.M., Rawlingson, A., Daniels, B., and Morris, A.J. (1998) Regulation of phospholipase D2: selective inhibition of mammalian phospholipase D isoenzymes by alpha- and beta-synucleins. *Biochemistry.* 37, 4901-4909
24. Shin, E.C., Cho, S.E., Lee, D.K., Hur, M.W., Paik, S.R., Park, J.H., and Kim, J. (2000) Expression patterns of alpha-synuclein in human hematopoietic cells and in Drosophila at different developmental stages. *Mol.Cells.* 10, 65-70
25. Li, Q.X., Campbell, B.C., McLean, C.A., Thyagarajan, D., Gai, W.P., Kapsa, R.M., Beyreuther, K., Masters, C.L., and Culvenor, J.G. (2002) Platelet alpha- and gamma-synucleins in Parkinson's disease and normal control subjects. *J.Alzheimers Dis.* 4, 309-315
26. Barbour, R., Kling, K., Anderson, J.P., Banducci, K., Cole, T., Diep, L., Fox, M., Goldstein, J.M., Soriano, F., Seubert, P., and Chilcote, T.J. (2008) Red blood cells are the major source of alpha-synuclein in blood. *Neurodegener Dis.* 5, 55-59
27. Hashimoto, M., Yoshimoto, M., Sisk, A., Hsu, L.J., Sundsmo, M., Kittel, A., Saitoh, T., Miller, A., and Masliah, E. (1997) NACP, a synaptic protein involved in Alzheimer's disease, is differentially regulated during megakaryocyte differentiation. *Biochem.Biophys.Res.Commun.* 237, 611-616
28. Nakai, M., Fujita, M., Waragai, M., Sugama, S., Wei, J., Akatsu, H., Ohtaka-Maruyama, C., Okado, H., and Hashimoto, M. (2007) Expression of alpha-synuclein, a presynaptic protein implicated in Parkinson's disease, in erythropoietic lineage. *Biochem.Biophys.Res.Commun.* 358, 104-110

29. Park, S.M., Jung, H.Y., Kim, H.O., Rhim, H., Paik, S.R., Chung, K.C., Park, J.H., and Kim, J. (2002) Evidence that alpha-synuclein functions as a negative regulator of Ca(++)-dependent alpha-granule release from human platelets. *Blood.* 100, 2506-2514
30. Forloni, G., Bertani, I., Calella, A.M., Thaler, F., and Invernizzi, R. (2000) Alpha-synuclein and Parkinson's disease: selective neurodegenerative effect of alpha-synuclein fragment on dopaminergic neurons in vitro and in vivo. *Ann.Neurol.* 47, 632-640
31. Kim, K.S., Park, J.Y., Jou, I., and Park, S.M. (2010) Regulation of Weibel-Palade body exocytosis by alpha-synuclein in endothelial cells. *J.Biol.Chem.* 285, 21416-21425
32. Sharma, P., Nag, D., Atam, V., Seth, P.K., and Khanna, V.K. (1991) Platelet aggregation in patients with Parkinson's disease. *Stroke.* 22, 1607-1608
33. Factor, S.A., Ortof, E., Dentinger, M.P., Mankes, R., and Barron, K.D. (1994) Platelet morphology in Parkinson's disease: an electron microscopic study. *J.Neurol.Sci.* 122, 84-89

CHAPTER 3.2

α-Synuclein Binds to Thrombin Exosites and Inhibits Thrombin-Mediated Platelet Aggregation

INTRODUCTION

α-synuclein (α-Syn) is a small soluble presynaptic protein that is highly conserved in vertebrates and has been implicated in Parkinson's disease (PD). Several mutations (i.e. A53T, A30P, and E46K) in the human α-Syn gene have been found to be associated with rare familial PD (1). In addition, protein deposits in PD's brain, called Lewy body, are composed by β-sheet rich α-Syn amyloid fibrils (2). Presently, the normal function of α-Syn remains poorly understood, although it has been linked with synaptic plasticity (3) and learning (4), neurotransmitter release and maintenance of synaptic vesicle pools (5). α-Syn was found to localize to the presynaptic membrane and was ubiquitously expressed in various hematopoietic cells including T cells, B cells, NK cells, monocytes, red blood cells and platelets (6). In fact, the protein is able to penetrate the platelets and constitute the major component of protein deposits in PD (2). At the level of platelets, α-Syn is loosely associated with the plasma membrane, the endomembrane system and, occasionally, with the membrane of secretory α-granules (7).

Thrombin is the final effector protease in the coagulation cascade (8) and plays a key role at the interface between blood coagulation, inflammation, and physiological and pathological cell proliferation (9). Moreover, it seems to be also involved in neurodegenerative diseases (10) due to its expression in a number of cells in the nervous system (NS) (11). The effects of thrombin on the NS are mediated by activation of Protease Activated Receptors (PARs), that have been linked to the development and regrowth on central NS related to memory, neurodegenerative diseases and dopaminergic reward pathway (12-14). It was reported that thrombin, at low concentration, induces retraction of neuritis in neuroblastoma cells, acts as mitogen and induces alterations in astrocytes morphology: all these effects seem to have a protective role in the NS (15). Conversely, in the presence of higher concentration of the enzyme, has been shown to induce apoptosis in motor neurons (16) and to determine in the brain a pro-inflammatory state (17). Interestingly, numerous alterations in morphology and platelets aggregation have been found in PD. Furthermore, α-

Syn has been shown to impair thrombin-induced platelets degranulation, through PAR-mediated activation (18). It was reported, in fact, that α-Syn functions as a negative regulator of Ca^{2+}-dependent α-granule release from human platelets (18), and it plays as a negative regulator in Weibel-Palade body exocytosis in endothelia cells (19). Besides cell biology data, clinical studies indicated that the incidence of myocardial infarction and ischemic stroke in 83 patients with PD is significantly lower than in controls, and that this effect seems to be correlated with the reduction of platelet aggregation (20). It seems that the platelets from PD patients have altered secretory pathways (21), owing to the presence of numerous large intracytoplasmic vacuoles formed from the open canalicular system. All these data suggest a possible implication of α-Syn in downregulating thrombin-induced platelets activation through binding to the protease.

In this study we investigated the possible interaction of the acid α-Syn with the basic thrombin molecule using biochemical and spectroscopic techniques. In particular, we investigated the effect of α-Syn on the procoagulant (i.e. fibrin generation and platelet aggregation) and anticoagulant (i.e. generation of active PC) functions of thrombin. These results might contribute to shed light on the possible cross-talk between coagulation/differentiation/inflammation pathways regulated by thrombin and Parkinson's disease.

MATERIALS AND METHODS

Materials

Human α-thrombin, protein-C, fibrinogen, and thrombomodulin were purchased from Haematologyic Technologies (Essex Junction, VT, USA); HD1 and HD22 aptamers were obtained from Primm (Milan, Italy); p-aminobenzamidine (PABA) and chromeogenic substrates (i.e. S-2238 D-Phe-Pip-Arg-p-nitroanilide; S-2366 pyroGlu-Pro-Arg-p-nitroanilide) were purchased from Sigma (St. Louis, MO, USA) and from Chromogenix (Milan, Italy), respectively; hirugen(54-65) peptide, fibrinogen γ′-chain peptide(408-427), and hirudin N-terminal domain Hir(1-47) were chemically synthesized (22, 23).

Production and Characterization of Recombinant α-Synuclein

Recombinant wild-type full length α-Syn (1-140), and *his-tagged* α-Syn (1-140), were expressed and refolded as previously described (24). Briefly, pRSETB expression vector

(Invitrogen, Carlsbad, CA, USA) was used to transform E. coli strain TOP10 and BL21pLysS cells. After inducing protein expression with isopropyl β-D-thiogalactoside (IPTG), harvested cells were sonicated in 40mM Tris-HCl pH 8.0, 0.5M NaCl buffer, and boiled for 10 minutes. The soluble fraction, containing α-Syn, was dialyzed over-night at 4°C in 40mM Tris-HCl pH 8.0, 0.1M NaCl, 2mM EDTA buffer, and purified by RP-HPLC on a C18 semi-preparative column (4.6 x 250 mm, 5 μm particle size, 300 Å porosity) from Grace-Vydac (Hesperia, CA, U.S.A.). The column was equilibrated with 0.1% (v/v) aqueous TFA and eluted with a linear 0.1% (w/w) TFA-acetonitrile gradient (30 - 55% in 30 minutes) at a flow rate of 1.5 ml/min. The absorbance of the effluent was recorded at 226 nm. The chemical identity of the purified proteins was established by ESI-TOF mass spectrometry (MS) on a Mariner instrument from Perseptive Biosystems (Stafford, TX, USA), while the purity of α-Syn preparations was established by SDS/PAGE (12% acrylamide gel). In addition, to confirm the correctness of amino acid sequence, a peptide mass fingerprint analysis was conducted. In details, to a solution of purified α-Syn (500 μl, 0.1 mg/ml) in 50mM Tris-HCl pH 7.8, 1mM $CaCl_2$ buffer was added trypsin, in protease/protein ration of 1:50 (w/w); the reaction was carried out for 3 hours at 37±0.1°C. The tryptic digest was then analyzed by RP-HPLC and MS spectrometry.

Chemical Synthesis and Characterization of C-terminal α-Syn Peptides

The peptides corresponding to residues (103-140), (103-121) and (122-140) of α-Syn were chemically synthesized by the solid-phase Fmoc method (25) using a model PS3 automated synthesizer from Protein Technologies International (Tucson, AZ, USA). Nα-Fmoc protected amino acids, solvents and reagents for peptide synthesis were purchased from Applied Biosystems (Foster City, CA, USA) or Bachem AG (Bubendorf, Switzerland). All other reagents and solvents were of analytical grade and purchased from Fluka-Sigma (St. Louis, MO, USA). The peptide chain was assembled stepwise on a *ChemMatrix* resin (Matrix Innovation, Quebec, Canada) derivatized with Fmoc-Ala (0.47 mequiv/g) or Fmoc-Asp (0.45 mequiv/) in the case of α-Syn (103-121). The crude peptides were fractionated by RP-HPLC on a C18 column (4.6 x 150 mm, 5 μm particle size, 300 Å porosity) from Grace-Vydac (Hesperia, CA, U.S.A.). The absorbance of the effluent was recorded at 226 nm. The peptide material was analyzed by mass spectrometry on a Mariner ESI-TOF instrument from Perseptive Biosystems (Stafford, TX, USA).

Spectroscopic Characterization of Monomeric α-Syn

Purified α-Syn (1-140) was subjected to alkaline treatment to obtain the monomeric form (26). Briefly, aliquots of lyophilized protein (2 mg) were dissolved immediately before use in 2mM NaOH (100 µl); the pH was adjusted to 11.0 with 1M NaOH (10 µl), and the protein was incubated for 10 min at room temperature (to dissolve any seeds). The pH was readjusted to 8 with 100mM Tris-HCl pH 7 buffer (200 µl). Solutions were centrifuged at 15000 rpm for 15 minutes to remove large aggregates. α-Syn (1-140) concentration was determined by UV absorption at 280 nm on a Jasco V-630 spectrophotometer (Tokyo, Japan) using a molar absorptivity value of 5960 $M^{-1} \cdot cm^{-1}$. For DLS measurements, polystyrene cuvettes (1-cm pathlength, 100µl) (Hellma, Müllheim, Germany) were used. Each measurement at 25°C consisted of a subset of runs determined automatically, each being averaged for 10 seconds. Scattering data were analyzed with the multimodal algorithm, as implemented in the Nano-6.20 software, and expressed as percentage mass size distribution. α-Syn (1-140) samples were filtered at 0.22µm on Vivaspin 500 filters (Sartorius, Germany) for 2 minutes at 8000 rpm and equilibrated for 1 min before analysis. The concentration of synthetic peptide was determined by UV absorption at 280 nm, using a ε^{M}_{280nm} for α-Syn (103-140) and α-Syn (122-140) of 4470 M^{-1} cm^{-1}. For α-Syn (103-122), the protein concentration was determined at 205nm, according to the method previously described by Scopes and co-workers: $c_{mg/ml} = Abs_{205nm} / 31 \cdot b$ (28), because the peptide does not contain Trp or Tyr residues.

Binding Measurements of α-Synuclein – Thrombin Interaction

The interaction of full-length α-synuclein and its synthetic peptides to thrombin was studied by spectroscopic techniques (i.e. fluorescence and circular dichroism) and surface plasmon resonance. The affinity (Kd) was estimated by recording the increase of tryptophan fluorescence of thrombin at the λ_{max} (i.e. 334 nm) as a function of protein/peptide concentration. The interaction was monitored by adding, under gentle magnetic stirring, to a solution of thrombin (1.5ml, 70nM) in HBS buffer (20mM HEPES pH 7.4, 0.15M NaCl, 0.1% PEG_{8000}) at 37±0.1°C, aliquots (2, 5, 10µl) of a suitable stock solution of ligand. Fluorescence spectra were recorded on a Jasco spectrofluorimeter model FP-6500, equipped with a Jasco ETC-223T Peltier system (Tokyo, Japan). Excitation and emission wavelengths were at 295 and 334 nm, using an excitation/emission slit of 3/10 nm, respectively. Under these conditions, Trp-photobleaching was always lower than 2%. The optical density of the solution at both 295 and 334 nm was always lower than 0.05 units and therefore no inner filter

effect occurred during titration experiments. Fluorescence intensities were corrected for dilution (<5% at the end of the titration) and subtracted for the contribution of the ligand, at the indicated concentration. The fluorescence values, measured in triplicate, were analyzed as a function of the peptide concentration by a single site binding isotherm equation (eq. 1) using the program Origin 7.5 (MicroCal Inc.):

$$(F-F_0)/\Delta Fmax = [RL]/[R] = [L]/(Kd + [L]) \quad \text{(eq.1)}$$

where the fluorescence intensity, F, of thrombin , R, at a given concentration of α-Syn ligand, L, is linearly related to the concentration of the complex [RL], according to the equation $F = [RL]\cdot F_{bound} + [R]_{free}\cdot F_{free}$. $F-F_0$ is the change in thrombin fluorescence in the absence, F_0, and presence, F, of the ligand, ΔF_{max} is the maximum signal change at infinite concentration of ligand, $[L]\infty$, and K_d is the dissociation constant of the complex, RL.

Surface Plasmon resonance (SPR) measurements were carried out on a Biacore X100 instrument (GE-Healthcare, Piscataway, NJ, USA), using a NTA sensor chip (carboxymethylated dextran pre-immobilized with nitrilotriacetic acid, NTA), according to the manufacturer's instructions. The sensor chip was first washed with EDTA scavenger solution (0.35M, 50µl), nickel solution ($NiCl_2$ 500µM, 50µl), and EDTA wash solution (3mM, 31µl). Then, an equimolar mixture of N-ethyl-N′-dimethylaminipropylcarbodiimide (EDC, 0.2M, 85µl) and N-hydroxysuccinimide (NHS, 0.2M, 85µl) was loaded; unreacted carboxymethyl-groups on the sensor chip were blocked by reaction with ethanolamine (1M, 126µl) at pH 8.5. Purified *his-tagged* α-Syn (1-140) (i.e. the ligand; 200nM, 90µl) was theninjected for 600 sec at a flow rate of 5 µl/min. Final immobilization levels of 224 resonance units (RU) were obtained. To avoid autoproteolysis, the inactive thrombin mutant S195A, produced in our laboratory, was used (29). All measurements were carried out at 25°C in Hepes-EP+ (10mM Hepes pH 7.4, 150mM NaCl, 3mM EDTA, 0.005% Tween20 polyoxyethylene sorbitan) at a flow rate of 30 µl/min. Each SPR trace was subtracted for unspecific binding (<2% of Rmax) of thrombin. The response units (RU) at the steady state were plotted as a function of [thrombin] and fitted to the Langmuir equation (eq.2) to yield the dissociation constant, Kd, of thrombin - *his-tagged* α-syn interaction:

$$R_{eq} = C\cdot R_{max}/(C + K_d) \quad \text{(eq.2)}$$

where R_{max} is the value in RU at saturating ligang concentration and R_{eq} is the change in RU at each given concentration C after reaching equilibrium.

Thrombin-α-Syn interaction was also probed by circular dichroism (CD), in the presence (i.e., fast form) and absence (i.e., slow form) of Na^+ and under physiological conditions. Far-UV CD spectra were recorded on a Jasco J-810 spectropolarimeter equipped with a thermostatted cell holder and a Peltier PTC-423S temperature control system (Tokyo, Japan), using a 1 mm-pathlength quartz cell. Each spectrum was the average of four accumulations, after base line subtraction. Under physiological conditions, the spectra were recorded in PBS (10mM Na_2HPO_4 pH 7.4, 0.15M NaCl) at 37±0.1°C, while in fast and slow conditions the signals were monitored at 25±0.1°C in 10mM Tris-HCl pH 7.4 buffer, containing NaCl (0.2M) and choline (0.2M), respectively (30).

Probing the Accessibility of Thrombin Active Site after α-Syn Binding

Binding of PABA (ε_{293nm} = 15mM$^{-1}\cdot$cm^{-1}), S2238 (D-Phe-Pip-Arg-para-Nitroanilide) (ε_{342nm} = 8270M$^{-1}\cdot$cm^{-1}) and Hir(1-47) (ε_{280nm}=2560M$^{-1}\cdot$cm^{-1}) to thrombin was performed by fluorescence measurements in the absence or presence of 20μM α-syn. Measurements were carried out at 37±0.1°C in HBS buffer. For PABA binding (31), thrombin samples were excited at 336 nm and the fluorescence intensity was recorded at 375 nm. The data were corrected for inner filter effect (eq.3) (31):

$$F_{corr} = F_{obs}\cdot 10^{-(Aex\cdot d/2)} \quad \text{(eq.3)}$$

where A_{ex} is the solution absorbance at the excitation wavelength and d is the cuvette path-length.

Data points were then fitted to the Langmuir equation (eq.4) using the program Origin 7.5 (MicroCal, Inc. (32):

$$F_{corr} = F_0 + \{(F_{max}\cdot[I])/(K_d+[I)\} \quad \text{(eq.4)}$$

where F_0 and F_{max} are the intensities of PABA fluorescence in the thrombin-free or thrombin-bound state, respectively, and K_d is the dissociation constant of thrombin-PABA complex.

For S228 binding, thrombin samples were excited at 295nm and the fluorescence recorded at 334nm as a function of substrate concentration; fluorescence data were fitted to the equation describing a simple one-site binding mechanism (eq.1). For Hir(1-47) binding, thrombin samples were excited at 295nm and the fluorescence recorded at 334nm as a function of inhibitor concentration. The data were analyzed within the framework of the tight binding model (eq.5) using the program Origin 7.5 (MicroCal, Inc.):

$$\Delta F = \{(\Delta F_{max}+[I]+K_d) - \{(\Delta F_{max}+[I]+K_d)^2 - 4\cdot\Delta F_{max}\,[I]\}^{1/2}\}/2 \quad \text{(eq.5)}$$

where K_d is the dissociation constant of the inhibitor-thrombin complex and ΔF_{max} is maximal fluorescence change at saturating Hir(1-47) concentrations, [I].

Probing the involvement of Thrombin Exosites

Binding of hirugen (exosite-I binder) and γ′-peptide (exosite-II binder) to thrombin, in the presence of 20μM α-Syn, were carried out by fluorescence measurements ($\lambda_{excitation}$ / $\lambda_{emission}$: 295nm/334nm), in HBS buffer at 37±0.1°C. The data were analyzed by eq. 1. In SPR competition experiments, exosite-I (i.e. HD1 and hirugen) and exosite-II (i.e. HD22 and γ′-peptide) binders were first incubated with thrombin mutant S195A and then injected over the *his-tagged* a-Syn (1-140) -coated NTA sensor chip, using the same experimental condition reported above.

Clotting Assays

The turbidity (i.e. absorbance at 350 nm) of a desalted fibrinogen solution was measured after addition of thrombin (1nM) at 37±0.1°C in HBS on a Jasco V-630 spectrophotometer (Tokyo, Japan), in the absence or presence of 0, 0.5, 1, 10μM α-Syn (1-140) (33). The effect of full-length α-Syn (1-140) and α-Syn (103-140) on whole blood clotting induced by thrombin, TRAP (Thrombin Receptor Activating Peptide: Ser-Phe-Leu-Leu-Arg-Asn) (34), and ADP in was estimated at 37°C by Multiple Electrode Aggregometry (MEA) using a Multiplate analyzer (Dynabyte, Munich, Germany). The Area Under the aggregating Curve (AUC) was calculated over 6-min reaction (35). Citrate-treated blood samples were taken from three healthy donors, 23-28 years of age, and non-smokers. The donors gave written informed consent for participation to this study, approved by the institutional ethics committee.

PC Activation

Protein C (PC) activation by thrombin alone or in the presence of 20μM α-syn (1-140) was monitored with or without thrombomodulin at 37°±0.1C in HBS, containing 5mM $CaCl_2$, according to the quenching method described elsewhere (36). At time intervals, aliquots of the reaction mixture were added to a HBS solution containing the aPC substrate S2366 (pyroGlu-Pro-Arg-p-nitroanilide) (200μM), and hirudin HM2 (1μM) to selectively inhibit thrombin. The initial velocity, v_i, of S2366 hydrolysis was determined by measuring the release of p-nitroanilide at 405 nm, using a Victor3 plate reader (Perkin-Elmer, Norwalk, CA)

and 96-well polystyrene plates (Sigma, St. Louis, MO, USA). At each time point, the concentration of the newly generated aPC was determined from a standard curve of v_i versus [aPC], obtained with aPC solutions of known concentration. The k_{cat}/K_m value of PC hydrolysis was obtained from the time-course of aPC generation, by the pseudo first-order kinetic model (eq.6), using the program Origin 7.5 (MicroCal, Inc.):

$$[P] = [P]\infty \cdot [1 - \exp(-t \cdot k_{obs})] \quad \text{(eq.6)}$$

where $[P]\infty$ is the concentration of the product at $t=\infty$ and k_{obs} is the observed kinetic constant given by $k_{obs} = [E] \cdot s$, in which [E] is the enzyme concentration and *s* is the specificity constant k_{cat}/K_m.

RESULTS

Chemical Characterization of Recombinant α-Synuclein

Wilde type α-Syn (1-140) were expressed in E. coli cells and purified by RP-HPLC. The chromatogram shows a major peak (Fig. 3.3A) having a mass of 14458.8 ± 0.1 a.m.u. (Fig.3.3B), very close to the average theoretical value deduced from the primary structure of α-Syn (1-140) (i.e. 14460.1 a.m.u.). In Fig. 3.3B-*Inset* SDS-PAGE analysis (12% acrylamide gel) of α-Syn (1-140) shows an apparent molecular weight of 20kDa, which is larger than the theoretical value of the protein, i.e. 14kDa. The abnormal slow mobility can be attributable to the poor binding of SDS by negative C-terminal region of α-Syn (37). Chemical characterization of the proteolytic fragments, resulting from limited proteolysis of α-Syn (1-140) with trypsin, allowed us to cover ~99% of protein sequence (Table 1), establishing that recombinant protein corresponds to the natural human protein.

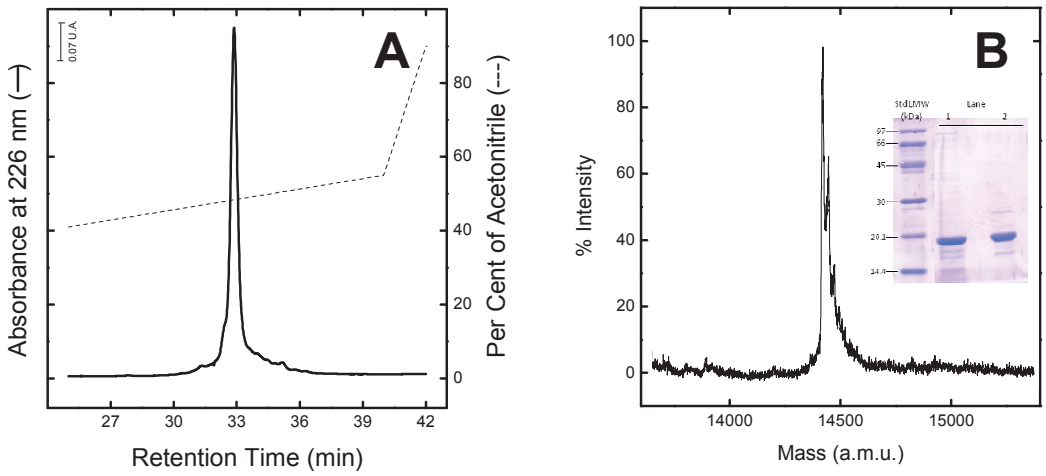

Figure 3.3 Chemical characterization of recombinant α-synuclein (1-140). (A) RP-HPLC analysis of purified α-Syn (1-140) (10μg) by a C18 column eluted with an acetonitrile-0.1% TFA gradient (---). **(B)** Deconvoluted ESI-TOF mass spectrum of RP-HPLC purified α-Syn (1-140). **(Inset)** SDS-PAGE (4-12% acrylamide) analysis of purified α-Syn (1-140) under reducing conditions. Lane 1: soluble fraction, containing crude α-Syn (1-140), after sonication; lane 2: purified α-Syn (1-140) (2μg). The molecular weight markers are indicated on the right.

Table 1: Peptide mass fingerprint analysis of α-synuclein (1-140)

Peak	Experimental MW (u.m.a.)	Theoretical MW (u.m.a.)	Δ MW	Sequence Deduced
1	403.24	403.48	0.24	^{7}GLSK^{10}
2	829.44	830.92	1.48	^{24}QGVAEAAGK^{32}
3	872.46	873.98	1.52	^{13}EGVVAAAEK^{21}
4	1071.60	1073.23	1.63	^{11}AKEGVVAAAEK^{21}
5	1294.72	1296.47	1.75	^{46}EGVVHGVATVAEK^{58}
6	1523.88	1525.75	1.87	^{46}EGVVHGVATVAEKTK^{60}
7	950.50	952.09	1.59	^{35}EGVLYVGSK^{43}
8	769.35	770.98	1.63	^{1}MDVFMK^{6}
9	1609.50	1607.85	1.65	^{81}TVEGAGSIAAATGFVKK^{97}
10	2156.12	2158.46	2.34	^{59}TKEQVTNVGGAVVTGVTAVAQK^{80}
	1477.74	1479.67	1.93	^{81}TVEGAGSIAAATGFVK^{96}
11	1927.06	1929.18	2.12	^{61}EQVTNVGGAVVTGVTAVAQK^{80}
	2156.22	2158.46	2.24	^{59}KEQVTNVGGAVVTGVTAVAQK^{80}
	1477.70	1479.67	1.97	^{81}TVEGAGSIAAATGFVK^{96}
12	4288.68	4289.42	0.74	^{103}NEEGAPQEGILEDMPVDPDNEAYEMPSEEGYQDYEPEA^{140}

α-Synuclein in Monomeric Form

To study the interaction with thrombin, α-synuclein should be in the momoneric form. For this purpose, α-Syn (1-140) has been subjected to different experimental conditions:

- HBS buffer
- 5M Guanidine Chloride
- 7% DMSO (dimethyl sulfoxide) v/v
- 2mM NaOH – 1M NaOH

Spectroscopic analytical techniques are usually used for protein aggregate detection (38), so the process has been validated by UV-Visible (UV-Vis) absorption and fluorescence emission. The UV-Vis spectra suggest that the protein after alkaline treatment is in the momoneric form (Fig. 3.4A). In fact the ratio Abs_{275nm} / Abs_{250nm} is equal to 2.6 ± 0.2 (i.e. characteristic value Tyrosine amino acid residue), and in the range 300-340 nm is not observed a significant scattering of light, possibly due to aggregation phenomena. Furthermore, the fluorescence emission spectroscopy indicates that the protein is not aggregated (Fig. 3.4B): the variation of the spectroscopic signal as a function of [analyte] is compatible with that obtained in the presence of a solution of N-Acetyl-Tyrosine amide (i.e. in α-Syn there are 4 Tyr, aromatic chromophores). It was previously reported that fluorescence and circular dichroism (CD) analyses allow investigating α-Syn fibrils formation (27). CD studies demonstrated that lower values of pH facilitate the aggregation process, probably by reducing the negative charge of α-Syn (present in physiological conditions). Consequently, it was proposed that hydrophobic interactions play a crucial role in α-Syn aggregation mechanism (39).

Dynamic light scattering measurements indicate in alkaline treated-α-Syn (1-140) the presence of a predominant specie (99%) having a hydrodynamic radius (Rh) of 3.6 ± 0.3 nm (Fig. 3.4D). The DLS data, expressed as the per cent of size distribution by mass, suggest that the sample is essentially monodispersed (Fig. 3.4C: no inflections observed) and essentially free of aggregates (Fig. 3.4C: baseline does not display significant noise beyond the log_{sec} 10000), and that the count rate is appropriate for a protein-like material (i.e. 342.3 kcps). Therefore, we can conclude that the alkaline treatment (2mM NaOH-1M NaOH) (26) is a conveninet method for obtaining full-length α-Syn in the monomeric form.

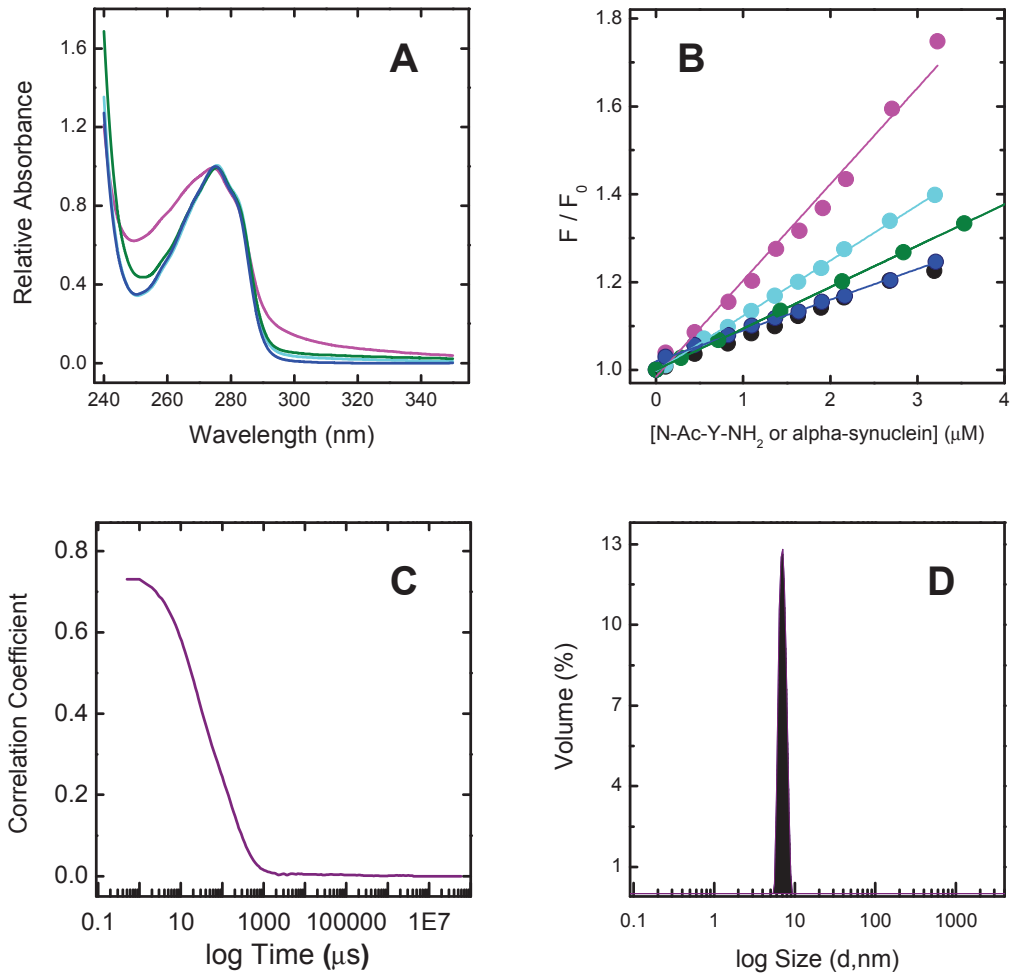

Figure 3.4 Characterization of monomeric α-synuclein (1-140). (A) UV-Vis absorption spectra of α-Syn (1-140) (2mg) in HBS buffer (—), 5M Guanidine Chloride (—), 7% DMSO (—), and 2mM NaOH – 1M NaOH (—). The spectra were reordered at 25±0.1°C, using a 0.5-cm pathlength cuvette **(B)** Variation of the fluorescence signal as a function of [α-Syn (1-140)] at 25±0.1°C, under different experimental conditions, as in panel A. Protein samples were excited at 300 nm using an excitation/emission slit of 5/10 nm and a 1-cm pathlength cuvette. In black is reported the model solution of N-Acetyl-Tyrosine amide. **(C)** Correlation curve of dynamic light scattering analysis of alkaline treated-α-Syn (1-140). **(D)** DLS data expressed as per cent mass. The samples (100μl) were centrifuged at 13000 r.p.m. for 5 min at 20°C and filtered at 0.22 μm.

α-Synuclein - Thrombin Interaction Probed by Fluorescence and SPR

The dissociation constants (Kd) of the interaction between α-Syn (1-140) and thrombin was determined by exploiting the decrease of the intrinsic fluorescence (λ_{ex} 295 nm, λ_{em} 334 nm) of the protease upon complex formation (Fig. 3.5A). In fact, the binding of α-Syn (1-140) to thrombin results in a decrease of the fluorescence quantum yield by about 30% (Fig. 3.5B), without any significant variation of the λ_{max}. Recent studies conducted in our laboratory contribute to elucidate the allosteric regulation of the thrombin active site (AS) by exosite specific lingands. In particular, exosite-I binders trigger a more open and accessible

conformation of the AS, increasing both the affinity for substrates/inhibitors and the catalytic efficiency of the enzyme. Conversely, exosite-II ligands do not significantly perturb the molecular recognition properties of thrombin. In this study, all tested peptide binders cause an increase in fluorescence intensity by 20-30%, whereas the λ_{max} remains unchanged. This suggests an overall conformational change of thrombin in which the chemical environment of tryptophan residues becomes more rigid. Most notably, our results are fully consistent with previous data reported in the literature showing that binding of allosteric modulators, such as Na^+ and exosite-I or exosite-II ligands, induces long-range effects on the structure of the enzyme (40-43).

In the case of α-synuclein, the decrease of fluorescence intensity can be attributed to quenching effect of carboxyl groups localized in the C-terminal portion on Trp-residues of thrombin. α-Syn (1-140) binding displays a saturable dose-dependent behaviour with a calculated stoichiometry of 1:1 and a K_d of 1.7 ± 0.5 μM.

The system α-synuclein - thrombin was also studied by surface plasmon resonance (SPR). Increasing concentrations of the inactive mutant S195A (Fig. 3.5C) were injected over a NTA sensor chip, loaded with purified *his-tagged* α-Syn (1-140), *via* Ni^{2+}/NTA chelation. Notably, the S195A mutant is catalytically inactive but retains the structural and molecular recognition properties of the wild type enzyme (44). Under the experimental conditions employed, the binding process was too fast to allow estimation of the rate constants and for this reason only equilibrium affinity analysis was performed to measure the Kd of thrombin binding (45). Our data (Fig. 3.5D) show that S195A binds to immobilized *his-tagged* α-Syn (1-140) with the same affinity (Kd = 2.4 ± 1.0 μM) obtained by spectroscopic technique (i.e. Kd = 1.7 ± 0.5 μM).

Mapping α-Synuclein - Thrombin Interaction Sites

A deeper understanding of the mechanism of α-synuclein binding to thrombin was achieved by studying the effect of α-Syn (1-140) on the affinity of competitive inhibitors of thrombin (i.e. PABA, S2238, and Hir (1-47)), which display different chemical complexity at enzyme catalytic pocket. PABA is a small inhibitor of trypsin-like serine proteases and forms a tight salt bridge with Asp189 at the bottom of their primary specificity site S1 (31). S2238 (D-Phe-Pip-Arg-p-nitroanilide) is a fibrinogen-like substrate and therefore it portrays on the procoagulant activity of thrombin. The substrate orients its bulky aromatic aminoacid D-Phe1 into the aryl binding site S3, pipecolyc acid in position 2 (Pip2) contacts Tyr60a and

Trp60d in the S2 site, while Arg3 harbours Asp189 in the S1 site of thrombin. S-2238 also interacts with S1′ primed site downstream to the scissile bond, where the pNA-group points to. Hir (1-47), the N-terminal domain of hirudin HM2 (23), binds to the active site (AS) of thrombin forming a parallel β-sheet, and through its first three amino acids extensively penetrates into the specificity pockets (46). In particular, Val1 on the inhibitor points to the S2 site, while Ser2 covers (but does not penetrate) the S1 site, and Tyr3 fills the apolar cavity of the S3 site (8). Binding of these inhibitors to thrombin was monitored by fluorescence spectroscopy in the absence or in the presence of 20μM α-Syn (1-140). The results indicate that α-Syn (1-140) does not influence the affinity of the inhibitors for thrombin AS (Table 2); therefore it is likely that the AS remains free and accessible for inhibitor/substrate binding.

The role of thrombin exosites in α-synuclein binding was assessed by studying the effect of 20μM α-Syn (1-140) on the affinity of specific exosites binders. For exosite-I, was used hirugen, corresponding to the C-terminal sequence of HV1 hirudin (54-65) (47, 48) whereas for exosite-II fibrinogen γ′-peptide, corresponding to the 408-427 sequence of the elongated fibrinogen γ′-chain (40). Our data (Table 2) suggest that, in the presence of 20μM α-Syn (1-140), is selectively reduced only the affinity of thrombin for the exosite II binder γ′-peptide, with an increased Kd value of 4 fold.

The involvement of thrombin exosite-II in α-Syn binding was qualitatively confirmed by SPR, saturating exosite-I (i.e. hirugen and HD1 aptamer) or exosite-II (i.e. fibrinogen γ′-peptide and HD22 aptamer) of S195A thrombin with different specific binders. The thrombin-ligand solutions were injected over *his-tagged* α-Syn (1-140) immobilized sensor chip and the decrease of the SPR signal (ΔRU) of the ternary complex was taken as an indication of compromised binding. SPR data indicate (Fig. 3.5E) that blockage of exosite-I results in 20-30% decrease of RU, while in the presence of exosite-II binders the response was completely abolished. In addition, the simultaneous blockage of both exosites with hirugen and γ′-peptide completely abrogates binding of S195A to *his-tagged* α-Syn (1-140).

These results confirm that both exosites are involved in the α-Syn (1-140)-thrombin interaction, suggesting that the role exosite-II is more important in promoting α-Syn binding to thrombin.

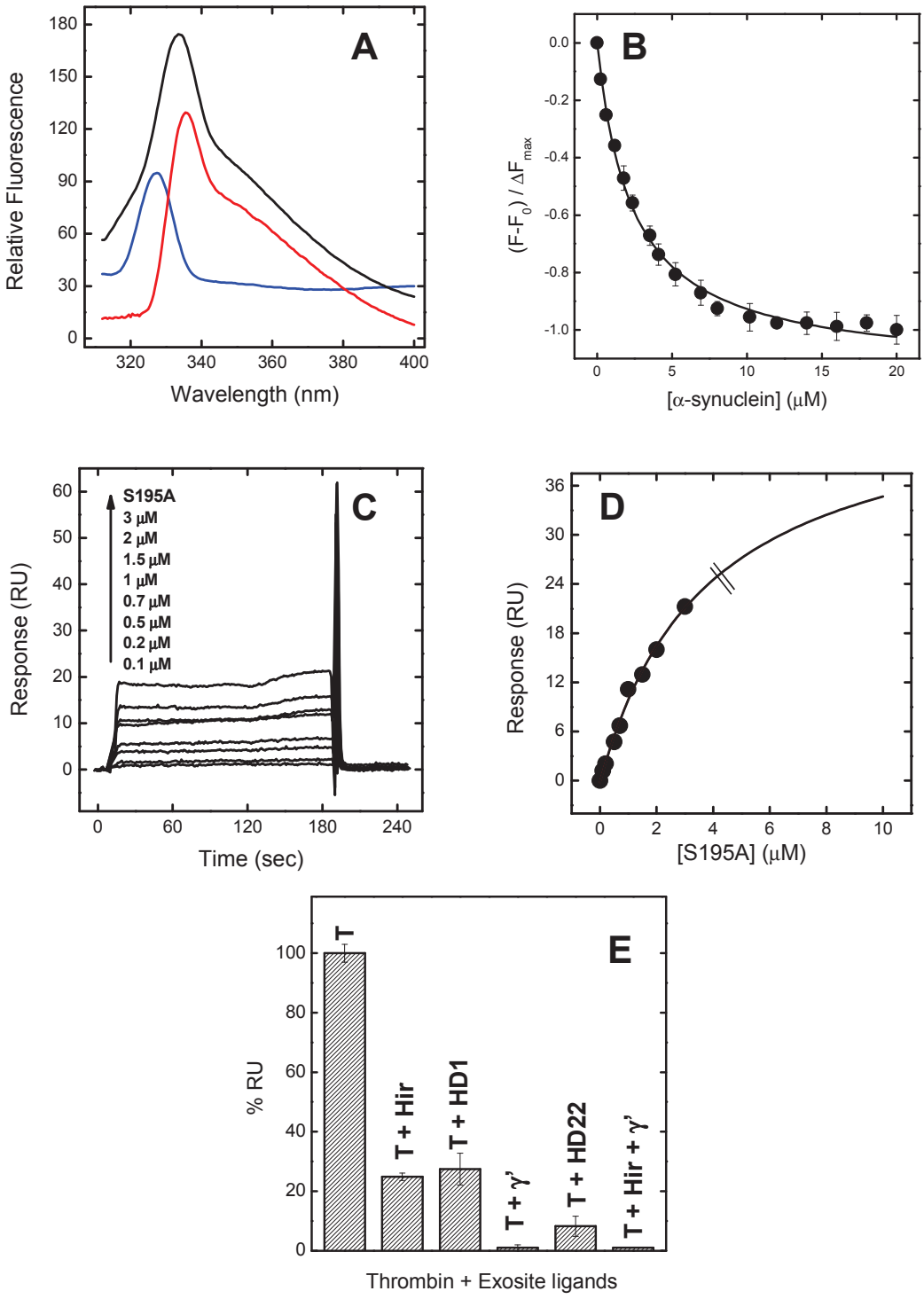

Figure 3.5 Analysis of α-Synuclein-thrombin interaction. (A) Interaction studied by tryptophan fluorescence: the intrinsic fluorescence of thrombin (—) decreases by about 20-30% (—) after adding α-Syn (1-140) (—). Fluorescence spectra were recorded at 37±0.1°C by exciting the sample at 300 nm, using an excitation/emission slit of 5/10 nm and a 1-cm pathlength cuvette. **(B)**. Plot of the fluorescence values, measured in triplicate, as a function of the protein concentration. The solid lines represent the least square fit with Kd of 1.7 ± 0.5 μM. **(C)** SPR signals relative to the binding of S195A to *his-tagged* α-Syn (1-140) loaded chip. **(D)** Plot of response signal (RU) as a function of [S195A]. Data fitting yields a Kd= 2.4 ± 1.0 μM. (E) Exosite-I: S195A (T, 1μM) was incubated for 30 min with 500nM HD1 or 20μM hirugen (Hir). Exosite-II: S195A (T, 1μM) was incubated with 1μM HD22 and 50μM fibrinogen γ'-peptide (γ'pep) or with a solution of 20μM hirugen + 50μM γ'-peptide. The resulting complexes were injected over the bound *his-tagged* α-Syn (1-140).

Table 2: Effect of α-synuclein on affinity* of SA/Exosite thrombin binders

Probe	- α-syn (1-140)	+ α-syn (1-140)
	Active Site	
PABA	114 ± 9 μM	96 ± 8 μM
S2238	0.82 ± 0.02 μM	0.71 ± 0.09 μM
Hir (1-47)	43 ± 4 μM	30 ± 5 μM
	Exosite -I	
Hirugen	2.04 ± 0.01 μM	2.75 ± 0.04 μM
	Exosite -II	
γ' peptide	4.4 ± 0.4 μM	19.5 ± 0.9 μM

*Kd values were calculated in HBS at 37±0.1°C in the presence or absesence of 20μM α-syn (1-140).

Conformational Study of α-Synuclein - Thrombin complex

To investigate whether the interaction of α-synuclein with thrombin alters the secondary structure of the protein we performed far-UV circular dichroism (CD) measurements. In fact, CD provides very convenient means of detecting such changes (49).

The shape of far-UV CD of human α-thrombin (Fig.3.6A) under physiological conditions (i.e. 0.15M NaCl, 37±0.1°C) resembles that of a protein possessing α-helical content (30). Indeed, the contribution of aromatic amino acids (i.e. Phe, Tyr, and Trp) and disulphide bonds induce a red shift in the typical bands of the helical conformation (220-222 nm and 208 nm → 210 nm and 225 nm) (30). The far-UV CD spectra of α-syn (1-140) (Fig.3.6A) presents a strong negative peak at 202 nm and a small shoulder at about 222 nm, indicating a random coil structure, possibly with the presence of some nascent and marginally stable α-helix content (37). In the presence of thrombin, the far-UV CD spectra is characterized by two minima, one at around 225 nm and one at 200 nm, with a substantial increase in the CD signal (Fig.3.6A). The signal for [α-syn (103-140)-thrombin] complex (Fig. 3.6B) is similar in shape but not in intensity, because the spectra are not normalized to molar concentration or Mean Residue Weight (MRW) (49). The difference between the experimental and the theoretical spectra suggests a weak conformational change of α-synuclein, after interaction with the serine protease. Interestingly, under "fast" conditions

(Fig. 3.6C; $\Delta_{Ellipticity}$ ~ 17%), i.e. with 0.2 M NaCl, this difference is greater than under the "slow" (Fig. 3.6D; $\Delta_{Ellipticity}$ ~ 11%), i.e. 0.2 M ChCl, demonstrating that the interaction is influenced by the initial conformation of thrombin, whereby the "fast" form has a more open and rigid conformation and exosite-I is completely structured and therefore more competent for ligand binding. Conversely, in the absence of Na^+, thrombin has a more flexible and collapsed conformation and exosite I is not fully expressed. Partial disruption of exosite-I in the "slow" form can dramatically reduce the affinity of α-Syn for thrombin.

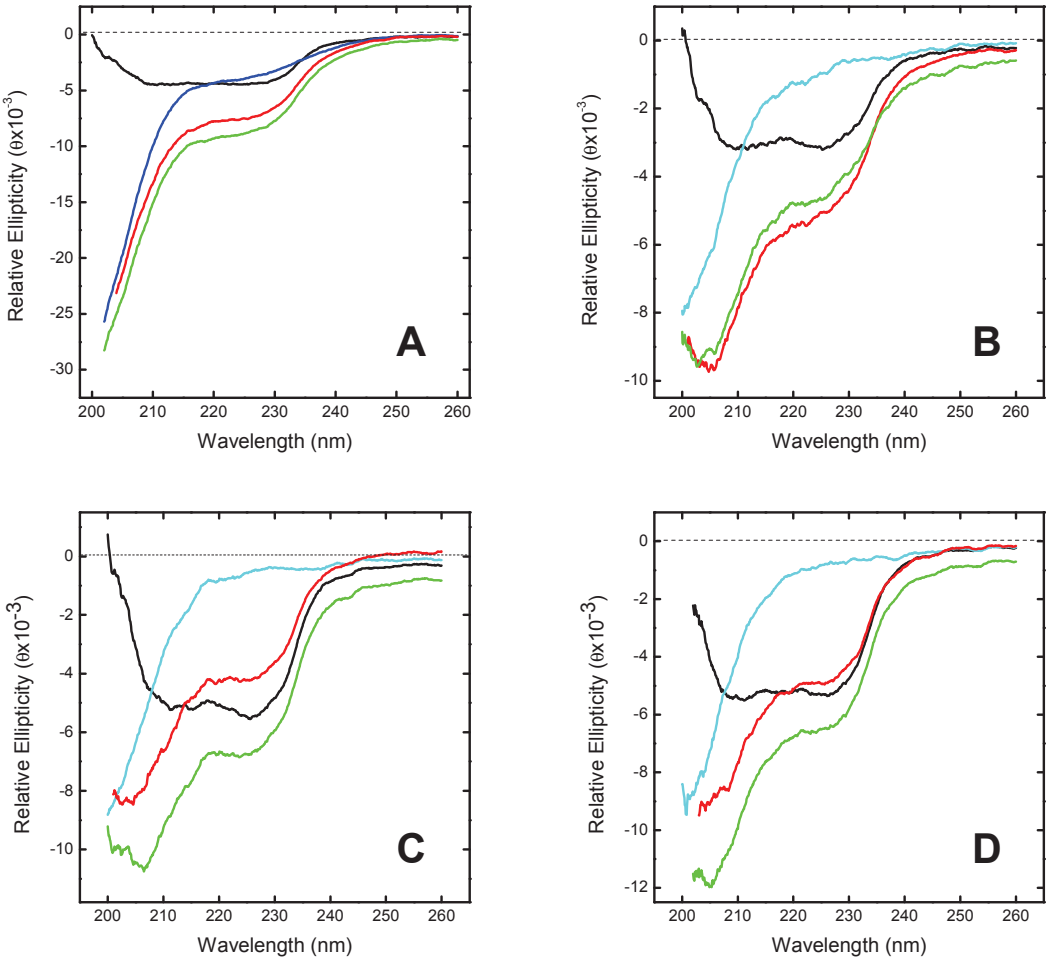

Figure 3.6 CD Analysis of α-synuclein-thrombin interaction. Far-UV CD spectra of: α-Syn (1-140) (—), α-Ssyn (103-140) (—), human thrombin (—), [α-Syn – thrombin] complex (—), and theoretical sum of α-Syn and thrombin's Far-UV CD spectra (—). **(A-B)** Physiological conditions: 37±0.1°C in PBS, using a 1 mm pathlength quartz cell. **(C)** Fast conditions: 25±0.1°C in Tris buffer containing 0.2M NaCl, using a 1 mm pathlength quartz cell. **(D)** Slow conditions: 25±0.1°C in Tris buffer containing 0.2M Choline, using a 1 mm pathlength quartz cell.

Effect of α-Synuclein on Thrombin Functions

Thrombin plays a pivotal role in the coagulation cascade, encountering a large number of different substrates. Here we investigated the effect of α-synuclein on pro-coagulant (i.e. fibrin generation and platelet aggregation) and anti-coagulant (i.e. protein C activation) functions of the serine protease. The effect of α-Syn (1-140) on the sol-gel transition associated with fibrin formation was monitored as an increase in turbidity (i.e. Abs_{350nm}) with time due to the light scattered by fibrin aggregates. Fibrin generation was started by addition of thrombin to a solution of purified human fibrinogen at increasing [α-Syn (1-140)]. The resulting clotting curves were analyzed to extract the values of ΔA_{max}, t_{max}, and t_c, where ΔA_{max} is the maximum slope of the clotting curve, t_{max} is the time needed to reach ΔA_{max}, and t_c (i.e. the clotting time) is the lag-time. Of note, t_{max} and t_c are correlated quantities: $t_{max} = 26.4 + 1.11 \cdot t_c$ (33). Our data show that in the presence of α-Syn (1-140) the clotting time is not significantly influence (Fig. 3.7A). Conversely, α-syn seems to affect ΔA_{max}, in a dose-dependent manner. Probably α-Syn (1-140) might influence the structure of fibrin clot; indeed ΔA_{max} is a parameter linked to the aggregation steps leading clot formation (33).

The effect of α-syn (1-140) on platelet aggregation was determined on whole blood, by Multiple Electrode Aggregometry (MEA) (35). MEA exploits the increase of electric impedance due to the adhesion and aggregation of platelets on the electrodes, upon addition of exogenous agonist (i.e. thrombin, TRAP, and ADP). Our results indicate that α-Syn (1-140) dose-dependently inhibits thrombin- and TRAP- induced platelet aggregation in whole blood (Fig 3.7B), by about 80% and 70% respectively. In the presence of ADP, instead, the effect is lower and the AUC value (Area Under the aggregating Curve) decreases by only 30%. These data were also confirmed by preliminary studies with PRP (Platelet Rich Plasma) in the presence of 20μM α-Syn (1-140), showing that thrombin-induced platelet aggregation is significantly slowed (Fig. 3.7C).

The effect of α-Syn (1-140) on the generation of activated PC (aPC) was investigated in the absence or presence of TM. The time-course of aPC generation was monitored by recording the release of pNA from the substrate S-2366, after thrombin inhibition (Fig. 3.7D). With or without TM, α-Syn (1-140) does not alter the efficiency with which thrombin hydrolyses PC. This trend confirms our conclusion that the active site of thrombin is not (or only marginally) involved in the formation of α-synuclein – thrombin complex.

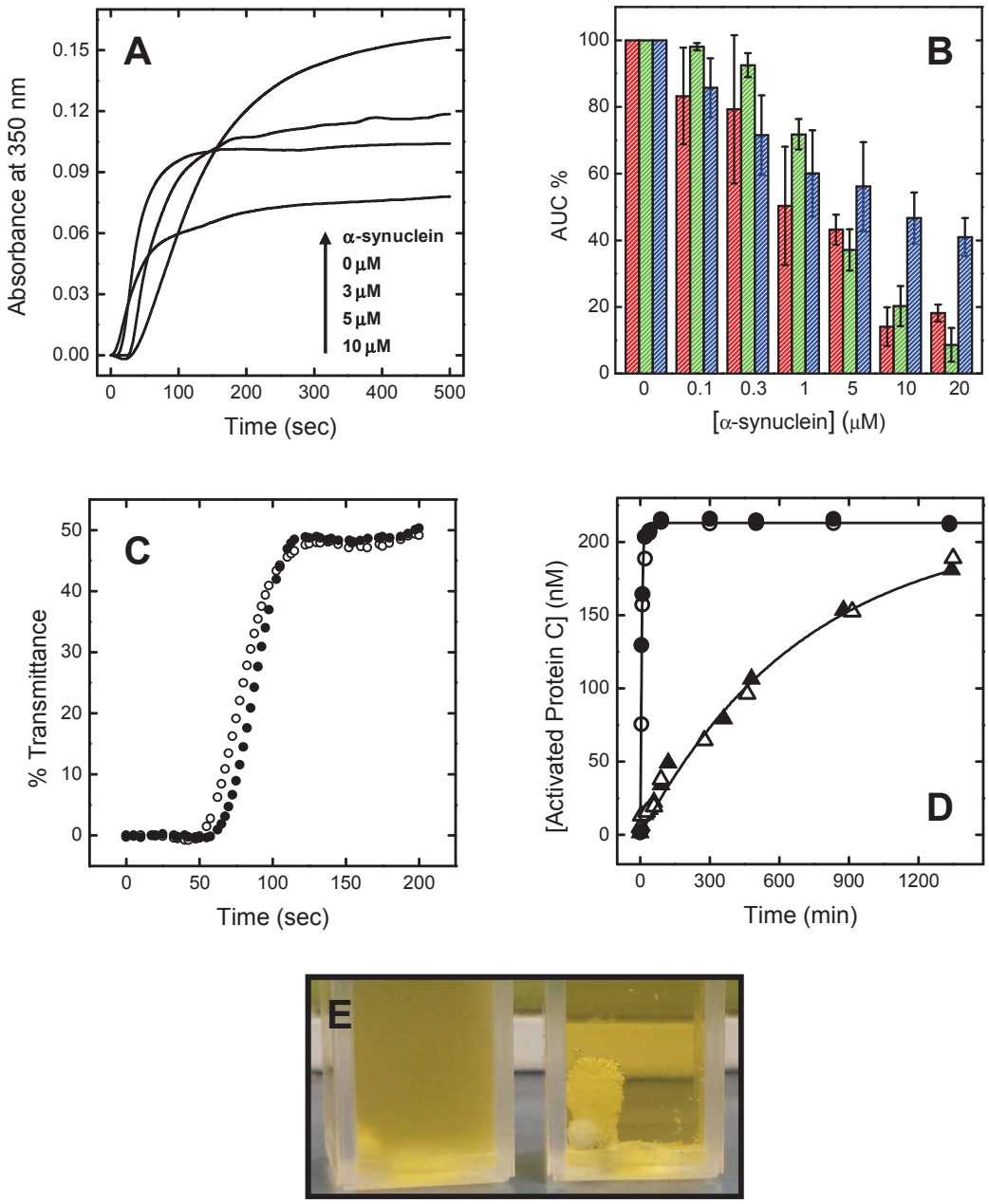

Figure 3.7 Effect of α-synuclein on thrombin functions. (A) Representative clotting curves for the generation of fibrin in the presence of α-Syn (1-140). To a human fibrinogen solution (0.44μM) in HBS at 37°C was added plasma thrombin (1nM), with different concentration of α-Syn (1-140) (0, 3, 5, and 10 μM) and the increase in turbidity (Abs at 350 nm) was recorded over time. **(B)** Effect of α-Syn (1-140) on platelet aggregation on whole blood, induced by addition of thrombin (6nM, —), TRAP (—) and ADP (—). The data are expressed as the AUC %, where AUC_0 = 100% is the Area Under the aggregation Curve at [α-Syn (1-140)] = 0. **(C)** Effect of α-Syn (1-140) (20μM) on thrombin- (6nM) platelet aggregation on PRP. The aggregation was performed at 37±0.1°C with stirring of 1000 r.p.m., monitoring the transmittance at 650 nm. In **(E)** is reported the platelet aggregated on PRP in presence (left) and in the absence (right) of 20μM α-Syn (1-140). **(D)** Effect of α-syn (1-140) on PC activation with (○,●) or without (Δ,▲) TM. To a solution of PC (200nM) was added human thrombin (5nM) in the absence (Δ) or in the presence (▲) of α-Syn (1-140) (20μM) at 37°C. Under conditions of pseudo-first reaction, the values of k_{cat}/K_m and $[aPC]_\infty$ were determined as follows: - α-Syn (1-140), k_{cat}/K_m= 0.3 ± 0.2 $mM^{-1}\cdot s^{-1}$ and $[aPC]_\infty$ = 194 ± 9 nM; + α-Syn (1-140), k_{cat}/K_m= 0.31 ± 0.2 $mM^{-1}\cdot s^{-1}$ and $[aPC]_\infty$ = 196 ± 5n M. The effect of α-Syn (1-140) on PC activation in the presence of 50nM TM (○,●) was determined as above, with [thrombin] = 10nM: - α-syn (1-140), k_{cat}/K_m = 215 ± 1 $mM^{-1}\cdot s^{-1}$ and $[aPC]_\infty$ = 198 ± 4nM; + α-Syn (1-140), k_{cat}/K_m = 212 ± 3$mM^{-1}\cdot s^{-1}$ and $[aPC]_\infty$ = 200 ± 3nM.

Effect of C-terminal α- Synuclein Peptides on Platelet Aggregation

The peptides corresponding to residues (103-140), (103-121) and (122-140) of α-Syn were chemically synthesized by solid-phase Fmoc method (25), and their identities were confirmed by MS analysis (Table 3). The affinity for thrombin was studied by spectroscopic technique, recording the variation of enzyme tryptophan fluorescence. The data were analyzed by the Langmuir equation and yields a Kd (Table 3) comparable to that obtained for the full-length protein (i.e. Kd =1.7 ± 0.5 μM). These data suggest that the C-terminal region is important for the formation of [α-synuclein - thrombin] complex.

Surprisingly, studies of platelet aggregation on whole blood show that the C-terminal peptide does not inhibit platelet aggregation induced by thrombin, TRAP or ADP (Fig. 3.8). This finding is consistent with recent results showing that the deletion mutant of α-Syn, which completely lacks C-terminal acidic tail, does not function as a negative regulator of α-granule release in platelets (18). In fact, it seems that only the intact protein plays a critical role in membrane translocation and platelet degranulation.

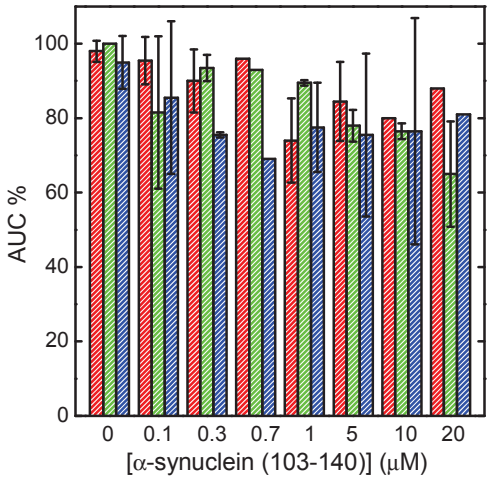

Figure 3.8 Effect of α-syn (103-140) on platelet aggregation on whole blood. The aggregation was induced by addition of thrombin (6nM, —), TRAP (—) and ADP (—) on whole blood in the presence of different concentrations of α-Syn (103-140) (0, 0.1, 0.3, 0.7, 1, 5, 10, and 20μM). The data are expressed as the AUC %, where AUC_0 = 100% is the Area Under the aggregation Curve at [α-Syn (103-140)] = 0.

Table 3: Small library of C-terminal α- synuclein peptides

Peptide	Experimental MW (u.m.a.)	Theoretical MW (u.m.a.)	Δ MW	Kd $_{thrombin}$
α-syn (103-140)	4289.5	4288.4	1.1	1.41 ± 0.05 μM
α-syn (103-121)	2055.1	2055.2	0.1	1.12 ± 0.10 μM
α-syn (122-140)	2251.2	2249.9	1.3	1.99 ± 0.09 μM

DISCUSSION

α-Synuclein Interacts with Thrombin

Previous studies have indicated that α-Syn may penetrate into platelets and subsequently affects α-granule release (18). The protein is also expressed in hematopoietic cells (6) and is implicated in the differentiation of megakaryocytes (50), suggesting that the biological function of α-Syn is not restricted to neuronal cells. The results of this study provide evidence that α-Syn binds to thrombin, inhibiting thrombin-mediated platelet aggregation (Fig. 3.7B). Using different molecular probes, we have demonstrated that α-Syn interacts with protease exosites, leaving the active site accessible (Fig. 3.5), thus displaying physiologically relevant affinity (Kd~2μM).

The theoretical model implies that the micromolar affinity of α-Syn for thrombin, expressed as the free energy change of binding (Kd~2μM; ΔG_b~-8.13kcal/mol), is distributed over the two interacting sites ($\Delta G_b=\Delta G_b^1+\Delta G_b^2$) and that it is fully manifested only when both thrombin exosites are available for binding. According to the model, in fact, when one of the two exosites is already occupied by a given ligand present in solution, α-Syn can still interact with thrombin, albeit with lower affinity (Kd~10mM), at the other exosite accessible on the protease surface to form a ternary complex. Hence, the binding properties of α-Syn can be dynamically regulated by the specificity and affinity of the ligand present in solution for either one of the two thrombin exosites. This simple model explains why in the presence of exosite ligands the interaction is not completely abolished (Table 2), while the concomitant blockage of both exosite abolishes binding (Fig. 3.5E). This interpretation is consitent with the observation that in the absence of Na^+, i.e. the slow form, the affinity of α-Syn for thrombin is much lower (Fig. 3.6D). In the slow form, in fact, exosite-I is not completely

formed and competent for ligand binding. In addition, the C-terminal region, α-Syn (103-140), appeared to interact with the serine protease (Table 3), suggesting that the acidic region of α-Syn is directly involved in the [α-Syn - thrombin] complex formation.

Effect of α-Synuclein on Platelet Aggregation

Multiple pathways contribute to platelet activation, involving different agonist such us thrombin, ADP, tromboxane, collagen, serotonin and epinephrine (51). Thrombin- platelets activation is mediated primarily by PAR-1, while PAR-4 expresses a lower sensitivity to the enzyme (52). Activation by thrombin results in cross linked platelet aggregation as fibrinogen strands bind to glycoprotein IIb/IIIa receptors. Adenosine diphosphate (ADP) is a nucleotide that is stored in the dense granules of platelets. Upon activation, platelets undergo shape change and release the contents of their α- and dense- granules. The release of internal stores of ADP promotes the activation of local free circulating platelets by binding to purinergic receptors, P2Y1 and P2Y12 on platelet membranes (53).

Our results suggest that full-length α-Syn inhibits thrombin-platelet aggregation, while the effect in the presence of ADP is less noticeable (Fig. 3.7B). Conversely, α-Syn (103-140) does not affect platelets activation (Fig. 3.8). The data reported here seem to indicate that the C-terminal region of α-Syn interacts with thrombin exosites, without influencing the catalytic activity of the protease. The observation that the C-terminal region of α-Syn (103-140) is able to interact with thrombin, but is not capable of inhibiting platelets aggregation can be explained according to a model in which α-Syn, secreted upon thrombin stimulation, localizes on the negatively charged surface of activated platelets (18), rich in phosphatidyl serine, likely through its highly electropositive N-terminal domain. Next, platelet-bound α-Syn would harbor thrombin exosite through its disordered negatively charged C-terminal domain, thus limiting further (useless) activation of platelets by thrombin (Fig. 3.9).

This model is consistent with the fact that, among cellular components of blood, α-Syn is most abundant in platelets (i.e. 264 ± 36 ng/ml), compared to leukocytes and erythrocytes (54), and that patients with Parkinson's disease have significantly lower incidence of myocardial infarction and ischemic stroke, compared to normal subjects and that the reduction of thrombotic events is caused by a reduced tendency of platelets to aggregate.

In conclusion, the results reported in this work allow us to propose a plausible molecular mechanism through which higher expression of α-Syn can affect the coagulation process in neurodegenerative diseases.

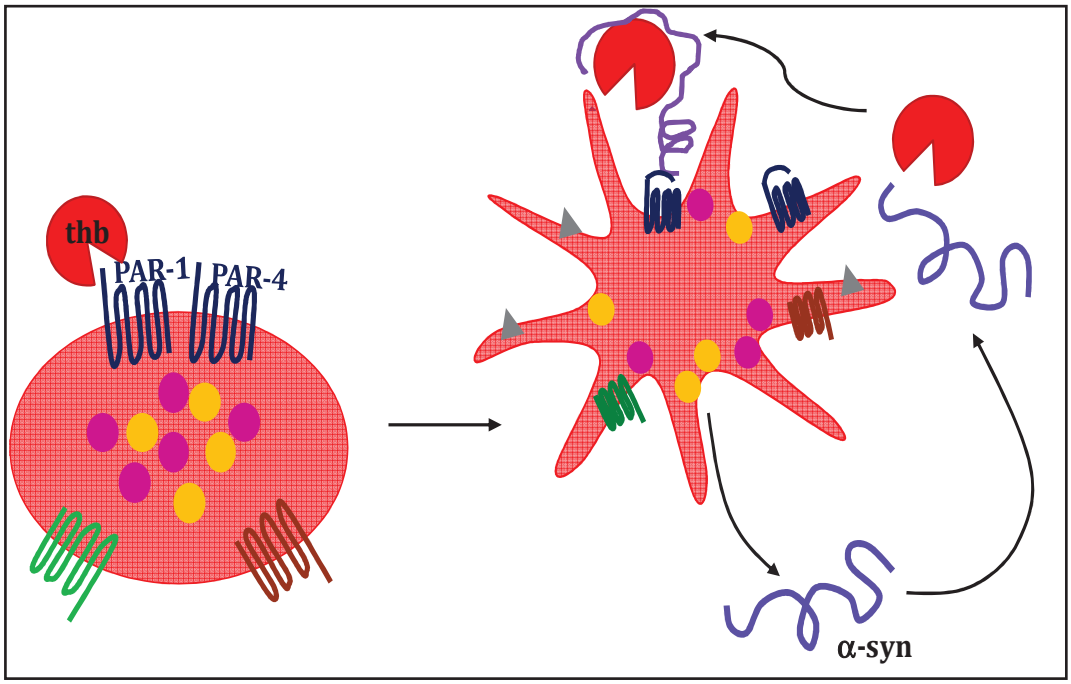

Figure 3.9 Schematic representation of interaction between α-synuclein and thrombin on the platelets surface. Upon thrombin activation platelets secret α-syn from α-granules; the protein interacts by C-terminal portion to thrombin exosites, while the N-terminal region binds to membrane surface in the vicinity of platelet receptors.

REFERENCES

1. Dikiy, I., and Eliezer, D. (2011) Folding and misfolding of alpha-synuclein on membranes. *Biochim.Biophys.Acta.*

2. Goedert, M. (2001) Alpha-synuclein and neurodegenerative diseases. *Nat.Rev.Neurosci.* 2, 492-501

3. Watson, J.B., Hatami, A., David, H., Masliah, E., Roberts, K., Evans, C.E., and Levine, M.S. (2009) Alterations in corticostriatal synaptic plasticity in mice overexpressing human alpha-synuclein. *Neuroscience.* 159, 501-513

4. George, J.M., Jin, H., Woods, W.S., and Clayton, D.F. (1995) Characterization of a novel protein regulated during the critical period for song learning in the zebra finch. *Neuron.* 15, 361-372

5. Murphy, D.D., Rueter, S.M., Trojanowski, J.Q., and Lee, V.M. (2000) Synucleins are developmentally expressed, and alpha-synuclein regulates the size of the presynaptic vesicular pool in primary hippocampal neurons. *J.Neurosci.* 20, 3214-3220

6. Shin, E.C., Cho, S.E., Lee, D.K., Hur, M.W., Paik, S.R., Park, J.H., and Kim, J. (2000) Expression patterns of alpha-synuclein in human hematopoietic cells and in Drosophila at different developmental stages. *Mol.Cells.* 10, 65-70

7. Hashimoto, M., Yoshimoto, M., Sisk, A., Hsu, L.J., Sundsmo, M., Kittel, A., Saitoh, T., Miller, A., and Masliah, E. (1997) NACP, a Synaptic Protein Involved in Alzheimer's Disease, Is Differentially Regulated during Megakaryocyte Differentiation. *Biochem.Biophys.Res.Commun.* 237, 611-616

8. Bode, W., and Huber, R. (1992) Natural protein proteinase inhibitors and their interaction with proteinases. *Eur.J.Biochem.* 204, 433-451

9. Siller-Matula, J.M., Schwameis, M., Blann, A., Mannhalter, C., and Jilma, B. (2011) Thrombin as a multi-functional enzyme. Focus on in vitro and in vivo effects. *Thromb.Haemost.* 106, 1020-1033

10. Choi, S.H., Joe, E.H., Kim, S.U., and Jin, B.K. (2003) Thrombin-induced microglial activation produces degeneration of nigral dopaminergic neurons in vivo. *J.Neurosci.* 23, 5877-5886

11. Dihanich, M., Kaser, M., Reinhard, E., Cunningham, D., and Monard, D. (1991) Prothrombin mRNA is expressed by cells of the nervous system. *Neuron.* 6, 575-581

12. Weinstein, J.R., Gold, S.J., Cunningham, D.D., and Gall, C.M. (1995) Cellular localization of thrombin receptor mRNA in rat brain: expression by mesencephalic

dopaminergic neurons and codistribution with prothrombin mRNA. *J.Neurosci.* 15, 2906-2919

13. Smith-Swintosky, V.L., Cheo-Isaacs, C.T., D'Andrea, M.R., Santulli, R.J., Darrow, A.L., and Andrade-Gordon, P. (1997) Protease-activated receptor-2 (PAR-2) is present in the rat hippocampus and is associated with neurodegeneration. *J.Neurochem.* 69, 1890-1896

14. Steinhoff, M., Vergnolle, N., Young, S.H., Tognetto, M., Amadesi, S., Ennes, H.S., Trevisani, M., Hollenberg, M.D., Wallace, J.L., Caughey, G.H., Mitchell, S.E., Williams, L.M., Geppetti, P., Mayer, E.A., and Bunnett, N.W. (2000) Agonists of proteinase-activated receptor 2 induce inflammation by a neurogenic mechanism. *Nat.Med.* 6, 151-158

15. Vaughan, P.J., Pike, C.J., Cotman, C.W., and Cunningham, D.D. (1995) Thrombin receptor activation protects neurons and astrocytes from cell death produced by environmental insults. *J.Neurosci.* 15, 5389-5401

16. Smirnova, I.V., Zhang, S.X., Citron, B.A., Arnold, P.M., and Festoff, B.W. (1998) Thrombin is an extracellular signal that activates intracellular death protease pathways inducing apoptosis in model motor neurons. *J.Neurobiol.* 36, 64-80

17. Nishino, A., Suzuki, M., Ohtani, H., Motohashi, O., Umezawa, K., Nagura, H., and Yoshimoto, T. (1993) Thrombin may contribute to the pathophysiology of central nervous system injury. *J.Neurotrauma.* 10, 167-179

18. Park, S.M., Jung, H.Y., Kim, H.O., Rhim, H., Paik, S.R., Chung, K.C., Park, J.H., and Kim, J. (2002) Evidence that alpha-synuclein functions as a negative regulator of Ca(++)-dependent alpha-granule release from human platelets. *Blood.* 100, 2506-2514

19. Kim, K.S., Park, J.Y., Jou, I., and Park, S.M. (2010) Regulation of Weibel-Palade body exocytosis by alpha-synuclein in endothelial cells. *J.Biol.Chem.* 285, 21416-21425

20. Sharma, P., Nag, D., Atam, V., Seth, P.K., and Khanna, V.K. (1991) Platelet aggregation in patients with Parkinson's disease. *Stroke.* 22, 1607-1608

21. Factor, S.A., Ortof, E., Dentinger, M.P., Mankes, R., and Barron, K.D. (1994) Platelet morphology in Parkinson's disease: an electron microscopic study. *J.Neurol.Sci.* 122, 84-89

22. Lancellotti, S., and De Cristofaro, R. (2009) Nucleotide-derived thrombin inhibitors: a new tool for an old issue. *Cardiovasc.Hematol.Agents Med.Chem.* 7, 19-28

23. De Filippis, V., Vindigni, A., Altichieri, L., and Fontana, A. (1995) Core domain of hirudin from the leech Hirudinaria manillensis: chemical synthesis, purification, and characterization of a Trp3 analog of fragment 1-47. *Biochemistry.* 34, 9552-9564

24. Albani, D., Peverelli, E., Rametta, R., Batelli, S., Veschini, L., Negro, A., and Forloni, G. (2004) Protective effect of TAT-delivered alpha-synuclein: relevance of the C-terminal domain and involvement of HSP70. *FASEB J.* 18, 1713-1715

25. Fields, G.B., and Noble, R.L. (1990) Solid phase peptide synthesis utilizing 9-fluorenylmethoxycarbonyl amino acids. *Int.J.Pept.Protein Res.* 35, 161-214

26. Munishkina, L.A., Phelan, C., Uversky, V.N., and Fink, A.L. (2003) Conformational behavior and aggregation of alpha-synuclein in organic solvents: modeling the effects of membranes. *Biochemistry.* 42, 2720-2730

27. Giehm, L., Lorenzen, N., and Otzen, D.E. (2011) Assays for alpha-synuclein aggregation. *Methods.* 53, 295-305

28. Scopes, R.K. (1974) Measurement of protein by spectrophotometry at 205 nm. *Anal.Biochem.* 59, 277-282

29. Pozzi, N., Acquasaliente, L., Frasson, R., Cristiani, A., Moro, S., Banzato, A., Pengo, V., Scaglione, G.L., Arcovito, A., De Cristofaro, R., and De Filippis, V. (2013) beta2-Glycoprotein I Binds Thrombin and Selectively Inhibits the Enzyme Procoagulant Functions. *J.Thromb.Haemost.*

30. De Filippis, V., De Dea, E., Lucatello, F., and Frasson, R. (2005) Effect of Na+ binding on the conformation, stability and molecular recognition properties of thrombin. *Biochem.J.* 390, 485-492

31. Evans, S.A., Olson, S.T., and Shore, J.D. (1982) p-Aminobenzamidine as a fluorescent probe for the active site of serine proteases. *J.Biol.Chem.* 257, 3014-3017

32. Birdsall, B., King, R.W., Wheeler, M.R., Lewis, C.A.,Jr, Goode, S.R., Dunlap, R.B., and Roberts, G.C. (1983) Correction for light absorption in fluorescence studies of protein-ligand interactions. *Anal.Biochem.* 132, 353-361

33. De Cristofaro, R., and Di Cera, E. (1991) Phenomenological analysis of the clotting curve. *J.Protein Chem.* 10, 455-468

34. Kinlough-Rathbone, R.L., Perry, D.W., Guccione, M.A., Rand, M.L., and Packham, M.A. (1993) Degranulation of human platelets by the thrombin receptor peptide SFLLRN: comparison with degranulation by thrombin. *Thromb.Haemost.* 70, 1019-1023

35. Toth, O., Calatzis, A., Penz, S., Losonczy, H., and Siess, W. (2006) Multiple electrode aggregometry: a new device to measure platelet aggregation in whole blood. *Thromb.Haemost.* 96, 781-788

36. Pozzi, N., Barranco-Medina, S., Chen, Z., and Di Cera, E. (2012) Exposure of R169 controls protein C activation and autoactivation. *Blood.* 120, 664-670

37. Huang, C., Ren, G., Zhou, H., and Wang, C.C. (2005) A new method for purification of recombinant human alpha-synuclein in Escherichia coli. *Protein Expr.Purif.* 42, 173-177

38. Mahler, H.C., Friess, W., Grauschopf, U., and Kiese, S. (2009) Protein aggregation: pathways, induction factors and analysis. *J.Pharm.Sci.* 98, 2909-2934

39. Uversky, V.N., Li, J., and Fink, A.L. (2001) Evidence for a partially folded intermediate in alpha-synuclein fibril formation. *J.Biol.Chem.* 276, 10737-10744

40. Lancellotti, S., Rutella, S., De Filippis, V., Pozzi, N., Rocca, B., and De Cristofaro, R. (2008) Fibrinogen-elongated gamma chain inhibits thrombin-induced platelet response, hindering the interaction with different receptors. *J.Biol.Chem.* 283, 30193-30204

41. Jackman, M.P., Parry, M.A., Hofsteenge, J., and Stone, S.R. (1992) Intrinsic fluorescence changes and rapid kinetics of the reaction of thrombin with hirudin. *J.Biol.Chem.* 267, 15375-15383

42. Bah, A., Garvey, L.C., Ge, J., and Di Cera, E. (2006) Rapid kinetics of Na+ binding to thrombin. *J.Biol.Chem.* 281, 40049-40056

43. Sabo, T.M., and Maurer, M.C. (2009) Biophysical investigation of GpIbalpha binding to thrombin anion binding exosite II. *Biochemistry.* 48, 7110-7122

44. Krem, M.M., and Di Cera, E. (2003) Dissecting substrate recognition by thrombin using the inactive mutant S195A. *Biophys.Chem.* 100, 315-323

45. Deinum, J., Gustavsson, L., Gyzander, E., Kullman-Magnusson, M., Edstrom, A., and Karlsson, R. (2002) A thermodynamic characterization of the binding of thrombin inhibitors to human thrombin, combining biosensor technology, stopped-flow spectrophotometry, and microcalorimetry. *Anal.Biochem.* 300, 152-162

46. De Filippis, V., Colombo, G., Russo, I., Spadari, B., and Fontana, A. (2002) Probing the hirudin-thrombin interaction by incorporation of noncoded amino acids and molecular dynamics simulation. *Biochemistry.* 41, 13556-13569

47. Skrzypczak-Jankun, E., Carperos, V.E., Ravichandran, K.G., Tulinsky, A., Westbrook, M., and Maraganore, J.M. (1991) Structure of the hirugen and hirulog 1 complexes of alpha-thrombin. *J.Mol.Biol.* 221, 1379-1393

48. Naski, M.C., Fenton, J.W.,2nd, Maraganore, J.M., Olson, S.T., and Shafer, J.A. (1990) The COOH-terminal domain of hirudin. An exosite-directed competitive inhibitor of the action of alpha-thrombin on fibrinogen. *J.Biol.Chem.* 265, 13484-13489

49. Kelly, S.M., Jess, T.J., and Price, N.C. (2005) How to study proteins by circular dichroism. *Biochim.Biophys.Acta.* 1751, 119-139

50. Hashimoto, M., Yoshimoto, M., Sisk, A., Hsu, L.J., Sundsmo, M., Kittel, A., Saitoh, T., Miller, A., and Masliah, E. (1997) NACP, a synaptic protein involved in Alzheimer's disease, is differentially regulated during megakaryocyte differentiation. *Biochem.Biophys.Res.Commun.* 237, 611-616

51. Jennings, L.K. (2009) Mechanisms of platelet activation: need for new strategies to protect against platelet-mediated atherothrombosis. *Thromb.Haemost.* 102, 248-257

52. Kahn, M.L., Zheng, Y.W., Huang, W., Bigornia, V., Zeng, D., Moff, S., Farese, R.V.,Jr, Tam, C., and Coughlin, S.R. (1998) A dual thrombin receptor system for platelet activation. *Nature.* 394, 690-694

53. Ruggeri, Z.M. (2002) Platelets in atherothrombosis. *Nat.Med.* 8, 1227-1234

54. Barbour, R., Kling, K., Anderson, J.P., Banducci, K., Cole, T., Diep, L., Fox, M., Goldstein, J.M., Soriano, F., Seubert, P., and Chilcote, T.J. (2008) Red blood cells are the major source of alpha-synuclein in blood. *Neurodegener Dis.* 5, 55-59

CHAPTER 4.1

Human Ceruloplasmin

Human ceruloplasmin (CP) is a protein from the α2-globulin fraction of human blood serum. This protein belongs to the family of multicopper oxidases (MCO), that includes ascorbate oxidase and laccase, and accounts for 95% of plasma copper (1). Copper ions in the CP molecule provide a large number of enzymatic activities. It was first isolated in 1944 (2) and has a molecular weight of some 132 kDa, being comprised of a single polypeptide chain of 1046 amino acid residues with a carbohydrate content of 7-8% (3). Serum CP is synthesized in the liver; however, its gene is also expressed in the brain, lungs, spleen, testis and some other organs of mammals (1).

Structure of Human Ceruoloplasmin

The first X-ray structural study of CP was reported in 1996 (i.e. 3.1 Å) (4) and shows that the molecule is comprised of six cupredoxin-type domains arranged in a triangular array. It is also shown that there are six integral copper ions, three of which form a trinuclear cluster at the interface of domains 1 and 6, whilst the remainder are arranged in three monuclear sites, one each in domains 2, 4 and 6 (Fig. 4.1). Each of the monuclear copper ions is coordinated to a cysteine and two histidine residues and those in domains 4 and 6 also coordinate weakly to a methionine residue; in domain 2, methionine is replaced by leucine at a van der Waals distance from the cation. Chemically, in domain 6 there are one type I Cu^{2+}, one type II Cu^{2+} and one type III Cu^{2+}, whereas the remaining type III $Cu2^{+}$ is coordinated by ligands of domain 1. Two additional type I (or 'blue') coppers are set apart from the catalytic centre, i.e. in domains 2 and 4 (4). Moreover, the lower surface of the molecule is relatively flat and positively charged, whereas the upper surface presents three large protuberances and is strongly negatively charged.

The arrangements of the trinuclear center and the mononuclear copper ion in domain 6 are essentially the same as that found in ascorbate oxidase and other members of the laccase family, strongly suggesting an oxidase role for CP in the plasma(5).

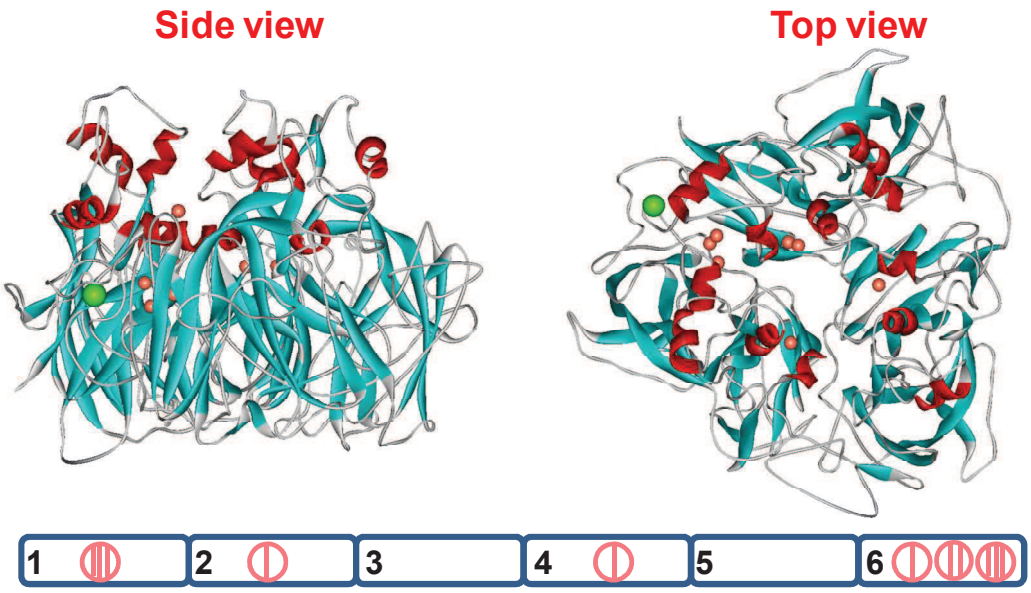

Figure 4.1 Overall organization of the human ceruloplasmin molecule (4ENZ.pdb). Left: side view; right: top view. β-sheets are colored in cyan, while helices are in red; copper (pink) and Ca^{+2} (green) ions are also shown. Below it is reported the distribution of copper ions. In domain 6 there are one type I Cu^{2+}, one type II Cu^{2+} and one type III Cu^{2+}, whereas the type III Cu^{2+} is coordinated by ligands of domain 1. Two more type I coppers are set apart from the catalytic centre, in domains 2 and 4.

Physiological Functions of Human Ceruloplasmin: a Moonlighting protein

Despite intensive studies of CP in the last 60 years, it is believed that only some of its most visible functions have been disclosed. CP is nowadays regarded as a "moonlighting" protein, because the protein can change its function in response to changes in substrate, localization and expression (6, 7).

CP plays a key role in copper storage (i.e. > 95% of plasma copper is bound to CP) and transport, as well as in iron metabolism and homeostasis. CP oxidizes Fe^{+2} to Fe^{+3}, which is then transferred in the plasma to apo-transferrin for delivery (8), and then holo-transferrin transports Fe^{3+} to haemoglobin of reticulocytes. Thus CP acquired its systematic name "ferro–O_2 oxidoreductase", although it is often termed "ferroxidase" (9). Importantly, the ferroxidase activity of CP reduces the concentration of free Fe^{+2} available for initiating Fe^{+2}–catalyzed lipid peroxidation, with a resulting marked antioxidant effect (6, 7, 10). Indeed, CP oxidizes highly toxic ferrous ions to the ferric state for further incorporation into, catalyzes Cu(I) oxidation (11) and promotes the oxidation of biogenic amines (norepinephrine, serotonin), synthetic amines (p-phenylenediamine (p-PD) and o-dianisidine (o-DA) (12).

Further, CP is the only plasma protein demonstrating the activity of NO-oxidase, NO_2-syntase (13), glutathione-linked peroxidase (14) and superoxide dismutase (15). These

properties make CP an effective antioxidant, able to prevent oxidative damage to proteins, DNA and lipids (16). The protein, in fact, can reduce the concentration of superoxide radical (O2•-) and nitric oxide (NO•) available for generating peroxynitrite (ONOO-) (13), a highly potent and tissue harmful oxidant (17).

Interaction of Human Ceruloplasmin with Other Proteins

CP seems to have an antioxidant-protective function. Recent studies indicated that the protein inhibits lipoxygenase (18) and several other leukocyte proteins/enzymes related to inflammatory and septic processes (19, 20). *In vitro* incorporation of Fe^{3+} into ferritin was shown to depend on the formation of CP-ferritin complex (21). In addition, the ability of CP to interact with myeloperoxidase (MPO) and to inhibit its pro-oxidant properties (22) likely imparts it with additional antioxidant activity in vivo: CP potently inhibits (Kd = 130 nM) leukocyte myeloperoxidase (MPO) both *in vitro* (23-26) and *in vivo* (23). In fact, the low-resolution crystallographic structure of MPO-CP complex shows that CP covers the enzyme active site, thus hindering MPO function (27). The protein interacts with the iron-binding protein lactoferrin (LF) (28, 29), and in the presence of MPO e LF forms a triple complex, under physiological conditions (23). CP may also be involved in regulating inflammation by interacting with macrophage migration inhibitory factor (30).

The interaction of CP with neuropeptide PACAP (31) probably plays a certain role in neuroregulation processes. Due to complex formation with ferroportin I, the membrane-bound CP found in astrocytes participates in regulation of iron levels in the central nervous system and in the prevention of free radical reaction. Finally, CP is suggested to participate in the regulation of clotting via its competition with blood coagulation factors FV and FVIII for protein C binding (32).

Human Ceruloplasmin in the Rheumatoid Arthritis

Rheumatoid arthritis (RA) is a chronic, systemic, inflammatory autoimmune disorder causing symmetrical polyarthritis of large and small joints, typically presenting between the ages of 30 and 50 years. RA primarily affects joints however it also affects other organs (i.e. skin, lungs, kidneys, heart and blood vessels) in 15–25% of individuals. The etiology of RA is not fully understood but involves a complex interplay of environmental and genetic factors. Complex interactions among multiple immune cell types and their cytokines, proteinases, and growth factors mediate joint destruction and systemic complications (33) (Fig. 4.2).

The plasma level of CP is an important diagnostic indicator of neoplastic and inflammatory diseases, such us carcinoma, leukemia, primary biliary cirrhosis, systemic lupus erythematosus and RA (34). It was observed that in inflamed tissues and in the synovial fluid of RA patients CP and thrombin concentrations are markedly increased (35). CP level tend to be higher in RA female patients as compared to male, instead there does not seem to be a correlation between the protein concentration and the age of subjects (34). In addition, significant positive correlation was found between the immunereactive CP, oxidase activity and copper in the patients with RA. However, significant correlations were also obtained for CP oxidase activity with C-reactive protein and erythrocyte sedimentation rate, which are accepted as biological inflammatory markers of RA (36). These results call into question the effectiveness with which the modulation of oxidative stress, influenced by CP, might have on the progress of disease.

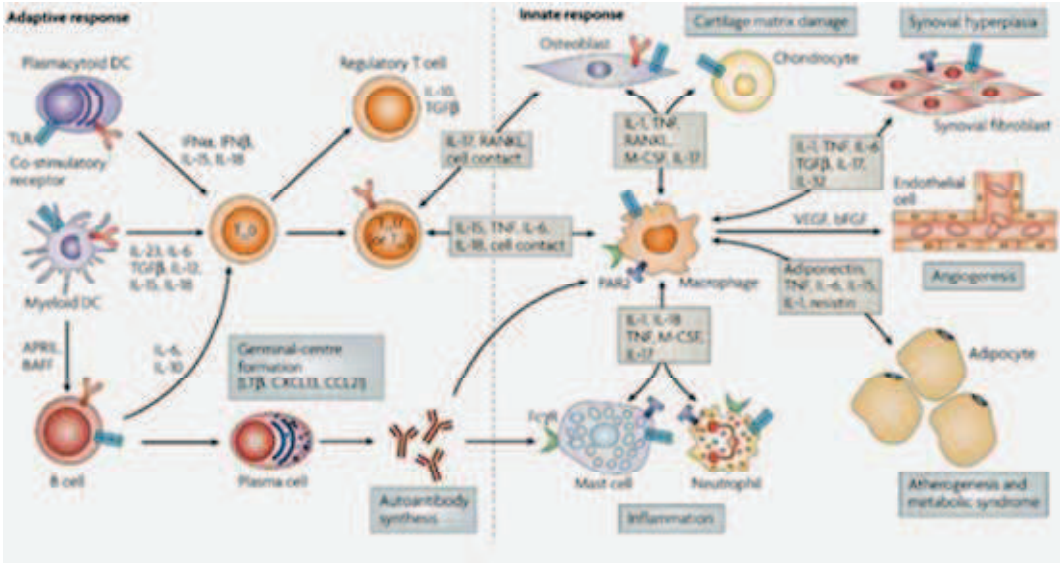

Figure 4.2 An overview of the cytokine-mediated regulation of synovial interactions. The component cells of the inflamed rheumatoid synovial membrane are depicted in innate and adaptive predominant compartments of the inflammatory response. Pivotal cytokine pathways are depicted in which activation of dendritic cells (DCs), T cells, B cells and macrophages underpins the disregulated expression of cytokines that in turn drive activation of effector cells, including neutrophils, mast cells, endothelial cells and synovial fibroblasts. This figure was adapted from (37).

REFERENCES

1. Vasilyev, V.B. (2010) Interactions of caeruloplasmin with other proteins participating in inflammation. *Biochem.Soc.Trans.* 38, 947-951
2. Holmberg, C.G. (1944) On the Presence of n laccase-like Enzyme in Nerum and its Relation to the Copper in Serum. *Acta Physiol.Scand.* 8, 227-229
3. Takahashi, N., Ortel, T.L., and Putnam, F.W. (1984) Single-chain structure of human ceruloplasmin: the complete amino acid sequence of the whole molecule. *Proc.Natl.Acad.Sci.U.S.A.* 81, 390-394
4. Zaitsev, V.N., Zaitseva, I., Papiz, M., and Lindley, P.F. (1999) An X-ray crystallographic study of the binding sites of the azide inhibitor and organic substrates to ceruloplasmin, a multi-copper oxidase in the plasma. *J.Biol.Inorg.Chem.* 4, 579-587
5. Bento, I., Peixoto, C., Zaitsev, V.N., and Lindley, P.F. (2007) Ceruloplasmin revisited: structural and functional roles of various metal cation-binding sites. *Acta Crystallogr.D Biol.Crystallogr.* 63, 240-248
6. Bielli, P., and Calabrese, L. (2002) Structure to function relationships in ceruloplasmin: a 'moonlighting' protein. *Cell Mol.Life Sci.* 59, 1413-1427
7. Shukla, N., Maher, J., Masters, J., Angelini, G.D., and Jeremy, J.Y. (2006) Does oxidative stress change ceruloplasmin from a protective to a vasculopathic factor?. *Atherosclerosis.* 187, 238-250
8. Hellman, N.E., and Gitlin, J.D. (2002) Ceruloplasmin metabolism and function. *Annu.Rev.Nutr.* 22, 439-458
9. Andrews, N.C. (2008) Forging a field: the golden age of iron biology. *Blood.* 112, 219-230
10. Floris, G., Medda, R., Padiglia, A., and Musci, G. (2000) The physiopathological significance of ceruloplasmin. A possible therapeutic approach. *Biochem.Pharmacol.* 60, 1735-1741
11. Stoj, C., and Kosman, D.J. (2003) Cuprous oxidase activity of yeast Fet3p and human ceruloplasmin: implication for function. *FEBS Lett.* 554, 422-426
12. Young, S.N., and Curzon, G. (1972) A method for obtaining linear reciprocal plots with caeruloplasmin and its application in a study of the kinetic parameters of caeruloplasmin substrates. *Biochem.J.* 129, 273-283
13. Shiva, S., Wang, X., Ringwood, L.A., Xu, X., Yuditskaya, S., Annavajjhala, V., Miyajima, H., Hogg, N., Harris, Z.L., and Gladwin, M.T. (2006) Ceruloplasmin is a NO oxidase and nitrite synthase that determines endocrine NO homeostasis. *Nat.Chem.Biol.* 2, 486-493

14. Park, Y.S., Suzuki, K., Taniguchi, N., and Gutteridge, J.M. (1999) Glutathione peroxidase-like activity of caeruloplasmin as an important lung antioxidant. *FEBS Lett.* 458, 133-136
15. Gutteridge, J.M., and Quinlan, G.J. (1992) Antioxidant protection against organic and inorganic oxygen radicals by normal human plasma: the important primary role for iron-binding and iron-oxidising proteins. *Biochim.Biophys.Acta.* 1159, 248-254
16. Kim, R.H., Park, J.E., and Park, J.W. (2000) Ceruloplasmin enhances DNA damage induced by hydrogen peroxide in vitro. *Free Radic.Res.* 33, 81-89
17. Pacher, P., Beckman, J.S., and Liaudet, L. (2007) Nitric oxide and peroxynitrite in health and disease. *Physiol.Rev.* 87, 315-424
18. Sokolov, A.V., Golenkina, E.A., Kostevich, V.A., Vasilyev, V.B., and Sud'ina, G.F. (2010) Interaction of ceruloplasmin and 5-lipoxygenase. *Biochemistry (Mosc).* 75, 1464-1469
19. Sokolov, A.V., Ageeva, K.V., Kostevich, V.A., Berlov, M.N., Runova, O.L., Zakharova, E.T., and Vasilyev, V.B. (2010) Study of interaction of ceruloplasmin with serprocidins. *Biochemistry (Mosc).* 75, 1361-1367
20. Sokolov, A.V., Pulina, M.O., Zakharova, E.T., Shavlovski, M.M., and Vasilyev, V.B. (2005) Effect of lactoferrin on the ferroxidase activity of ceruloplasmin. *Biochemistry (Mosc).* 70, 1015-1019
21. Van Eden, M.E., and Aust, S.D. (2000) Intact human ceruloplasmin is required for the incorporation of iron into human ferritin. *Arch.Biochem.Biophys.* 381, 119-126
22. Segelmark, M., Persson, B., Hellmark, T., and Wieslander, J. (1997) Binding and inhibition of myeloperoxidase (MPO): a major function of ceruloplasmin?. *Clin.Exp.Immunol.* 108, 167-174
23. Sokolov, A.V., Pulina, M.O., Ageeva, K.V., Ayrapetov, M.I., Berlov, M.N., Volgin, G.N., Markov, A.G., Yablonsky, P.K., Kolodkin, N.I., Zakharova, E.T., and Vasilyev, V.B. (2007) Interaction of ceruloplasmin, lactoferrin, and myeloperoxidase. *Biochemistry (Mosc).* 72, 409-415
24. Sokolov, A.V., Prozorovskii, V.N., and Vasilyev, V.B. (2009) Study of interaction of ceruloplasmin, lactoferrin, and myeloperoxidase by photon correlation spectroscopy. *Biochemistry (Mosc).* 74, 1225-1227
25. Griffin, S.V., Chapman, P.T., Lianos, E.A., and Lockwood, C.M. (1999) The inhibition of myeloperoxidase by ceruloplasmin can be reversed by anti-myeloperoxidase antibodies. *Kidney Int.* 55, 917-925

26. Park, Y.S., Suzuki, K., Mumby, S., Taniguchi, N., and Gutteridge, J.M. (2000) Antioxidant binding of caeruloplasmin to myeloperoxidase: myeloperoxidase is inhibited, but oxidase, peroxidase and immunoreactive properties of caeruloplasmin remain intact. *Free Radic.Res.* 33, 261-265
27. Samygina, V.R., Sokolov, A.V., Bourenkov, G., Petoukhov, M.V., Pulina, M.O., Zakharova, E.T., Vasilyev, V.B., Bartunik, H., and Svergun, D.I. (2013) Ceruloplasmin: macromolecular assemblies with iron-containing acute phase proteins. *PLoS One.* 8, e67145
28. Zakharova, E.T., Shavlovski, M.M., Bass, M.G., Gridasova, A.A., Pulina, M.O., De Filippis, V., Beltramini, M., Di Muro, P., Salvato, B., Fontana, A., Vasilyev, V.B., and Gaitskhoki, V.S. (2000) Interaction of lactoferrin with ceruloplasmin. *Arch.Biochem.Biophys.* 374, 222-228
29. Pulina, M.O., Zakharova, E.T., Sokolov, A.V., Shavlovski, M.M., Bass, M.G., Solovyov, K.V., Kokryakov, V.N., and Vasilyev, V.B. (2002) Studies of the ceruloplasmin-lactoferrin complex. *Biochem.Cell Biol.* 80, 35-39
30. Meyer-Siegler, K.L., Iczkowski, K.A., and Vera, P.L. (2006) Macrophage migration inhibitory factor is increased in the urine of patients with urinary tract infection: macrophage migration inhibitory factor-protein complexes in human urine. *J.Urol.* 175, 1523-1528
31. Tams, J.W., Johnsen, A.H., and Fahrenkrug, J. (1999) Identification of pituitary adenylate cyclase-activating polypeptide1-38-binding factor in human plasma, as ceruloplasmin. *Biochem.J.* 341 (Pt 2), 271-276
32. Walker, F.J., and Fay, P.J. (1990) Characterization of an interaction between protein C and ceruloplasmin. *J.Biol.Chem.* 265, 1834-1836
33. Majithia, V., and Geraci, S.A. (2007) Rheumatoid arthritis: diagnosis and management. *Am.J.Med.* 120, 936-939
34. Lopez-Avila, V., Sharpe, O., and Robinson, W.H. (2006) Determination of ceruloplasmin in human serum by SEC-ICPMS. *Anal.Bioanal Chem.* 386, 180-187
35. Nakano, S., Ikata, T., Kinoshita, I., Kanematsu, J., and Yasuoka, S. (1999) Characteristics of the protease activity in synovial fluid from patients with rheumatoid arthritis and osteoarthritis. *Clin.Exp.Rheumatol.* 17, 161-170
36. Louro, M.O., Cocho, J.A., Mera, A., and Tutor, J.C. (2000) Immunochemical and enzymatic study of ceruloplasmin in rheumatoid arthritis. *J.Trace Elem.Med.Biol.* 14, 174-178

37. McInnes, I.B., and Schett, G. (2007) Cytokines in the pathogenesis of rheumatoid arthritis. Nat.Rev.Immunol. 7, 429-442

CHAPTER 4.2

Thrombin Proteolytically Hinders the Antioxidant Activity of Human Ceruloplasmin: Implications in the Pathogenesis of Rheumatoid Arthritis

INTRODUCTION

Human ceruloplasmin (CP) is a circulating copper-containing glycoprotein (1046 amino acids, ~ 132 kDa) produced in the liver and first described as a component of α_2-globulin fraction of human plasma (1). CP belongs to the multicopper oxidase family (2) and it is nowadays regarded as a "moonlighting" protein, because changes its function as a function of in substrate, localization and expression (3, 4). CP plays a key role in copper storage and transport, as well as in iron metabolism and homeostasis (2). The ferroxidase activity of CP reduces the concentration of free Fe^{+2} available for initiating Fe^{+2}–catalyzed lipid peroxidation, with a resulting marked antioxidant effect (3-5). CP protects tissues form damage induced by reactive oxygen and nitrogen species (ROS and RNS) by exerting both superoxide dismutase (6) and NO oxidase functions (7), that decrease the concentration of superoxide radical ($O2\cdot^-$) and nitric oxide ($NO\cdot$) available for generating peroxynitrite (ONOO-) (7). CP is also a key component of the physiological acute phase response (3, 5), i.e. CP plasma concentration is triplicated in acute phase inflammation (8) while its disfunction has been associated with cardiovascular and neurodegenerative diseases (4)

CP structure contains six cupredoxin-type domains, each consisting of 150-190 amino acid residues (9-11). The even domains 2, 4 and 6 bind a copper ion each, while the interface between domains 1 and 6 hosts a trinuclear copper centre, which is close to a Ca^{2+}-binding site in domain 1. The oxygen reductase function of CP has been associated with the trinuclear copper center, whereas the ferroxidase activity is accomplished by the copper site in domain 6. In keeping with its antioxidant/protective function, it was recently reported that CP inhibits lipoxygenase and several other leukocyte proteins/enzymes related to inflammatory and septic processes (12-14). Furthermore, we and others have discovered that CP potently inhibits (Kd =130nM) leukocyte myeloperoxidase (MPO) both *in vitro* and *in vivo* (15-19). Interestingly, the catalytic pocket of MPO contains heme, which is instrumental for ROS and RNS generation (20). The low-resolution crystallographic structure of MPO-CP complex (4ejx) shows that CP

covers the enzyme active site, thus hindering MPO function (11). Although MPO represents a front-line defense against bacteria in innate immunity, the aberrant production/release of MPO from activated neutrophiles, even in the absence of infection, can damage host tissues, amplify inflammation and set the basis for the onset of several different diseases (20). In particular, compared with healthy controls, plasma MPO concentrations are significantly higher in patients with rheumatoid arthritis (RA) (21), a systemic autoimmune disease characterized by synovial inflammation and hyperplasia, leading to progressive cartilage and bone destruction (22). In this scenario, the potent inhibitory effect of CP on MPO oxidase function further emphasizes the role of this cooper-protein in promoting the antioxidant response in human plasma (3, 19, 23).

Thrombin is a serine protease, strategically positioned at the interface of coagulation, inflammation and cell proliferation (24-26). Thrombin has a chymotrypsin-like fold (27) and accomplishes most of its activities through the hydrolytic active site, located in a deep crevice at the interface of two β-barrels, two positively charged exosites (exosite-I and exosite-II) located at opposite sides from the catalytic cleft. The procoagulant functions of thrombin entail conversion of soluble fibrinogen into insoluble fibrin and activation of platelets through cleavage of protease activated receptor 1 (PAR-1). Thrombin also acts as a proinflammatory and chemotactic mediator by inducing, *via* PAR cleavage, the production of inflammatory cytokines in monocytes and macrophages (28). As observed with CP, thrombin concentration is markedly increased in inflammed tissues and specifically in the synovial fluid of RA patients (29).

In this study we have demonstrated that thrombin cleaves CP both *in vitro* and in the synovial fluid of RA patients only at two peptide bonds, thus generating a nicked species (CP*) formed by a stable non-covalent complex of three proteolytic fragments. Strikingly, CP* retains the ferroxidase function of intact CP, but has lost the MPO inhibitory function. We conclude that antioxidant/antiinflammatory function of CP is regulated by proteolysis of thrombin. These results are unprecedented and set the basis for elucidating the biochemical mechanisms underlying the progression of inflammation in RA patients and, hopefully, for developing novel therapeutic strategies.

MATERIALS AND METHODS

Materials

Acrylamide and reagents for electrophoresis were purchased from Medigen Laboratories (Novosibirsk, Russia); the reagents for surface plasmon resonance were from GE-Healthcare (Piscataway, NJ, USA); phenylmethylsulphonyl fluoride (PMSF), 2,2′-azino-bis(3-ethyl benzthiazoline-6-sulphonic acid) disodium salt (ABTS), $Fe(NH_4)_2(SO_4)_2 \cdot 6H_2O$, (D)-Phe-Pro-Arg-chloromethyl ketone (PPACK), thiourea, H_2O_2, and the chromogenic substrate Z-Ala-Ala-Arg-pNA•HBr were from Merck (Darmstadt, Germany). All other salts, detergents, solvents and reagents were of analytical grade and purcahased from Merck or Fluka. Hirudin HM2 from Hirudinaria manillensis was a generous gift of Dr. Orsini (Farmitalia-Carlo Erba, Italy); HD1 and HD22 aptamers were obtained from Primm (Milan, Italy hirugen(54-65) peptide, fibrinogen γ′-chain peptide(408-427), and hirudin N-terminal domain Hir(1-47) were chemically synthesized (30).

Biological Samples

Samples of human serum from healthy subjects were obtained from clotted venous blood after centrifugation at 5°C for 15 min at 500 g in the presence 0.01% (w/v) gentamycin as a bacteriostatic agent. 24 patients (12 males and 12 females) aged between 50 and 70, with established diagnosis of rheumatoid arthritis (RA) were examined. The patients enrolled in this study were under monitoring at the Institute of Experimental Medicine (St. Petersburg, Russia), having a history of RA at a different stage of progression of the disease. The protocols for all clinical studies were scrutinized and approved by the Ethical Committee of the Institute of Experimental medicine and all subjects gave their informed consent to the study. Synovial fluid (5-10 ml) was collected after knee joint puncture. Samples of each patient's synovial fluid were centrifuged at 5°C for 15 min at 500 g or 5 min at 15000 g, divided into aliquots (500 μl) and then rapidly placed at -80°C. Frozen samples were thawed at 37°C and used for further analyses.

Determination of the Copper Content in Biological Fluids

The levels of copper in serum and synovial fluid samples were determined as described (31). Briefly, the specimens were treated with threefold excess (w/w) of $HClO_4$:H_2SO_4 (4:1) solution. The mixture was centrifuged at 13000 g for 15 min, and the copper concentration in

the supernatant was determined by atomic absorption spectrometry using a PinAAcle 900 instrument (Perkin-Elmer, USA).

Purification of CP from Human Plasma

CP was isolated from human blood plasma by affinity chromatography on protamine-Sepharose as previously described (14), followed by benzamidine affinity chromatography to eliminate traces of contaminant serine proteases. All preparations had Abs 610_{nm}/Abs 280_{nm} >0.049 and contained more than 95% intact CP, as given by the presence of the 132-kDa electrophoretic band.

Limited Proteolysis of CP with Thrombin

To a solution of purified, intact hCP (2 mg/ml, 100 µl) in 10mM Tris-HCl pH 7.4, in 0.1M NaCl (TBS) human thrombin was added (50 NIH units/ml, final concentration). At time intervals, aliquots (10 µl) were taken, added with an equal volume of reducing sample loading buffer, and heated at 100°C for 3 min to stop the proteolytic reaction. Denatured samples were then analyzed by SDS-PAGE (4-10% acrylamide) and Coomassie stained.

Identification of Thrombin Cleavage Sites on CP by Edman Degradation and Peptide Mass Fingerprint Analysis

Electrophoretic bands corresponding to proteolytic hCP fragments were electrotransferred onto Immobilon membrane (BioRad, Hercules, CA, USA) using a semi-dry transfer device (Hoefer Scientific, Holliston, MA, USA) in Tris-HCl 20%ethanol-containing buffer. Coomassie stained bands on the Immobilon sheet were cut and subjected to Edman degradation on a Procise-491 automated protein sequencer (Applied Biosystems, Carlsbad, CA, USA). Proteolytic fragments were identified by in situ tryptic digestion of the corresponding electrophoretic bands followed by peptide mass fingerprint analysis. Briefly, 1-mm3 pieces of selected bands were excised from the gel and twice soaked for 30 min at 37°C in 100 µl of 0.1M NH_4HCO_3 containing 40% (v/v) acetonitrile to extract the dye. The aqueous/organic solution was discarded and, to dehydrate the gel, 100 µl of neat acetonitrile were added to the gel pieces. After acetonitrile was discarded and the gel air- dried, 4 µl of tosyl-phenyl-chloromethylketone(TPCK)-treated trypsin (Promega, Madison, WI, USA) (15 µg/ml) in 50mM NH_4HCO_3 were added. Hydrolysis was allowed to proceed for 18 h at 37°C and then 8 µl of peptide extracting mixture were added under gentle stirring. After

centrifugation at 2000 rpm for 3 min, the supernatant was collected and analyzed by mass spectrometry on an Ultraflex-II MALDI-TOF spectrometer (Bruker, Germany). Routinely, 1 µl of the supernatant solution was added with 0.3 µl of the matrix 2,5-dihydrobenzoic acid (10 mg/ml in 0.5% aqueous TFA containing 20% acetonitrile) and the resulting mixture was air-dried. Mass spectra were recorded in the reflectron positive ion mode with a mass accuracy of 50 ppm after internal calibration against the peaks of tryptic autolysis. Protein fragments were identified using the MASCOT search software (http://www.matrixscience.com).

Electrophoresis and Western Blotting

Polyacrylamide gel electrophoresis in the presence of SDS (SDS-PAGE) and Western blotting analyses were performed as described (16).CP bands were detected using a rabbit polyclonal anti-hCP antibody (Ab) (1:10000 dilution), as a primary Ab, and a peroxidase-conjugated goat anti-rabbit IgG (Calbiochem, Darmstadt,Germany) as a secondary Ab (1:5000 dilution). When holo- and apo-CP were being analyzed, samples for electrophoresis were prepared in the absence of SDS and without heat treatment (32).

Size-Exclusion Chromatography (SEC)

The molecular weight of CP and CP* was estimated by SEC. Aliquots of intact and nicked CP were loaded on a (1.6 x 30 cm) Superose-12 (GE-Healthcare, Piscataway, NJ, USA) column connected to an Äkta-Purifier biochromatography system and eluted at a flow rate of 0.3 ml/min with 25mM Tris-HCl pH 7.4, 0.15M NaCl. Nicked CP (CP*) was obtained by proteolysis of CP with thrombin at 37°C for 5 h. The molecular weight of CP and CP* was estimated after calibrating the column with the protein standards BSA (67 kDa), ovalbumin (44 kDa), carbonic anhydrase (29 kDa), RNAse (13.7 kDa), and aprotinin (6.5 kDa), according to the equation KD = (Ve-V0) (Vi-V0), where KD is the distribution constant, Ve is the elution volume of CP or CP*, whereas V0 and Vi are the void and interstitial volume of the column. V0 and Vi were calculated by loading blue dextran (2000 kDa) and the threepeptide Gly-Tyr-Gly (295 Da), respectively.

Spectroscopic Techniques

UV-Vis spectra were recorded on a V-630 spectrophotometer (Jasco, Tokyo, Japan). The concentration of thrombin and CP was determined by measuring the absorbance at 280 nm, using an extinction coefficient, $\varepsilon_{0.1\%}$, of 1.96 and 1.61 $mg^{-1} \cdot cm^2$ respectively. Fluorescence spectra were recorded on a Jasco FP-6500 spectrofluorimeter equipped with a thermostatted

cell holder and a Peltier ETC-273T temperature control system. Circular dichroism (CD) spectra were recorded on a Jasco J-810 spectropolarimeter equipped with a thermostatted cell holder and a Peltier PTC-423S temperature control system. Spectra were recorded on 0.1- or 1-cm pathlength cuvette in the far- and near-UV region, respectively. Each spectrum is was the average of four accumulations, after base line subtraction. Ellipticity data were expressed as the mean residue ellipticity, $[\theta] = (\theta \cdot MRW)/(10 \cdot l \cdot c)$, where θ is the measured ellipticity in degrees, MRW is the mean residue weight, l is the cuvette pathlength, and c is the protein concentration in g/ml.

CP Ferroxidase Activity

During the time-course proteolysis of hCP (2 mg/ml) with thrombin at increasing time points, the ferroxidase activity of the proteolytic reaction was determined at 25°C by recording the increase of absorbance at 310 nm, resulting from the formation of Fe^{+3} complex with N,N′-dimethylformamide (DMF) at a fixed $[Fe^{+2}]$. Aliquots (10 µl) of the hCP proteolysis mixture (0.8 µM, final concentration) was added to solutions of 1% (v/v) DMF in 0.1M sodium acetate buffer pH 5.5, containing 30µM thiourea and 200µM ferrous $Fe(NH_4)_2(SO_4)_2$•6H2O. The inhibition of hCP ferroxidase activity by thrombin was measured at 37°C in the presence of increasing concentrations of human thrombin (0 - 360nM), irreversibly inhibited at the active site with equimolar concentrations of phenylmethylsulphonyl fluoride (PMSF). The initial rate (v) of Fe^{+3} generation was plotted as a function of substrate concentration, $[Fe^{+2}]$, according to the Hanes-Woolf equation (eq.1):

$$[Fe^{+2}]/v = (1/v_{max}) \cdot [Fe^{+2}] + (Km_{app}/v_{max}) \quad \text{(eq.1)}$$

where v_{max} is the values of the maximum reaction rate and, Km_{app} is the apparent Michaelis constant.

After plotting the values of Km_{app} versus [PMSF-thrombin] and fitting the data points to the eq.2 the value of the inhibition constant, KI, was extrapolated as the intercept of the straight line:

$$Km_{app} = Km \cdot (1 + [I]/KI) \quad \text{(eq.2)}$$

where [I] is the concentration of PMSF-thrombin.

Myeloperoxidase (MPO) Activity

MPO was purified from the extract of frozen human leukocytes obtained from healthy donors, as detailed elsewhere (33). MPO activity in the synovial fluid of RA patients was assayed by monitoring the absorbance increase at 414 nm, caused by oxidation of the chromogenic

substrate 2,2′-azino-bis(3-ethyl benzthiazoline-6-sulphonic acid) disodium salt (ABTS) into the ABTS•+ radical. A reference curve was obtained with increasing concentrations (0.05–0.4μM) of purified MPO in 0.1M sodium-acetate buffer pH 5.5, containing 100μM H_2O_2 and 1mM ABTS. Upon adding H_2O_2 to the mixture, the reaction rate was measured as ΔA 414_{nm}/min on a SF-2000-02 spectrophotometer (OKB Spectr, Russia) using the Kinetics software. The concentration of MPO (ng/ml) in the synovial fluid samples was determined form the reference curve previously obtained with known concentrations of purified MPO. The MPO inhibitory activity of hCP or hCP/CP* mixtures, during proteolysis of hCP with thrombin, was determined at 25°C by measuring the rate ABTS•+ formation at 414 nm in the same buffer at a fixed [MPO].

Thrombin Activity

The concentration of thrombin (NIH/ml) in the synovial fluid of RA patients was determined at 25°C by measuring the rate of p-nitroaniline (pNA) release at 405 nm from the chromogenic substrate Z-Ala-Ala-Arg-pNA·HBr (0.1 mg/ml) in PBS. A reference curve at 25°C was obtained with increasing concentrations (0.05 – 2.0 NIH/ml) of purified human thrombin. The effect of hCP on the hydrolytic activity of thrombin was determined by measuring at 37°C the release of pNA from the substrate S2238 (D-Phe-Pip-Arg-pNA) in Hepes buffer pH 7.4, containing 0.1M NaCl and 0.1% PEG-8000, in the presence of increasing CP concentrations.

Production of Recombinant Thrombin

Recombinant wild-type thrombin was expressed and refolded as previously described. Briefly, pET23(+) plasmid vector containing the cDNA corresponding to wild-type human prethrombin-2 (preThb-2) sequence (Dr. J. Huntington, University of Cambridge, UK) was used to transform E. coli strain BL21(DE3)pLysS cells. After inducing preThb-2 expression with isopropyl β-D-thiogalactoside (IPTG), harvested cells were sonicated and inclusion bodies recovered by centrifugation. Refolding of preThb-2 chain was carried out by diluting drop wise solubilized inclusion bodies (in 6M Gdn-HCl) into the renaturing solution: 20mM Tris-HCl buffer, pH 8.5, 0.6M L-arginine hydrochloride, 0.5M NaCl, 1mM EDTA, 10% glycerol, 0.2% Brij-58, and1mM L-cysteine. After dialysis and centrifugation, correctly folded pThb-2 was purified on a heparin-sepharose column followed by treatment with ecarin to generate active α-thrombin, which was purified on a heparin-sepharose column. Mutations

in the preThb2 cDNA were introduced by the oligonucleotide-directed mutagenesis method, using the QuickChange mutagenesis kit (Stratagene, La Jolla, CA). The purity of thrombin preparation (~98%) was established by SDS/PAGE (12% acrylamide gel) and RP-HPLC on a C4 analytical column (4.6 x 150 mm, 5 μm particle size, 300 Å porosity) from Grace-Vydac (Hesperia, CA, U.S.A.). The column was equilibrated with 0.1% (v/v) aqueous TFA and eluted with a linear 0.1% (w/w)-TFA-acetonitrile gradient at a flow rate of 0.8 ml/min. The absorbance of the effluent was recorded at 226 nm. The chemical identity of the purified proteins was established by ESI-TOF mass spectrometry on a Mariner instrument from Perseptive Biosystems (Stafford, TX, U.S.A.).

Binding Measurement

Dynamic Light Scattering (DLS) measurement were carried out with Zetasizer Nano S (Malvern Instruments, Worcestershire, UK); the translational diffusion coefficient (D) was obtained experimentally, while the molecular hydrodynamic radius (RH) was calculated from the Stokes-Einstein equation: $RH = KB \cdot T/6\pi \cdot \eta \cdot D$, where KB is the Boltzman constant, T is the absolute temperature, and η is the solution viscosity. A calibration curve was obtained by linear fitting the experimental RH values of monomeric globular protein standards versus their known molecular weight (LogMW). Polystyrene cuvettes (1-cm pathlength, 100 μl) (ZEN-0117, Hellma) were used for all measurements. Each measurement consisted of a subset of runs determined automatically, each being averaged for 10 s. Scattering data were analysed with the multimodal algorithm, as implemented in the Nano-6.20 software, and expressed as percentage mass size distribution. Protein samples were filtered at 0.22 μm on Vivaspin 500 filters (Sartorius, Germany) for 2 minutes at 8.000 rpm and equilibrated for 1 min before analysis.

The interaction between CP and inactive S195A thrombin was monitored at 25°C in 5mM Tris-HCl pH 7.4, 0.2M NaCl, 0.1% PEG-8000 by a Jasco (Tokyo, Japan) model FP-6500 spectrofluoriometer, equipped with a Peltier model ECT-327T temperature control system (Jasco). Samples were excited at 280 nm and the fluorescence intensity was recorded at 335 nm, corrected for dilution and subtracted for the signal of S195A at each concentration. The data were fitted to the Langmuir equation (eq.3) using the program Origin 7.5 (MicroCal, Inc.):

$$\Delta F = F\text{-}F^{\circ} = (\Delta F_{max} \cdot [L])/(Kd + [L]) \qquad \text{(eq.3)}$$

where Kd is the dissociation constant of the complex, RL, and ΔFmax is the maximum fluorescence change at infinite concentration of ligand, $[L]\infty$.

Surface Plasmon resonance (SPR) measurements were carried out on a Biacore X100 instrument (GE-Healthcare, Piscataway, NJ, USA). Purified CP (50 μg/ml) in 10mM ammonium acetate buffer pH 4.0, was injected for 10 min at a flow rate of 5 μl/min and covalently immobilized on a carboxymethylated dextran chip (CM5) using the amine coupling chemistry, according to the manufacturer's instructions. The sensor chip was first activated with an equimolar (0.2M) mixture of N-ethyl-N′-dimethylaminipropylcarbodiimide (EDC) and N-hydroxysuccinimide (NHS) and then reacted with a solution of CP (i.e., the ligand). Unreacted carboxymethyl-groups on the sensor chip were blocked by reaction with 1M ethanolamine at pH 8.5. Final immobilization levels of 18500 resonance units (RU) were obtained, corresponding to approximately 18.5 ng of bound CP/mm^2. To avoid proteolysis, the inactive thrombin mutant S195A was used, when active human thrombin was irreversibly inhibited at active site with PPACK. In competition experiments exosite-I (i.e. hirugen) and exosite-II (i.e γ′-peptide) binders were first incubated thrombin-PPACK and then injected over the CP-coated sensor chip. All measurements were carried out at 25° in Hepes-EP+ (10mM Hepes pH 7.4, 150mM NaCl, 3mM EDTA, 0.005% Tween20 polyoxyethylene sorbitan) at a flow rate of 30 μl/min. Each SPR trace was subtracted for unspecific binding (<2% of Rmax) of thrombin. The dissociation constant, Kd, of hCP-thrombin complex was determined by plotting the value of RU at the steady state as a function of [thrombin] and the data were fitted to the Langmuir equation (eq. 4) describing the one-site binding model or to eq. 5, describing a two-site nonequivalent binding model:

$$R_{eq}/R_{max} = [Thrombin] / ([Thrombin] + Kd) \quad \text{(eq.4)}$$

$$R_{eq}/R_{max} = [Thrombin] / ([Thrombin] + Kd_1) + [Thrombin] / ([Thrombin] + Kd_2) \quad \text{(eq.5)}$$

where R_{eq} is the RU at a given [Thrombin], after reaching equilibrium, R_{max} is the RU value at saturating [Thrombin], and Kd_1 and Kd_2 are the dissociation constants for type 1 and type 2 binding sites for thrombin on CP.

Structural Analysis and Docking Simulations

Protein structures were visualized with the ViewerPro 4.2 software (Accelerys Inc., San Diego, CA, USA) while B-factor flexibility plot was generated with the program What If (34). Docking of thrombin into CP structure was performed with Ultrafast-FFT GPU-based HEX 6.3 software (35), starting from the structures of CP at 2.6 Å (4ENZ.pdb) (11) and PPACK-inhibited thrombin (1PPB.pdb) (27), after removal of the inhibitor coordinates. The structure of the ternary complex formed by MPO, CP and thrombin was obtained starting

from the structure of the MPO-CP complex (4EJX.pdb) (11). Simulations were run using default parameters and "shape + electrostatics" option, without introducing any additional geometric/energetic constraint. A hundred poses were generated and ranked according to the HEX scoring function. The top three poses were almost identical and used for interpreting binding data.

Treatment of RA Patients with Hirudin-Based Ointment

A group of 19 patients (11 males and 8 females) were treated with RefludanTM (Leu1,Thr2-63-desulphohirudin; Bayer Healthcare Pharmaceuticals) prepared as an ointment. The treatment lasted for 14 days with applications of the ointment on affected joints every second day. Each application contained 200 μg of hirudin. Five additional patients did not receive this therapy and were used as controls. For each patient, the swelling of the knee joint was measured and taken as an indicator of the arthritis progression.

RESULTS

Thrombin Cleaves CP at Two Exposed and Flexible Loops

Proteolysis (0-120 min) of purified CP by thrombin was carried out under limited proteolysis conditions (thrombin:hCP ratio 1:100) and analyzed by SDS-PAGE (lanes 1-8 in Fig. 4.3A). Five major bands at 116, 72, 67, 50 and 19 kDa are incrementally generated over time from the CP band at 132 kDa. Interestingly, the intensity of the 116-kDa band first increases at short reaction times (5-15 min) and then decreases, likely because of further proteolysis. Notably, the proteolytic pattern obtained by treatment of CP with thrombin closely resembles that resulting from prolonged storage of purified CP preparations kept under sterile conditions in buffer solution at 4°C for 3 months (lane 9) or frozen in liquid nitrogen and stored at –70°C for one year (lane 10). Western blot analysis in Fig. 4.1B reveals that, upon storage for two weeks at 37°C, spontaneous proteolytic degradation of hCP in blood serum (lane 2) is abolished in the presence of specific thrombin inhibitors, like full-length hirudin (lane 3) and its N-terminal 1-47 fragment (lane 4) (36, 37).

Rigorous chemical characterization of the proteolytic fragments, resulting either from proteolysis of CP with thrombin or prolonged storage of purified CP, was carried out by Edman sequencing on electroblotted bands and by peptide mass fingerprint analysis after in situ tryptic digestion of the proteolytic bands. This procedure allowed us to cover ~67% of hCP sequence (i.e. 698 out of 1046 amino acids in Fig. 4.4) and establish that:

1. the cleavage sites in the two set of experiments (i.e. limited proteolysis with thrombin and prolonged storage) are the same;
2. the bands at 116 and 19 kDa originate from thrombin cleavage of the peptide bond Lys887-Val888 in full-length CP, to generate fragments 1-887 and 888-1046, respectively;
3. the bands at 67 and 72 kDa result from cleavage of the peptide bond Arg481-Ser482 in CP to generate fragments 1-481 and 482-1046, respectively;
4. the 67-kDa band (fragment 1-481) results from the proteolytic attack on intact CP (132-kDa-band) or on fragment 1-887 (116-kDa band);
5. the 50-kDa accumulates at longer reaction times as the result of proteolysis at both sites Arg481-Ser482 and Lys887-Val888, to generate fragment 482-887.

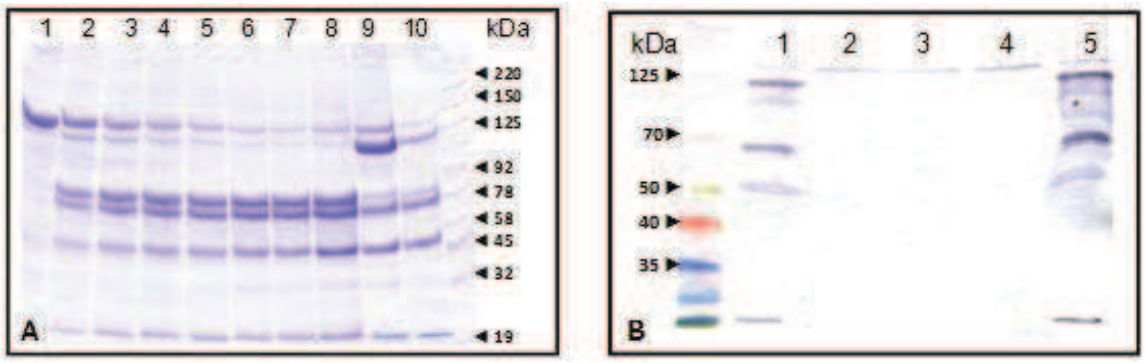

Figure 4.3 Limited proteolysis of purified CP by thrombin and identification of proteolyzed CP species in blood serum. (A) SDS-PAGE analysis of CP proteolysis. Lanes 1-8: proteolysis of plasma purified hCP (2 mg/ml, 10 µl) with thrombin (50 NIH units/ml) at 25°C, after 0, 5, 10, 15, 30, 45, 60 and 120 min reaction. lanes 9 and 10: aliquots (10 µl) of purified CP samples (2 mg/ml) undergoing spontaneous proteolytic degradation upon prolonged storage under different conditions; lane 11: molecular weight protein standards. **(B) Effect of hirudin on the spontaneous proteolysis of CP in blood serum.** Western blotting was carried out using rabbit anti-hCP Abs and peroxidase-conjugated goat anti-rabbit IgG. Lane 1: molecular weight protein standards; lane 2: aliquot (2 µl) of human serum incubated at 37ºC for two weeks under sterile conditions; lane 3: as in lane 2, in the presence of hirudin HM2 (100 nM); lane 4: as in lane 2, in the presence of hirudin (1-47) (100 nM); lane 5: aliquot (2 µl) of freshly prepared human serum; lane 6: aliquot (0.2 µg) of purified hCP undergoing spontaneous proteolytic degradation, corresponding to lane 10 in panel **A**.

```
        10          20          30          40          50          60
KEKHYYIGII ETTWDYASDH GEKKLISVDT EHSNIYLQNG PDRIGRLYKK ALYLQYTDET

        70          80          90         100         110         120
FRTTIEKPVW LGFLGPIIKA ETGDKVYVHL KNLASRPYTF HSHGITYYKE HEGAIYPDNT

       130         140         150         160         170         180
TDFQRADDKV YPGEQYTYML LATEEQSPGE GDGNCVTRIY HSHIDAPKDI ASGLIGPLII

       190         200         210         220         230         240
CKKDSLDKEK EKHIDREFVV MFSVVDENFS WYLEDNIKTY CSEPEKVDKD NEDFQESNRM

       250         260         270         280         290         300
YSVNGYTFGS LPGLSMCAED RVKWYLFGMG NEVDVHAAFF HGQALTNKNY RIDTINLFPA

       310         320         330         340         350         360
TLFDAYMVAQ NPGEWMLSCQ NLNHLKAGLQ AFFQVQECNK SSSKDNIRGK HVRHYYIAAE

       370         380         390         400         410         420
EIIWNYAPSG IDIFTKENLT APGSDSAVFF EQGTTRIGGS YKKLVYREYT DASFTNRKER

       430         440         450         460         470         480
GPEEEHLGIL GPVIWAEVGD TIRVTFHNKG AYPLSIEPIG VRFNKNNEGT YYSPNYNPQS

       490         500         510         520         530         540
RSVPPSASHV APTETFTYEW TVPKEVGPTN ADPVCLAKMY YSAVDPTKDI FTGLIGPMKI

       550         560         570         580         590         600
CKKGSLHANG RQKDVDKEFY LFPTVFDENE SLLLEDNIRM FTTAPDQVDK EDEDFQESNK

       610         620         630         640         650         660
MHSMNGFMYG NQPGLTMCKG DSVVWYLFSA GNEADVHGIY FSGNTYLWRG ERRDTANLFP

       670         680         690         700         710         720
QTSLTLHMWP DTEGTFNVEC LTTDHYTGGM KQKYTVNQCR RQSEDSTFYL GERTYYIAAV

       730         740         750         760         770         780
EVEWDYSPQR EWEKELHHLQ EQNVSNAFLD KGEFYIGSKY KKVVYRQYTD STFRVPVERK

       790         800         810         820         830         840
AEEEHLGILG PQLHADVGDK VKIIFKNMAT RPYSIHAHGV QTESSTVTPT LPGETLTYVW

       850         860         870         880         890         900
KIPERSGAGT EDSACIPWAY YSTVDQVKDL YSGLIGPLIV CRRPYLKVFN PRRKLEFALL

       910         920         930         940         950         960
FLVFDENESW YLDDNIKTYS DHPEKVNKDD EEFIESNKMH AINGRMFGNL QGLTMHVGDE

       970         980         990        1000        1010        1020
VNWYLMGMGN EIDLHTVHFH GHSFQYKHRG VYSSDVFDIF PGTYQTLEMF PRTPGIWLLH

      1030        1040
CHVTDHIHAG METTYTVLQN EDTKSG
```

Figure 4.4 (C) Amino acid sequence of mature hCP (entry code: P00450). The peptide segments identified during peptide mass fingerprint analysis are underlined.

Nicked CP (CP*) Retains the Native Fold of the Intact Protein

Purified intact CP was reacted with thrombin at 37°C for 2 hours, such that the amount of intact CP, estimated from the intensity of the 132-kDa band, was < 5% compared to that of CP*. Thrombin traces were eliminated from the proteolysis mixture by affinity chromatography on a benzamidine-Sepharose column. The completeness of the proteolytic reaction at the scissile bonds Arg481-Ser482 and Lys887-Val888 was checked by SDS-PAGE (4-10% acrylamide), showing the presence of fragments 1-481 (67 kDa band), 482-887 (50 kDa band) and 888-1046 (19 kDa band), and the concomitant absence of intact CP (1-1046; 132 kDa band) and that of the overlapping fragment 1-887 (116 kDa band). The persistence of a minor band at 72 kDa, corresponding to the overlapping fragment 482-1046, indicates that the peptide bond Lys887-Val888 is slightly more resistant to thrombin proteolysis than Arg481-Ser482 bond, consistent with the substrate specificity of thrombin which prefers an Arg-residue at P1 (38).

Size-exclusion chromatography (SEC) analysis (Fig. 4.5) indicates that intact and nicked CP (CP*) are eluted at the same volume of effluent, thus suggesting that the molecular size and global fold of CP remain unchanged after proteolysis, with an estimated molecular weight of about 160 kDa, in agreement with the molecular weight of CP = 132 kDa.

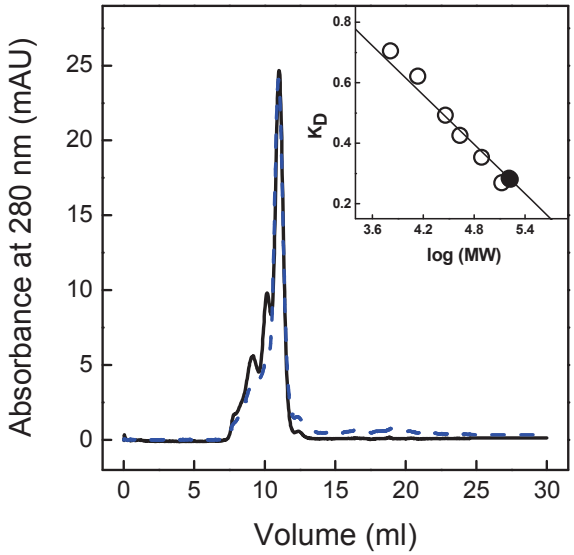

Figure 4.5 Size-exclusion chromatography of intact (CP —) and nicked CP (CP*— —). Aliquots (0.2 ml; 0.5 mg/ml) of CP and CP* were loaded on a Superose-12 column eluted at flow of 0.3 ml/min, with 25mM Tris-HCl pH 7.4, 0.15M NaCl buffer. The absorbance of the effluent was recorded at 280 nm using a 0.2cm pathlength detection cell. **(Inset)** Column calibration with protein standards (○). From the calibration curve, a molecular weight of ~160 kDa was estimated for both CP and CP* (●).

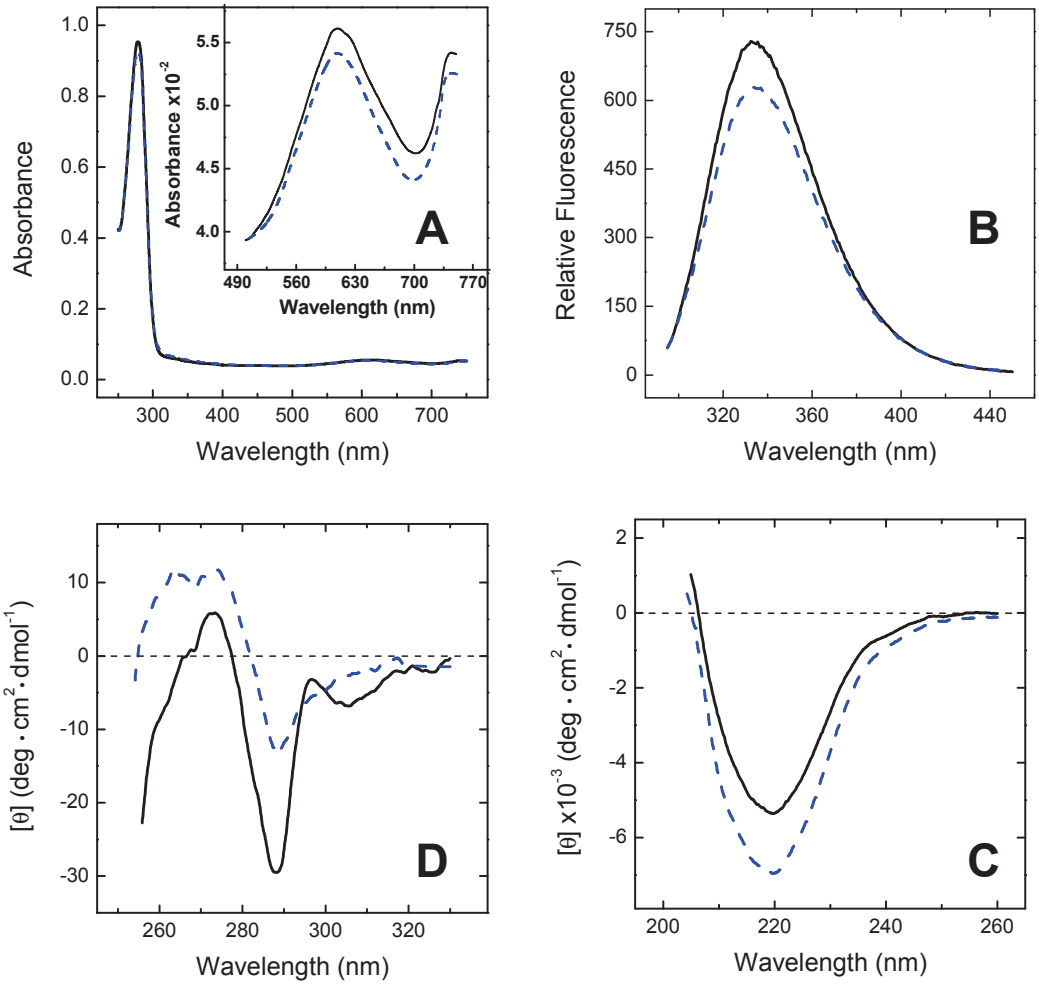

Figure 4.6 Conformational characterization of intact (CP —) and nicked CP (CP*— —). (A) UV/Vis absorption spectra of CP and CP*. The spectra were reordered at 25±0.1°C, using a 1 cm pathlength cuvette. **(B)** Fluorescence spectra of CP and CP* were obtained by excited protein samples at 280 nm with an excitation/emission slit of 1 and 3, respectively. CD spectra of CP and CP* in the far- **(C)** and near-UV **(D)** region. All measurements were carried out at 25±0.2°C in 20mM Tris-HCl buffer pH 7.4, at a protein concentration of 0.2 mg/ml, except near-UV CD measurements (0.5 mg/ml).

Very similar conclusions can be drawn from UV/Vis absorption (Fig. 4.6A) and emission fluorescence (Fig.4.6B) spectra, indicating that the chemical environment surrounding copper-binding sites (i.e. UV-Vis) and aromatic amino acids (i.e. fluorescence) remains essentially unchanged after proteolysis. Likewise, far-UV CD spectra indicate that CP* retains the β-sheet secondary structure of CP (Fig. 4.6C), whereas the lower CD signal of CP* in the near-UV region (Fig. 4.6D) is suggestive of a looser tertiary packing in the nicked protein, as already observed with copper-free apo-CP (39). Overall, our results strongly suggest that, after 2-h proteolysis with thrombin, CP* can be essentially regarded as a fragment complementing system in which fragments 1-481, 482-887, and 888-1046 tightly interact to form a non-covalent complex possessing native-like structure.

Thrombin-Mediated Proteolysis of CP Hinders MPO Inhibitory Activity without Altering Ferroxidase Activity

The time-course proteolysis reaction of CP with thrombin was monitored by SDS-PAGE (Fig. 4.7A) and at each time-point the functional properties of CP/CP* were studied with respect to its ability to promote oxidation of Fe^{+2}-ion and to inhibit the oxidase activity of leukocyte MPO (Fig. 4.7B). Aliquots of the proteolysis reactions were taken, treated with PMSF to irreversibly inhibit thrombin, and then tested with respect to their ferroxidase and MPO activities. Our data unequivocally demonstrate that the ferroxidase activity of CP is not affected by proteolysis; whereas inhibition of MPO is dramatically reduced during proteolysis, and after 2-h reaction, when the relative amount of intact CP is negligible the inhibition of MPO is totally abolished (Fig. 4.7B). Notably, incubation of CP with the catalytically inactive thrombin S195A mutant does not decrease the ability of CP to inhibit MPO oxidase activity. Moreover, control experiments demonstrate that thrombin does not alter the function of MPO in the absence of CP. These results provide clear-cut evidence that the inhibition of MPO can be reverted by thrombin through proteolysis of CP.

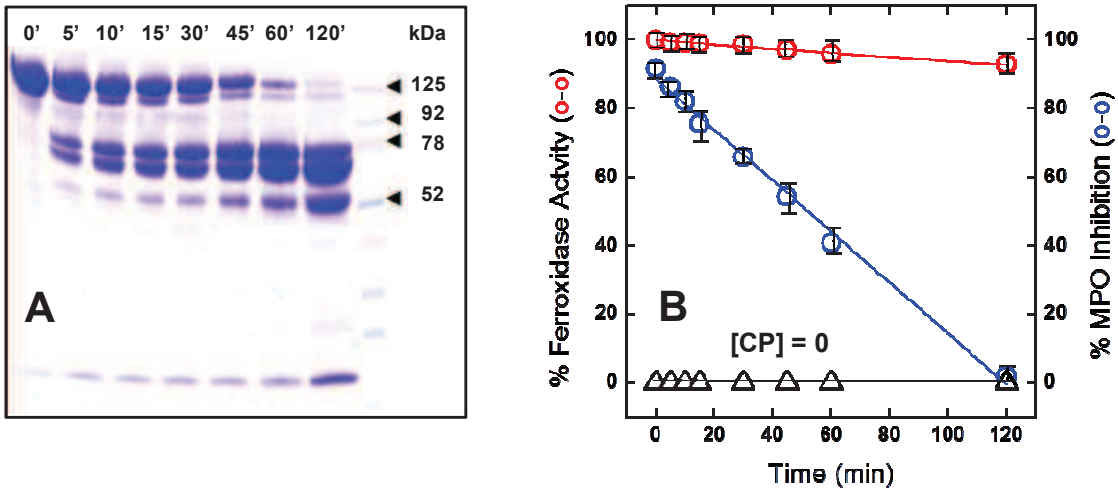

Figure 4.7 Effect of thrombin cleavage on the ferroxidase and MPO inhibitory activity of CP. (A) SDS-PAGE analysis of the proteolysis reaction of CP with thrombin. At the indicated time points, aliquots (10 µl) of the proteolysis reaction were taken ad analyzed on a 4-10% acrylamide gel. **(B)** Freshly purified CP (120 nM) was treated at 25°C with human thrombin (1.2nM) in TBS pH 7.4. At the time points as in panel **A**, aliquots were taken, thrombin was inactivated by adding an equimolar concentration of PMSF, and the ferroxidase and MPO inhibitory activity of hCP was determined. The ferroxidase activity (○-○) of CP*, generated during proteolysis with thrombin, was determined at 25°C by the rate of Fe^{+3}-DMF complex formation at 310 nm in 0.1M sodium acetate buffer pH 5.5, containing 30mM thiourea and 200mM Fe^{+2}. The MPO inhibitory activity (○-○) of the newly generated CP* was determined at 25°C by measuring the rate ABTS•+ formation at 414 nm in the same buffer with [MPO] = 20nM. Control measurement (Δ-Δ) was carried out in the absence of CP.

Probing Thrombin-CP Interaction

The interaction of thrombin with CP was investigated by several different spectroscopic techniques, including dynamic light scattering (DLS) (Fig. 4.8A), fluorescence spectroscopy (Fig. 4.8B) and surface plasmon resonance (SPR) (Fig. 4.8C, 4.8D). To avoid proteolysis of CP during analysis, human thrombin was irreversibly inhibited at the active site with (D)-Phe-Pro-Arg-choromethyl ketone (PPACK) and used in DLS measurements, whereas the inactive thrombin S195A mutant was used in fluorescence and SPR analyses. Notably, mutation of Ser195 with Ala abrogates the catalytic activity of thrombin without altering its binding properties [Johnson et al., 2005#37; Pozzi et al., 2013#32]. 41

The molecular diameter (d) of PPACK-thrombin (Thb) and CP alone were determined by DLS as 4. ±0.1nm and 7.5±0.1 nm (Fig. 4.8A), respectively, with a polydispersity index significantly higher for PPACK-thrombin (0.29) compared to that of CP (0.17). From the calibration curve (Fig. 4.8A, Inset) the apparent molecular weight (MW) of PPACK-thrombin and CP was estimated at 40 kDa and 140 kDa, respectively, in agreement with the MW of the two proteins (Thb = 36kDa and CP = 132kDa). Interestingly, the d-value of CP gradually increased after addition of Thb, from 0.5:1 to 5:1 molar ratio, together with the increase in the polydispersity index. At a Thb:CP molar ratio of 3:1, a d-value of 8.5±0.2nm was determined, corresponding to an apparent MW of about 190 kDa (Fig. 4.8A, Inset). This value is reasonably compatible with the formation of a 1:1 complex between two proteins, like Thb and CP, that both contain extended carbohydrate chains.

The affinity of thrombin for CP was determined quantitatively by recording the decrease of fluorescence intensity of CP after addition of the catalytically inactive thrombin S195A mutant. Fitting data points with an equation that describes the one-site binding model, yields an equilibrium dissociation constant, Kd, of 267±30nM (Fig. 4.8B).

CP-thrombin interaction was also studied by Surface Plasmon Resonance (SPR). CP was first immobilized on a CM5 sensor chip and then incremental concentrations of PPACK-thrombin or S195A were injected in the mobile phase (Fig. 4.8C). The data relative to the binding of PPACK-thrombin were interpolated with one-site binding model, and resulted in a good fit, with a Kd of 56±2nM (Fig. 4.8D, ●-●), comparable to that estimated by fluorescence measurements. When the same equation was used to interpolate the data of S195A binding (Fig. 4.8D, ○-○), a poor fit was obtained (dashed line), with a Kd = 3.2±0.8μM. Notably, after interpolating the data points with the equation that describing a two-site binding model, a much better fit was obtained (continuous line). Analysis of binding data suggests the presence

of at least two binding sites on CP: a high-affinity site (Kd_1 of 65±8nM) and a low-affinity site (Kd_2 of 9.0±1.1μM).

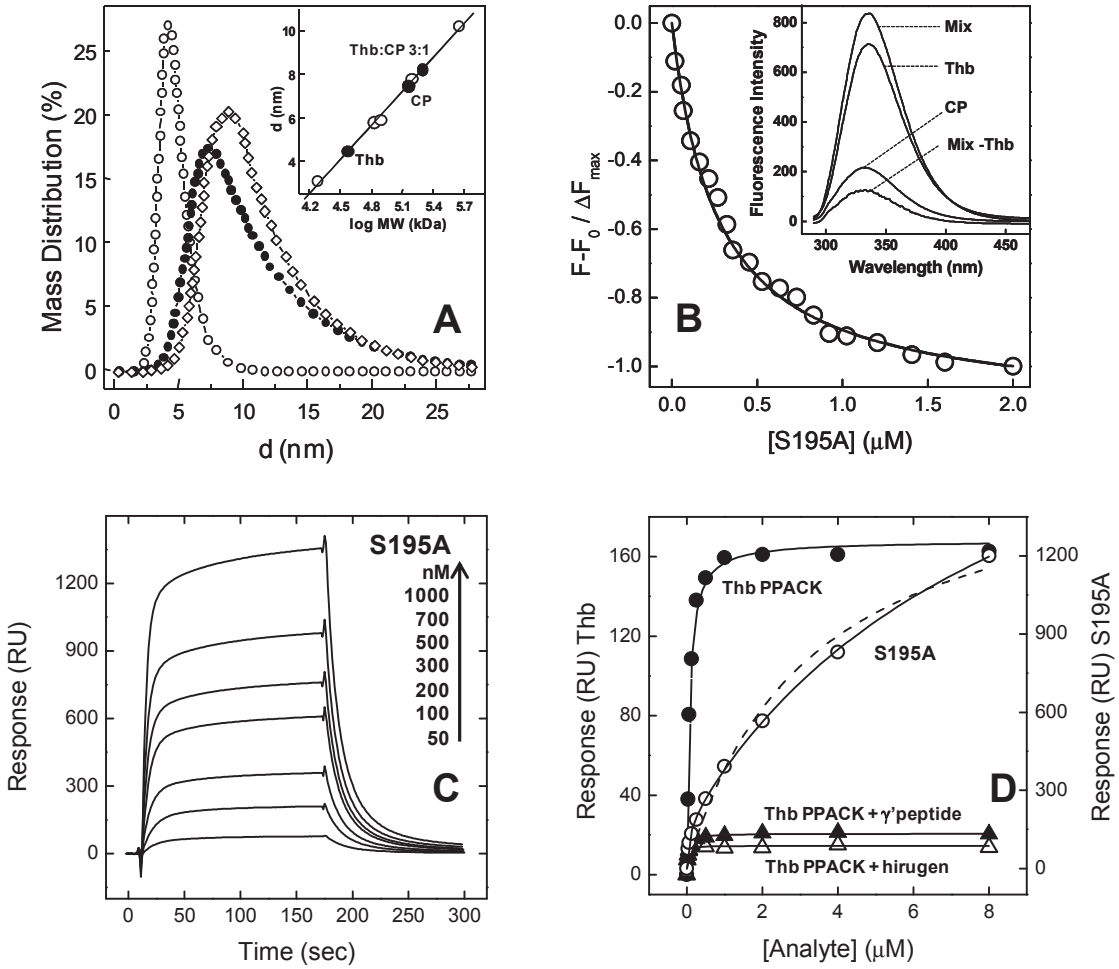

Figure 4.8 Probing CP-thrombin interaction by Dynamic Light Scattering (DLS) and fluorescence spectroscopy and SPR. (A) DLS spectra of isolated PPACK-thrombin (Thb: 100 μg/ml, ○-○), isolated CP (100 μg/ml, ●-●), and PPACK-Thb:CP mixture (◊-◊) in a 3:1 molar ratio (3μM Thb with 1μM CP). **(Inset)** Plot of the experimental molecular diameter (d) of standard proteins *versus* log MW. **(B)** Fluorescence binding of thrombin S195A mutant to CP (50 nM) yields a K_d = 267±30nM. **(Inset)** At each S195A concentration, the fluorescence of CP-Thb mixture (Mix) was subtracted for the contribution of thrombin alone (Thb) at the same concentration, to yield the fluorescence change associated with complex formation (Mix-Thb). **(C)** Sensograms of CP-S195A interaction. **(D)** SPR analysis of thrombin-CP interaction and mapping of thrombin binding sites. ●-●: binding of active site-inhibited PPACK-thrombin to immobilized CP; Δ-Δ: binding of PPACK-thrombin having exosite 1 saturated with hirugen; ▲-▲: binding of PPACK-thrombin having exosite 2 saturated with γ'-peptide; ○-○: binding of thrombin S195A mutant to immobilized CP. The data are expressed as the plot of RU at increasing [thrombin]. Fitting PPACK-thrombin binding data results in K_d = 56 ± 2 nM; Fitting of S195A binding data with eq. describing a two-site binding model, give a Kd1 = 65 ± 8 nM and a Kd2 = 9.0 ± 1.1 μM.

The role of thrombin exosites in CP binding was assessed in SPR competition experiments (Fig. 4.8D), whereby PPACK-thrombin solutions were first incubated with saturating concentrations of ligands specific for exosite 1 (i.e. hirugen) or exosite 2 (i.e. fibrinogen γ′-peptide) and then injected over the CP-bound sensor chip. The decrease in the SPR signal (%RU) was interpreted as an indication that the blocked exosite was involved in the interaction with CP. The results indicate that blockage of either one of the two thrombin exosites results in the reduction of RU by > 90%, such that a reliable Kd could not be estimated.

Mutual Effects of Thrombin and CP Binding:

Active Site-Blocked Thrombin Inhibits the Ferroxidase Activity of CP whereas CP does not Affect the Hydrolytic Activity of Thrombin

The effect of thrombin binding on CP function was investigated by measuring the rate of Fe^{+2} oxidation by CP as a function of [Fe^{+2}] at increasing concentration of PMSF-thrombin (Fig. 4.9A, 4.9B). Covalent blockage of thrombin active-site with PMSF was necessary to prevent binding of the protease to potential proteolytic sites on CP surface and therefore to study the effect of thrombin binding on CP function independently from proteolysis. Remarkably, PMSF-thrombin inhibited the ferroxidase activity of CP in a concentration-dependent manner and Hanes-Wolff analysis of the reaction rates indicated that that PMSF-thrombin increased the value of Km_{app} (from 57 to 138μM), without substantially affecting v_{max} (Fig. 4.9A). These findings are compatible with a competitive mechanism of CP inhibition by thrombin, whereby the enzyme covers the ferroxidase site of CP and competitively impairs binding of Fe^{+2} at that site. From the secondary plot of Km_{app} versus [PMSF-thrombin] (Fig. 4.9B), a value of the equilibrium inhibition constant (KI) was determined as 220±20nM, very close to the Kd value of PPACK-thrombin binding estimated from fluorescence measurements (Kd = 267±30nM).

The effect of CP binding on thrombin hydrolytic activity was measured by recording the time-course release of pNA from the chromogenic substrate S2238 in the presence of increasing [CP] (Fig. 4.9C). Our results indicate that the rate of pNA release is unchanged even at [CP] = 20μM, a concentration approximately 100-fold higher than the Kd value of thrombin-CP complex. This finding provides experimental evidence that, after CP binding, the active site of thrombin remains accessible and functional.

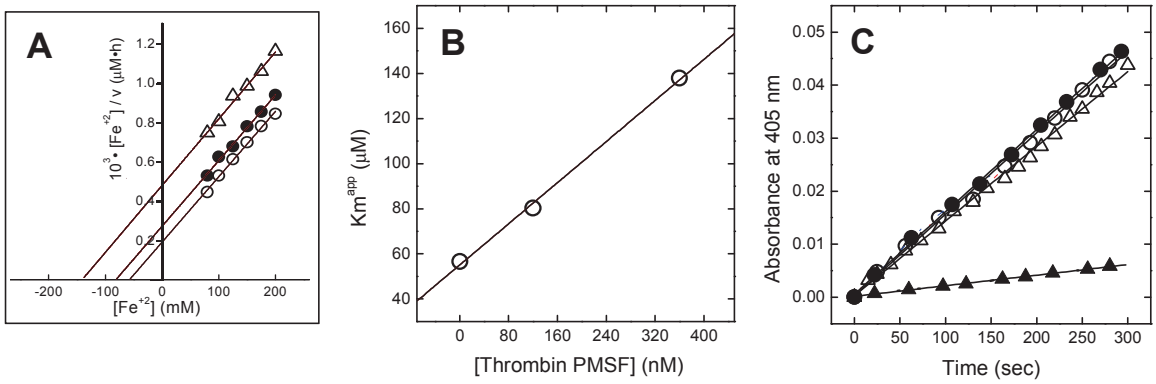

Figure 4.9 Mutual effects of thrombin and CP binding. (A) Effect of thrombin on the ferroxidase activity of CP. To a solution of purified hCP were added increasing concentrations of PMSF-inactivated thrombin (○, 0 nM; ●, 120 nM; ∆, 360 nM). The resulting ferroxidase activity of hCP 1 yields K_m^{app} values of 57±2, 80±3 and 138±6 μM and V_{max} values of 301±20, 302±18 and 300±25 nM·h^{-1}. **(B)** Secondary plot of Km_{app} *versus* [PMSF-thrombin]. Data fitting yields a K_I = 220±20 nM**. (C)** Effect of CP on the hydrolytic activity of human thrombin. The release of pNA from the substrate S2238 (20μM) by thrombin (100pM) was measured at 37°C in the absence (○) and in the presence of 2μM (●) and 20μM (Δ) CP. As a control, the time course hydrolysis of S2238 was carried out without adding thrombin (▲), in the presence of 1μM CP.

The Synovial Fluid of Patients with Rheumatoid Arthritis (RA) Contains Proteolyzed CP, Apo-CP and Variable Amount of MPO and Thrombin

Samples of synovial fluid taken from 24 patients with a history of RA were analyzed by SDS-PAGE and Western blotting with rabbit anti-CP polyclonal Ab (Fig. 4.10A). For comparison, blood serum samples were also analyzed. As expected, serum CP (lane K in Fig. 4.10A) migrated as a single band at 132 kDa, corresponding to intact CP, with only a faint reactive band at 116 kDa. Conversely, CP-related species from synovial fluid samples migrated as multiple reactive bands at lower MW. For instance, intact CP was the predominant species in sample 5, even though several other reactive bands at 116, 72, 67, and 50 kDa were present. The latter bands were variably represented in all other samples analyzed, whereas the 132-kDa band was missing, thus indicating that CP undergoes proteolytic degradation in the synovial fluid. This conclusion was confirmed by adding an aliquot (1μl) of sample n.1, corresponding to lane 1 in Fig. 4.10A, to a solution of purified CP. As shown by Western blotting analysis (Fig. 4.10B), low-molecular weight CP-species were produced over time and the fragmentation pattern resembled that obtained after in vitro proteolysis of purified CP with thrombin. Strikingly, as already shown for thrombin-mediated proteolysis of CP in vitro the data in Fig. 4.10D demonstrate that proteolytic degradation of CP induced by the synovial fluid sample n.1 is inhibited by hirudin. This finding demonstrates the involvement of thrombin in the proteolytic degradation of CP in the synovial fluid of RA patients.

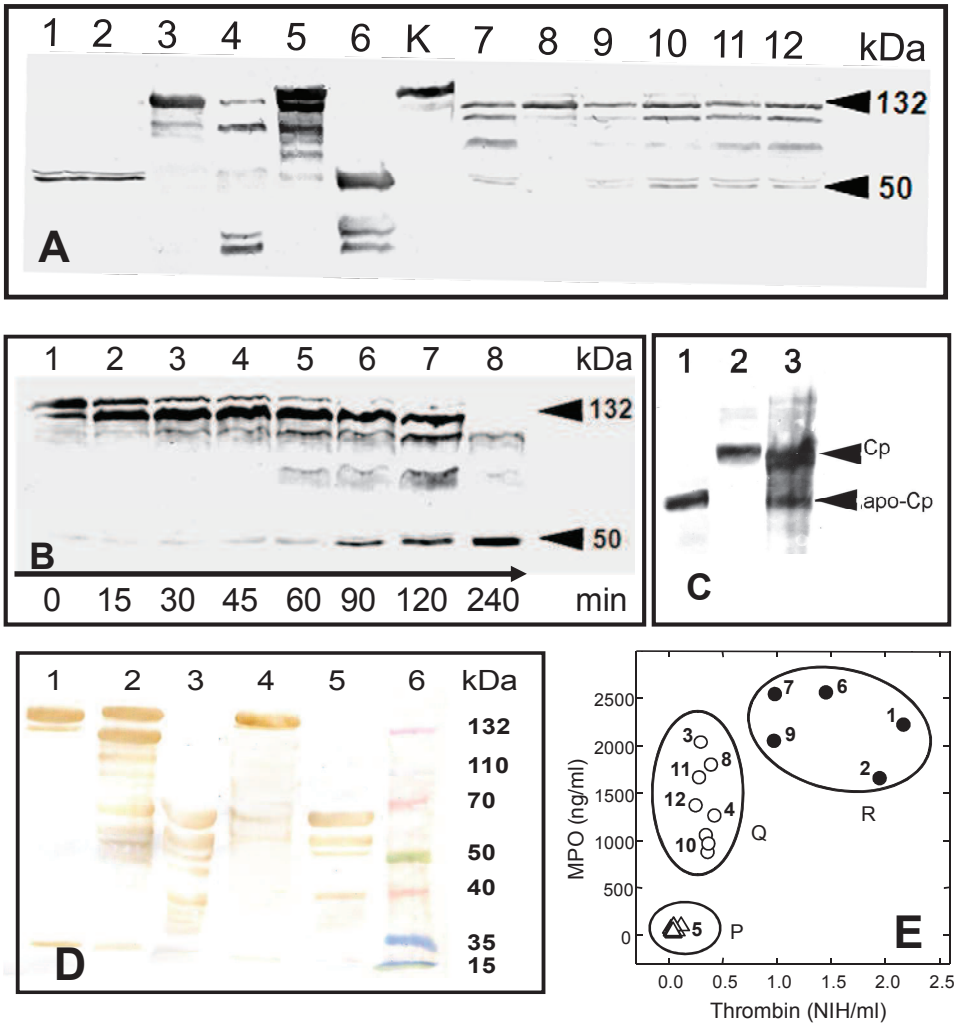

Figure 4.10 Identification of proteolyzed CP in the synovial fluid of rheumatoid arthritis (RA) patients and quantification of MPO and thrombin in the synovial fluid of RA patients. Samples were analyzed by SDS-PAGE and Western blotting using rabbit anti-hCP Ab and peroxidase-conjugated goat anti-rabbit IgG. **(A)** Proteolyzed CP species in samples from RA patients. Lanes 1-4 and 6-12: synovial fluid samples (5µl) of RA patients displaying different extent of proteolytic degradation and lacking the 132 kDa band, characteristic of intact hCP; lane 5: representative sample (5µl) of the synovial fluids containing the 132 kDa band; lane K: blood plasma (2µl). **(B)** Proteolytic degradation of purified CP by the synovial fluid of RA patients. Lanes 1-8: freshly purified CP (2mg/ml; 10µl) in TBS was added with 0.5µl of synovial fluid sample corresponding to lane 1 in panel **A**. Aliquots (5µg) of the reaction mixture were taken and analyzed over time, as indicated. (**C**) Identification of apo- and holo-CP in the synovial fluid of RA patients. Lane 1: purified apo-CP (1µg), obtained by treating holo-CP with KCN; lane 2: purified holo-CP (1µg); lane 3 synovial fluid sample (5µl) from a RA patient. To prevent copper depletion, samples for electrophoresis were prepared in the absence of SDS and without heat treatment. Notably, apo-CP migrates faster than holo-CP. **(D)** Effect of hirudin on the proteolysis of purified CP. Lane 1: purified CP (20µg); lane 2: purified CP (20µg) added with synovial fluid sample (1µl), corresponding to lane 1 in panel A, after 1-h incubation at 37°C; lane 3: as in lane 2, after 12-h incubation; lane 4: as in lane 2, in the presence of hirudin (2µg); lane 5: aliquot (10µl) of synovial fluid sample (lane 1 in panel A); lane 6: molecular weight protein standards. **(E)** Quantization of MPO and thrombin in the synovial fluid of RA patients. The levels of thrombin and MPO in synovial fluid samples were determined as detailed in the Methods. The numbers refer to the samples analyzed in panel **A**. Three different clusters can be identified (P, Q, and R), with different thrombin/MPO titers and intact CP. Cluster P (Δ) contains 11 samples with low titers of both MPO and thrombin and variable amount of intact CP, as given by the presence of the 132 kDa band; clusters Q (○) and R (●) contain 8 or 5 samples, with variably high titers of thrombin and MPO respectively, in which intact CP is absent, whereas titers are.

Notably, Western blotting analysis of the synovial fluid in RA patients revealed the presence of significant amount of (copper-free) apo-CP (Fig. 4.10C). However, the average total copper concentration (i.e. Cu_{bound} + Cu_{free}) in the synovial fluid of the 24 patients tested was determined as 0.96±0.19mg/l, very close to the plasma concentration of copper in normal individuals (31). After dialysis of synovial fluid samples with a 3-kDa cut-off membrane, about 2/3 of total copper remained in the well, while the residual copper (1/3) was found in the dialysate. This finding demonstrates that significant copper depletion from CP occurs in RA patients.

The levels of MPO and thrombin in the synovial fluid of RA patients are reported in Fig. 4.10E. Although no clear trend can be delineated, three clusters (i.e. P, Q and R) can be identified according to the levels of MPO and thrombin. Cluster P comprises 11 out of 24 samples, all containing very low titers of MPO and thrombin and low amount of proteolyzed CP, cluster P is characterized by the presence of a distinctive band at 132 kDa, corresponding to intact CP (i.e. sample n. 5 in Fig. 4.10A). The samples belonging to cluster Q (8 out of 24) display relatively high MPO and low thrombin levels. Although intact CP is missing in these samples (i.e. sample n. 3, 4, 8, 10, 11, 12), the presence of bands at high molecular weight is suggestive of reduced proteolytic activity. Cluster R contains 5 samples, all displaying high MPO and thrombin titers. In these samples (i.e. sample n. 1, 2, 6, 7, 9), CP extensively degraded, as documented by the absence of high molecular weight bands and by the concomitant accumulation of a 50-kDa band, considered as the end-point of proteolytic degradation of CP (40).

Hirudin Treatment Ameliorates the Clinical Symptoms of Rheumatoid Arthritis

From the group of 24 Russian patients with RA previously analyzed, 19 patients were treated with an ointment containing hirudin, whereas 5 patients were untreated and used as controls. At the end of the treatment (14 days), eight patients reported moderate pain relief, but the reduction of edema remained within the error margins. Notably, CP was somewhat proteolyzed in the synovial fluid of these patients. Strikingly, 11 patients reported cessation of pain, and the edema of their joints was noticeably reduced when compared to controls. Furthermore, much of CP in their synovial fluid was intact, as judged by the relative abundance of the 132-kDa band in SDS-PAGE. The remaining five untreated patients reported exacerbation of pain, increased swelling of the knee joint and extensive proteolytic degradation of CP. Although the number of patients enrolled in this study is too small to draw

statistically significant conclusions, the levels of intact CP in synovial fluid samples seem to positively correlate with hirudin treatment.

DISCUSSION

Structural Analysis of CP Cleavage by Thrombin

Along the 1046 amino acid-sequence of CP, there are many potential cleavage sites for thrombin (i.e. 40 Arg- and 65 Lys-residues). In addition, the sequence of the thrombin proteolytic sites on CP surface, i.e. PQSR481↓S482VPP and PYLK887↓V888FNP, only partially conform to the consensus substrate specificity reported for the protease, i.e. P4(ϕal)-P3(x)-P2(Pro)-P1(Arg)↓P1′(s)-P2′(ϕar)-P3′(Arg)-P4′(ϕal) (38), where x stands for any amino acid and ϕal and ϕar are apolar aliphatic or aromatic residues. Nevertheless, CP proteolysis is limited exclusively at the peptide bonds Arg481-Ser482 and Lys887-Val888 (Fig. 4.11A), while and the resulting noncovalent complex CP*, has a native-like fold (Fig 4.5, 4.6) that is quite resistant to further proteolysis even at higher thrombin:CP ratio (up to 1:5) or after prolonged reaction time (up to 5h).

The unique susceptibility of CP to thrombin hydrolysis can be explained on the basis of the three-dimensional structure of CP (10, 11) and on the general structural requirements for limited proteolysis (41). Beyond substrate specificity among competing sites on the protein surface, in fact, limited proteolysis is dictated by the exposure of the cleavable site and, most importantly, by its conformational flexibility. Indeed, proteolysis occurs at exposed and flexible loops and rarely at sites embedded in rigid secondary structure elements (41). In the case of CP, >50% of the amino acid residues are embedded in β-sheets (39%) or α-helices (13%) and therefore are protected from proteolysis. Conversely, Arg481-Ser482 bond is in the loop region connecting domain 3 and 4 on the outer surface of CP, while Lys887-Val888 bond is in the loop bridging domain 5 and 6 in the flat/basal region of the molecule (Fig. 4.11B). Furthermore, both cleavable sites are characterized by high surface exposure and conformational flexibility, compared to other potentially competing segments, such that they are not visible in the crystallographic CP structure. Although proteolysis of CP by thrombin has important functional implications, our results also account for the so-called “spontaneous” degradation of CP occurring during prolonged storage of highly purified preparations and set a point to the long-lasting debate on the single-chain nature of circulating bioactive CP (42, 43).

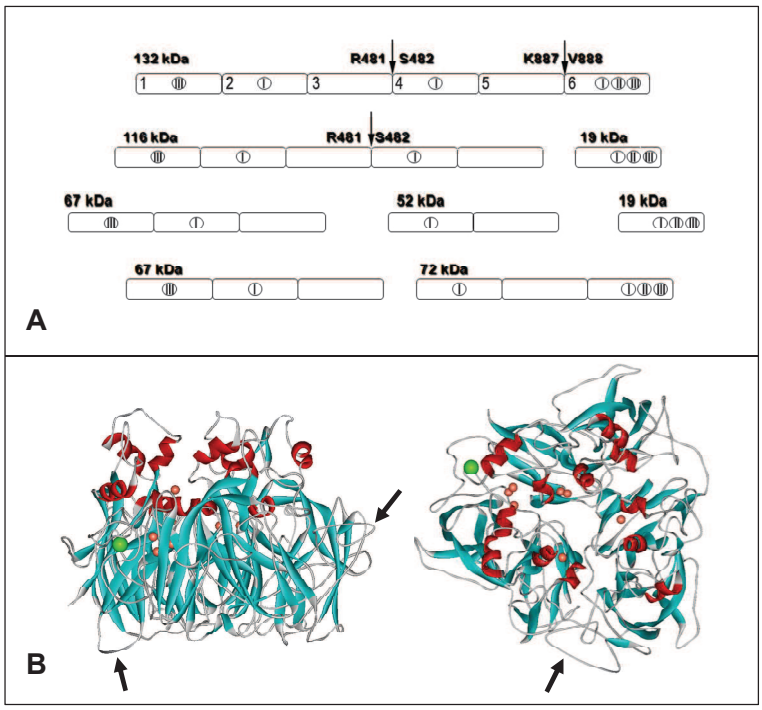

Figure 4.11 Analysis of thrombin proteolytic sites on CP structure. (A) Scheme of CP domain architecture and identification of thrombin proteolytic sites (indicated by arrows), as obtained from peptide mass fingerprint analysis. **(B)** Ribbon drawing of the crystallographic structure of CP (4ENZ.pdb). Left panel: side view; right panel: top view. β-sheets are colored in cyan, while helices are in red; copper (orange), Na^{+} (violet) and Ca^{+2} (green) ions are also shown, together with the Fe^{+2} ion (magenta) in the putative ferroxidase site. Unresolved chain segments in the X-ray structure of CP are delimited by sequence numbers, while arrows indicate thrombin cleavage sites. In the ferroxidase site, Fe^{+2} is coordinated by Glu272, Glu935, His940 and Asp1025, and is at ~8Å form the mononuclear copper center underneath, where the copper ion is coordinated by His975, Cys1021 and His1026.

Proteolysis has Opposite Effects on CP Functions

The structural integrity of CP is important for the glutathione-dependent peroxidase activity of the protein (44) and for CP-mediated loading of iron into ferritin (45). In agreement with these studies, the data shown in Fig. 4.7 indicate that limited proteolysis by thrombin abrogates the MPO inhibitory function of CP. However, the data also show that the ferroxidase activity of CP is not affected by thrombin-induced proteolysis. These opposite effects can be rationalized by analyzing the structure of intact CP and proposing reasonable mechanisms explaining how peptide bond cleavage might perturb the ferroxidase site of CP and its MPO binding site.

Considered that nicked CP* essentially retains the native-like structure of the intact protein (Fig 4.5, 4.6) and that the ferroxidase site in intact CP, and perhaps also in the nicked CP*, is separated from the scissile bonds R481-S482 and K887-V888 by about 45 and 50 Å, respectively, it is very unlikely that local perturbations, possibly evoked after peptide bond cleavage, are transmitted long-range to the ferroxidase site in such a way to alter its function.

Therefore, the ferroxidase activity of CP is predicted to remain unchanged after proteolysis, as experimentally verified (Fig. 4.7). On the other hand, the abrogation of MPO inhibition observed with CP* (Fig. 4.7) is nicely explained by the crystallographic structure of CP-MPO complex, very recently solved at low resolution (4EJX Z.pdb) (11). This structure shows that CP interacts with MPO through its lower flat and positively charged surface, thus hindering access of substrates to the deep pocket leading to MPO active site, where the heme-group is bound (Fig. 4.12A). In particular, the 884-890 loop containing the scissile bond Lys887-Val888 in CP makes numerous contacts with a wide hydrophobic pocket surrounding the heme-group of MPO in the protein region across the N-termini of the light and heavy chains, thus limiting substrate accessibility. Importantly, the role of this loop in CP-MPO interaction has been confirmed by the synthetic peptide 883PYLK↓VFNPRR892, which can effectively inhibit the peroxidase activity of MPO (11). Of note, the other scissile bond Arg481-Ser482 in the 475-483 loop on CP structure is located in the upper region of the molecule and does not seem to participate in CP-MPO interaction. On these grounds it is conceivable that cleavage of the 884-890 loop in CP can dramatically alter both the stereochemical and electrostatic properties of this segment in such a way that free CP* looses affinity for MPO.

Thrombin-CP Interaction

A major achievement of this work is that thrombin has an intrinsic affinity for CP, and that this affinity is only marginally related to the binding of CP at the protease active site, leading to CP hydrolysis. Quantitative data on thrombin-CP interaction were obtained by different techniques, including fluorescence, SPR and inhibition of ferroxidase activity. The affinity of thrombin for CP, obtained from fluorescence binding experiments of the inactive S195A thrombin mutant (Kd=267±30nM) (Fig. 4.9B), was identical to that deduced from inhibition of CP ferroxidase activity by active-site blocked PMSF-thrombin (KI=220±20nM) (Fig. 4.6). A comparable Kd value was obtained from SPR measurements of active-site blocked PPACK-thrombin to immobilized CP (Kd=56±2nM) (Fig. 4.9D). In these experiments a single binding site for thrombin was identified on CP structure. Conversely, when SPR experiments were carried out with thrombin S195A mutant, having the active site empty, at least two binding sites were identified on CP: a low-affinity site (Kd_2=9.0±1.1μM) and a high-affinity site (Kd_1=65±30nM), having a Kd value identical to that determined for PPACK-thrombin (Kd=56±nM) (Fig. 4.9D). A key aspect emerging from SPR experiments is that interaction is abrogated after saturating either one of the two exosites with specific

peptide binders (i.e. hirugen or fibrinogen γ′-peptide), thus demonstrating that both thrombin exosites are involved in CP binding (Fig. 4.9D).

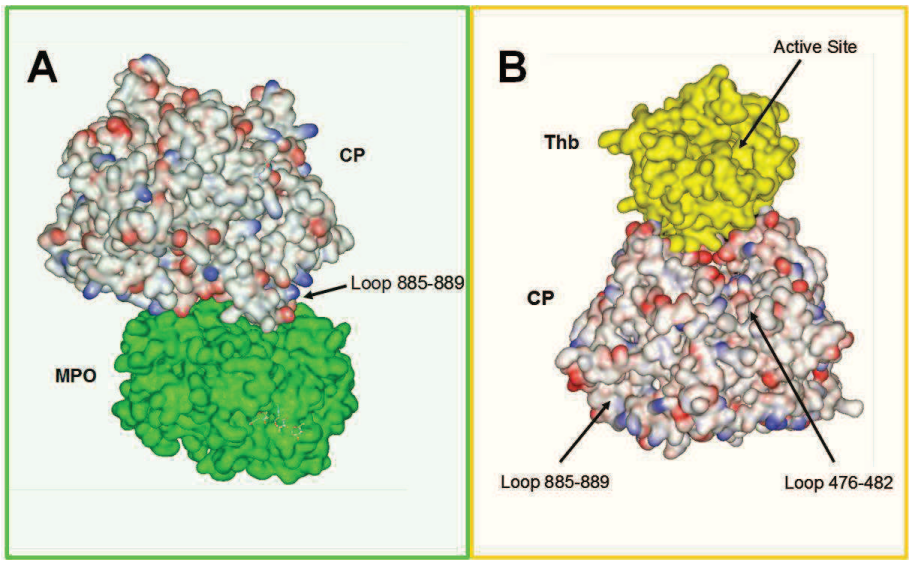

Figure 4.12 Structural Models of complexes of CP with MPO and thrombin. (A) Crystallographic structure of MPO-CP complex (4EJX.pdb) (11). CP structure is shown as a color-coded surface, whereas MPO is shown in green. **(B)** Theoretical model of thrombin-CP complex. The approximate position of the catalytic site is indicated by an arrow. The loop regions on CP structure that are cleaved by thrombin are also indicated. The docking model was obtained using the HEX software, starting from the coordinates of isolated CP (4ENZ.pdb) and thrombin (1PPB.pdb).

To interpret our binding data, a theoretical docking model of thrombin-CP interaction was generated (Fig. 4.12B, 4.13). The model clearly shows geometric and electrostatic complementarity between the positively charged exosites on the convex surface of thrombin and the large negative, concave surface in the upper region of CP molecule, where the ferroxidase site is located. Importantly, the model also shows that thrombin covers the ferroxidase site of CP and impairs substrate entrance and product release, while leaving the protease active site fully accessible for ligand/substrate binding. This is a key structural insight for explaining the observed mutual effect of CP and thrombin binding, whereby PMSF-thrombin competitively inhibits the ferroxidase activity of CP (Fig. 4.9A, B), whereas CP does not alter the hydrolytic activity of the protease (Fig. 4.9C). Finally, evaluation of SPR binding data in the light of the docking model allows us to propose that the high-affinity binding site spans the negative concave surface in the upper region of CP, whereas the low-affinity site(s) can map in the cleavable loop regions 885-889 or 476-482. When thrombin active site is filled with PPACK, only the high-affinity site is available. Instead, in S195A the active site is empty, so both binding sites are available on CP surface.

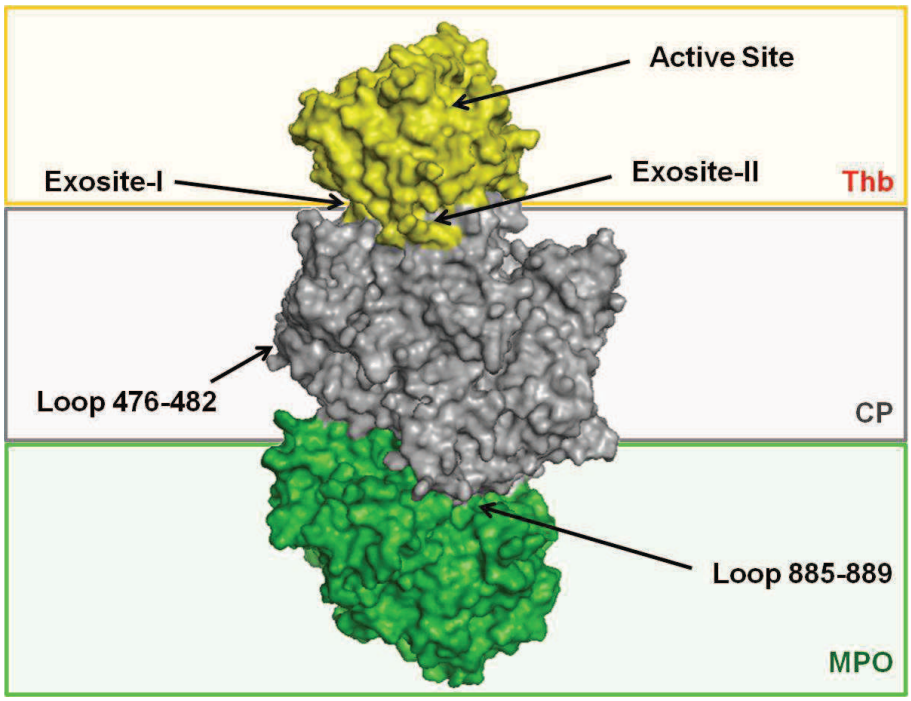

Figure 4.13 Theoretical model of the ternary complex MPO-CP-Thb. The docking model was obtained using the HEX software, starting from the coordinates of MPO-CP complex (4JEX.pdb) and thrombin (1PPB.pdb). MPO interacts with the bottom, flat surface of CP which is positively charge, whereas thrombin binds to the upper surface of CP, which is negatively charged. The active site of the serine protease remains free and accessible for substrate binding.

Relevance of CP Proteolysis by Thrombin in the Pathogenesis of Rheumatoid Arthritis

The fragmentation pattern of purified CP, obtained after in vitro proteolysis with thrombin or after prolonged storage (Fig. 4.3A and Fig.4.7A), is similar to that of CP present in the synovial fluid of patients with rheumatoid arthritis (RA) (Fig. 4.10A). More importantly, the proteolytic degradation of purified CP, induced by addition of exogenous thrombin or of synovial fluid samples from RA patients, is effectively blocked by hirudin, a highly potent inhibitor that displays absolute specificity for thrombin (Fig. 4.1B and Fig. 4.10D) (36). These observations provide strong indication that thrombin can proteolyses CP both in vitro and in vivo. Thrombin, however, is not the only CP cleaving protease: CP is also highly susceptible to digestive (i.e. trypsin and chymotrypsin), fibrinolytic (i.e. plasmin) and leukocyte (i.e. elastase and cathepsin G) proteases, which extensively degrade CP into small fragments devoid of any functional activity. Conversely, we have shown that thrombin-mediated proteolysis is "limited" at only two sites and selectively abrogates the ability of CP to inhibit the oxidase activity of MPO, whereas it does not alter the ferroxidase function. Hence, it is possible to speculate that thrombin, at variance with other proteases, might

regulate via proteolysis CP function in vivo, especially in those clinical settings where the concentrations of CP, thrombin and MPO are increased, such as in RA.

RA is a widespread, chronic inflammatory disease more frequently affecting the synovial membrane of flexible joints (46). Even though the initiation of RA is thought to be driven by T lymphocytes, activation of the coagulation cascade as been proposed as an important nonimmunological pathway amplifying and perpetuating the features of chronic inflammation in RA joints (22). Increased permeability of the inflamed synovial microvasculature leads to extravasations of inflammatory leukocytes and clotting factors, such that intact extrinsic coagulation pathway has been demonstrated within the RA synovium, with higher expression in RA patients of tissue factor, fibrinogen (>2-fold) and thrombin (>7-fold) (29) compared with osteoarthritis patients. Thrombin activation leads to abundant deposition of fibrin, a distinctive feature of RA joints, which in turn exacerbates the disease either by mechanically altering the functionality of the affected joint and by forming a matrix onto which inflammatory leukocytes can be activated via αMβ2 integrin receptor (47). Activated leukocytes then start releasing proteases, inflammatory cytokynes, and MPO, which is the major route to the burst of ROS and RNS production, thus amplifying inflammation and tissue damage. In inflamed tissues thrombin induces the release of pro-inflammatory cytokines from monocytes and macrophages, including interleukin-6 (IL-6) (28). Besides its role in sustaining inflammatory processes, IL-6 also markedly increases the expression of CP (8), which would downregulate inflammation via MPO inhibition (19). The cellular effects of thrombin in RA seem to be mediated by activation of PAR1, which is abundantly expressed in inflamed rheumatoid synovial tissues (48). However, soft tissue inflammation and synovitis were reduced by only 30 or 20% in PAR1 deficient mice compared to controls (49). The cellular effects of thrombin in RA seem to be mediated by activation of the thrombin receptor PAR1, which is abundantly expressed in inflamed rheumatoid synovial tissues.

These results, while strongly supporting the role of the thrombin-PAR-1 axis in animal models of RA, also suggest that other mechanisms, different from PARs activation, may function to sustain inflammation and tissue damage in rheumatoid joints. In this study, we propose that thrombin may act as an indirect stimulator of MPO prooxidative function by releasing the breaks that CP exerts on the enzyme. Our data also show the concomitant presence of apo-CP (Fig. 8C) and higher levels of free copper in the synovial fluid of arthritic patients.

REFERENCES

1. Holmberg, C.G. (1944) On the Presence of n laccase-like Enzyme in Nerum and its Relation to the Copper in Serum. *Acta Physiol.Scand.* 8, 227-229
2. Hellman, N.E., and Gitlin, J.D. (2002) Ceruloplasmin metabolism and function. *Annu.Rev.Nutr.* 22, 439-458
3. Bielli, P., and Calabrese, L. (2002) Structure to function relationships in ceruloplasmin: a 'moonlighting' protein. *Cell Mol.Life Sci.* 59, 1413-1427
4. Shukla, N., Maher, J., Masters, J., Angelini, G.D., and Jeremy, J.Y. (2006) Does oxidative stress change ceruloplasmin from a protective to a vasculopathic factor?. *Atherosclerosis.* 187, 238-250
5. Floris, G., Medda, R., Padiglia, A., and Musci, G. (2000) The physiopathological significance of ceruloplasmin. A possible therapeutic approach. *Biochem.Pharmacol.* 60, 1735-1741
6. Gutteridge, J.M., and Quinlan, G.J. (1992) Antioxidant protection against organic and inorganic oxygen radicals by normal human plasma: the important primary role for iron-binding and iron-oxidising proteins. *Biochim.Biophys.Acta.* 1159, 248-254
7. Shiva, S., Wang, X., Ringwood, L.A., Xu, X., Yuditskaya, S., Annavajjhala, V., Miyajima, H., Hogg, N., Harris, Z.L., and Gladwin, M.T. (2006) Ceruloplasmin is a NO oxidase and nitrite synthase that determines endocrine NO homeostasis. *Nat.Chem.Biol.* 2, 486-493
8. Gitlin, J.D. (1988) Transcriptional regulation of ceruloplasmin gene expression during inflammation. *J.Biol.Chem.* 263, 6281-6287
9. Zaitsev, V.N., Zaitseva, I., Papiz, M., and Lindley, P.F. (1999) An X-ray crystallographic study of the binding sites of the azide inhibitor and organic substrates to ceruloplasmin, a multi-copper oxidase in the plasma. *J.Biol.Inorg.Chem.* 4, 579-587
10. Bento, I., Peixoto, C., Zaitsev, V.N., and Lindley, P.F. (2007) Ceruloplasmin revisited: structural and functional roles of various metal cation-binding sites. *Acta Crystallogr.D Biol.Crystallogr.* 63, 240-248
11. Samygina, V.R., Ochoa-Lizarralde, B., Popov, A.N., Cabo-Bilbao, A., Goni-de-Cerio, F., Molotkovsky, J.G., Patel, D.J., Brown, R.E., and Malinina, L. (2013) Structural insights into lipid-dependent reversible dimerization of human GLTP. *Acta Crystallogr.D Biol.Crystallogr.* 69, 603-616
12. Sokolov, A.V., Ageeva, K.V., Kostevich, V.A., Berlov, M.N., Runova, O.L., Zakharova, E.T., and Vasilyev, V.B. (2010) Study of interaction of ceruloplasmin with serprocidins. *Biochemistry (Mosc).* 75, 1361-1367

13. Sokolov, A.V., Golenkina, E.A., Kostevich, V.A., Vasilyev, V.B., and Sud'ina, G.F. (2010) Interaction of ceruloplasmin and 5-lipoxygenase. *Biochemistry (Mosc).* 75, 1464-1469
14. Sokolov, A.V., Pulina, M.O., Zakharova, E.T., Shavlovski, M.M., and Vasilyev, V.B. (2005) Effect of lactoferrin on the ferroxidase activity of ceruloplasmin. *Biochemistry (Mosc).* 70, 1015-1019
15. Sokolov, A.V., Prozorovskii, V.N., and Vasilyev, V.B. (2009) Study of interaction of ceruloplasmin, lactoferrin, and myeloperoxidase by photon correlation spectroscopy. *Biochemistry (Mosc).* 74, 1225-1227
16. Sokolov, A.V., Pulina, M.O., Ageeva, K.V., Ayrapetov, M.I., Berlov, M.N., Volgin, G.N., Markov, A.G., Yablonsky, P.K., Kolodkin, N.I., Zakharova, E.T., and Vasilyev, V.B. (2007) Interaction of ceruloplasmin, lactoferrin, and myeloperoxidase. *Biochemistry (Mosc).* 72, 409-415
17. Griffin, S.V., Chapman, P.T., Lianos, E.A., and Lockwood, C.M. (1999) The inhibition of myeloperoxidase by ceruloplasmin can be reversed by anti-myeloperoxidase antibodies. *Kidney Int.* 55, 917-925
18. Park, Y., Lee, I.S., Joo, E.J., Hahn, B.S., and Kim, Y.S. (2009) A novel and one-step purification of human ceruloplasmin by acharan sulfate affinity chromatography. *Arch.Pharm.Res.* 32, 693-698
19. Chapman, A.L., Mocatta, T.J., Shiva, S., Seidel, A., Chen, B., Khalilova, I., Paumann-Page, M.E., Jameson, G.N., Winterbourn, C.C., and Kettle, A.J. (2013) Ceruloplasmin is an endogenous inhibitor of myeloperoxidase. *J.Biol.Chem.* 288, 6465-6477
20. Klebanoff, S.J. (2005) Myeloperoxidase: friend and foe. *J.Leukoc.Biol.* 77, 598-625
21. Stamp, L.K., Khalilova, I., Tarr, J.M., Senthilmohan, R., Turner, R., Haigh, R.C., Winyard, P.G., and Kettle, A.J. (2012) Myeloperoxidase and oxidative stress in rheumatoid arthritis. *Rheumatology (Oxford).* 51, 1796-1803
22. Majithia, V., and Geraci, S.A. (2007) Rheumatoid arthritis: diagnosis and management. *Am.J.Med.* 120, 936-939
23. Vasilyev, V.B. (2010) Interactions of caeruloplasmin with other proteins participating in inflammation. *Biochem.Soc.Trans.* 38, 947-951
24. Huntington, J.A. (2005) Molecular recognition mechanisms of thrombin. *J.Thromb.Haemost.* 3, 1861-1872
25. Di Cera, E. (2007) Thrombin as procoagulant and anticoagulant. *J.Thromb.Haemost.* 5 Suppl 1, 196-202

26. Coughlin, S.R. (2005) Protease-activated receptors in hemostasis, thrombosis and vascular biology. *J.Thromb.Haemost.* 3, 1800-1814
27. Bode, W., and Huber, R. (1992) Natural protein proteinase inhibitors and their interaction with proteinases. *Eur.J.Biochem.* 204, 433-451
28. Kastl, S.P., Speidl, W.S., Katsaros, K.M., Kaun, C., Rega, G., Assadian, A., Hagmueller, G.W., Hoeth, M., de Martin, R., Ma, Y., Maurer, G., Huber, K., and Wojta, J. (2009) Thrombin induces the expression of oncostatin M via AP-1 activation in human macrophages: a link between coagulation and inflammation. *Blood.* 114, 2812-2818
29. Nakano, S., Ikata, T., Kinoshita, I., Kanematsu, J., and Yasuoka, S. (1999) Characteristics of the protease activity in synovial fluid from patients with rheumatoid arthritis and osteoarthritis. *Clin.Exp.Rheumatol.* 17, 161-170
30. Pozzi, N., Acquasaliente, L., Frasson, R., Cristiani, A., Moro, S., Banzato, A., Pengo, V., Scaglione, G.L., Arcovito, A., De Cristofaro, R., and De Filippis, V. (2013) beta2-Glycoprotein I Binds Thrombin and Selectively Inhibits the Enzyme Procoagulant Functions. *J.Thromb.Haemost.* 11, 1093-1102
31. Linder, M.C., Lomeli, N.A., Donley, S., Mehrbod, F., Cerveza, P., Cotton, S., and Wotten, L. (1999) Copper transport in mammals. *Adv.Exp.Med.Biol.* 448, 1-16
32. Sato, M., and Gitlin, J.D. (1991) Mechanisms of copper incorporation during the biosynthesis of human ceruloplasmin. *J.Biol.Chem.* 266, 5128-5134
33. Sokolov, A.V., Ageeva, K.V., Pulina, M.O., Cherkalina, O.S., Samygina, V.R., Vlasova, I.I., Panasenko, O.M., Zakharova, E.T., and Vasilyev, V.B. (2008) Ceruloplasmin and myeloperoxidase in complex affect the enzymatic properties of each other. *Free Radic.Res.* 42, 989-998
34. Vriend, G. (1990) WHAT IF: a molecular modeling and drug design program. *J.Mol.Graph.* 8, 52-6, 29
35. Ritchie, D.W., and Venkatraman, V. (2010) Ultra-fast FFT protein docking on graphics processors. *Bioinformatics.* 26, 2398-2405
36. Markwardt, F. (1991) Hirudin and derivatives as anticoagulant agents. *Thromb.Haemost.* 66, 141-152
37. De Filippis, V., De Dea, E., Lucatello, F., and Frasson, R. (2005) Effect of Na+ binding on the conformation, stability and molecular recognition properties of thrombin. *Biochem.J.* 390, 485-492
38. Gallwitz, M., Enoksson, M., Thorpe, M., and Hellman, L. (2012) The extended cleavage specificity of human thrombin. *PLoS One.* 7, e31756

39. De Filippis, V., Vassiliev, V.B., Beltramini, M., Fontana, A., Salvato, B., and Gaitskhoki, V.S. (1996) Evidence for the molten globule state of human apo-ceruloplasmin. *Biochim.Biophys.Acta.* 1297, 119-123
40. Prozorovski, V.N., Rashkovetski, L.G., Shavlovski, M.M., Vasiliev, V.B., and Neifakh, S.A. (1982) Evidence that human ceruloplasmin molecule consists of homologous parts. *Int.J.Pept.Protein Res.* 19, 40-53
41. Fontana, A., Polverino de Laureto, P., De Filippis, V., Scaramella, E., and Zambonin, M. (1997) Probing the partly folded states of proteins by limited proteolysis. *Fold.Des.* 2, R17-26
42. Poulik, M.D. (1968) Heterogeneity and structure of ceruloplasmin. *Ann.N.Y.Acad.Sci.* 151, 476-501
43. Kingston, I.B., Kingston, B.L., and Putnam, F.W. (1979) Complete amino acid sequence of a histidine-rich proteolytic fragment of human ceruloplasmin. *Proc.Natl.Acad.Sci.U.S.A.* 76, 1668-1672
44. Kim, I.G., and Park, S.Y. (1998) Requirement of intact human ceruloplasmin for the glutathione-linked peroxidase activity. *FEBS Lett.* 437, 293-296
45. Van Eden, M.E., and Aust, S.D. (2000) Intact human ceruloplasmin is required for the incorporation of iron into human ferritin. *Arch.Biochem.Biophys.* 381, 119-126
46. Scott, D.L., Wolfe, F., and Huizinga, T.W. (2010) Rheumatoid arthritis. *Lancet.* 376, 1094-1108
47. Flick, M.J., Du, X., and Degen, J.L. (2004) Fibrin(ogen)-alpha M beta 2 interactions regulate leukocyte function and innate immunity in vivo. *Exp.Biol.Med.(Maywood).* 229, 1105-1110
48. Morris, R., Winyard, P.G., Brass, L.F., Blake, D.R., and Morris, C.J. (1996) Thrombin receptor expression in rheumatoid and osteoarthritic synovial tissue. *Ann.Rheum.Dis.* 55, 841-843
49. Yang, Y.H., Hall, P., Little, C.B., Fosang, A.J., Milenkovski, G., Santos, L., Xue, J., Tipping, P., and Morand, E.F. (2005) Reduction of arthritis severity in protease-activated receptor-deficient mice. *Arthritis Rheum.* 52, 1325-1332

APPENDIX

Appendix A

Abbreviations and Symbols

Å	Angstrom
ABTS	2,2′-azino-bis(3-ethyl benzthiazoline-6-sulphonic acid) disodium salt
CD	Circular Dichroism
Da	Dalton
DLS	Dynamic Light Dcattering
DMF	N,N′-dimethylformamide
DMSO	dimethyl sulfoxide
EDC	N-ethyl-N′-dimethylaminipropylcarbodiimide
EDTA	Ethylene Diamino Tetracetic Acid
ESI	Electrospray ionization
Gdn-HCl	Guanidine Chloride
HEPES	4-(2-hydroxyethyl)-1-piperazineethanesulfonic acid
HPLC	High-pressure liquid chromatography
IPTG	IsoPropyl-β-D-ThioGalactopyranoside
LPS	Lypopolysaccharide
MALDI	Matrix-Assisted Laser Desorption Ionization
MS	Mass spectrometry
MW	Molecular Weight
NAPAP	.Nα-(2-naphthyl-sulphonyl-glycyl)-D,L-p-amidinophenylalanyl-piperidine
NHS	N-hydroxysuccinimide
PABA	p-aminobenzamidine
PEG	PolyEthylene Glycol
PMSF	Phenylmethylsulphonyl fluoride
PPACK	D-Phe-Pro-Arg-chloromethyl ketone
RP	Reverse-phase
S-2238	D-Phe-Pip-Arg-p-nitroanilide
S-2366	pyroGlu-Pro-Arg-p-nitroanilide
SDS	Sodium Dodecyl Sulfate

SDS-PAGE	SDS-PolyAcrylamide Gel Electrophoresis
SEC	Size-exclusion chromatography
SPR	Surface Plasmon Resonance
TFA	Trifluoroacetic acid
TOF	Time-of-flight
Tris	Tris(hydroxymethyl)aminomethane
UV	ultraviolet

Appendix B

Amino Acids

Ala	A	Alanine
Arg	R	Arginine
Asp	D	Aspartic acid
Asn	N	Asparagine
Cys	C	Cysteine
Gly	G	Glycine
Gln	Q	Glutamine
Glu	E	Glutamic acid
His	H	Histidine
Ile	I	Isoleucine
Lys	K	Lysine
Leu	L	Leucine
Met	M	Methionine
Phe	F	Phenylalanine
Pro	P	Proline
Ser	S	Serine
Thr	T	Threonine
Tyr	Y	Tyrosine
Trp	W	Tryptophan
Val	V	Valine

Appendix C

Thrombin Numbering Scheme

Chym	T1h	F1g	G1f	S1e	G1d	E1c	A1b	D1a	C1	G2	L3	R4
Ch-A	1	2	3	4	5	6	7	8	9	10	11	12
Ch-B	-	-	-	-	-	-	-	-	-	-	-	-
ProT	285	286	287	288	289	290	291	292	293	294	295	296

Chym	P5	L6	F7	E8	K9	K10	S11	L12	E13	D14	K14a	T14b
Ch-A	13	14	15	16	17	18	19	20	21	22	23	24
Ch-B	-	-	-	-	-	-	-	-	-	-	-	-
ProT	297	298	299	300	301	302	303	304	305	306	307	308

Chym	E14c	R14d	E14e	L14f	L14g	E14h	S14i	Y14j	I14k	D14l	G14m	R15
Ch-A	25	26	27	28	29	30	31	32	33	34	35	36
Ch-B	-	-	-	-	-	-	-	-	-	-	-	-
ProT	309	310	311	312	313	314	315	316	317	318	319	320

Chym	I16	V17	E18	G19	S20	D21	A22	E23	I24	G25	M26	S27
Ch-A	37	38	39	40	41	42	43	44	45	46	47	48
Ch-B	1	2	3	4	5	6	7	8	9	10	11	12
ProT	321	322	323	324	325	326	327	328	329	330	331	332

Chym	P28	W29	Q30	V31	M32	L33	F34	R35	K36	S36a	C37	Q38
Ch-A	49	50	51	52	53	54	55	56	57	58	59	60
Ch-B	13	14	15	16	17	18	19	20	21	22	23	24
ProT	333	334	335	336	337	338	339	340	341	342	343	344

Chym	E39	L40	L41	C42	G43	A44	S45	L46	I47	S48	D49	R50
Ch-A	61	62	63	64	65	66	67	68	69	70	71	72
Ch-B	25	26	27	28	29	30	31	32	33	34	35	36
ProT	345	346	347	348	349	350	351	352	353	354	355	356

Chym	W51	V52	L53	T54	A55	A56	H57	C58	L59	L60	Y60a	P60b
Ch-A	73	74	75	76	77	78	79	80	81	82	83	84
Ch-B	37	38	39	40	41	42	43	44	45	46	47	48
ProT	357	358	359	360	361	362	363	364	365	366	367	368

Chym	P60c	W60d	D60e	K60f	N60g	F60h	T60i	E61	N62	D63	L64	L65
Ch-A	85	86	87	88	89	90	91	92	93	94	95	96
Ch-B	49	50	51	52	53	54	55	56	57	58	59	60
ProT	369	370	371	372	373	374	375	376	377	378	379	380

Chym	V66	R67	I68	G69	K70	H71	S72	R73	T74	R75	Y76	E77
Ch-A	97	98	99	100	101	102	103	104	105	106	107	108

Ch-B	61	62	63	64	65	66	67	68	69	70	71	72
ProT	381	382	383	384	385	386	387	388	389	390	391	392

Chym	R77a	N78	I79	E80	K81	I82	S83	M84	L85	E86	K87	I88
Ch-A	109	110	111	112	113	114	115	116	117	118	119	120
Ch-B	73	74	75	76	77	78	79	80	81	82	83	84
ProT	393	394	395	396	397	398	399	400	401	402	403	404

Chym	Y89	I90	H91	P92	R93	Y94	N95	W96	R97	E97a	N98	L99
Ch-A	121	122	123	124	125	126	127	128	129	130	131	132
Ch-B	85	86	87	88	89	90	91	92	93	94	95	96
ProT	405	406	407	408	409	410	411	412	413	414	415	416

Chym	D100	R101	D102	I103	A104	L105	M106	K107	L108	K109	K110	P111
Ch-A	133	134	135	136	137	138	139	140	141	142	143	144
Ch-B	97	98	99	100	101	102	103	104	105	106	107	108
ProT	417	418	419	420	421	422	423	424	425	426	427	428

Chym	V112	A113	F114	S115	D116	Y117	I118	H119	P120	V121	C122	L123
Ch-A	145	146	147	148	149	150	151	152	153	154	155	156
Ch-B	109	110	111	112	113	114	115	116	117	118	119	120
ProT	429	430	431	432	433	434	435	436	437	438	439	440

Chym	P124	D125	R126	E127	T128	A129	A129a	S129b	L129c	L130	Q131	A132
Ch-A	157	158	159	160	161	162	163	164	165	166	167	168
Ch-B	121	122	123	124	125	126	127	128	129	130	131	132
ProT	441	442	443	444	445	446	447	448	449	450	451	452

Chym	G133	Y134	K135	G136	R137	V138	T139	G140	W141	G142	N143	L144
Ch-A	169	170	171	172	173	174	175	176	177	178	179	180
Ch-B	133	134	135	136	137	138	139	140	141	142	143	144
ProT	453	454	455	456	457	458	459	460	461	462	463	464

Chym	K145	E146	T147	W148	T149	A149a	N149b	V149c	G149d	K149e	G150	Q151
Ch-A	181	182	183	184	185	186	187	188	189	190	191	192
Ch-B	145	146	147	148	149	150	151	152	153	154	155	156
ProT	465	466	467	468	469	470	471	472	473	474	475	476

Chym	P152	S153	V154	L155	Q156	V157	V158	N159	L160	P161	I162	V163
Ch-A	193	194	195	196	197	198	199	200	201	202	203	204
Ch-B	157	158	159	160	161	162	163	164	165	166	167	168
ProT	477	478	479	480	481	482	483	484	485	486	487	488

Chym	E164	R165	P166	V167	C168	K169	D170	S171	T172	R173	I174	R175
Ch-A	205	206	207	208	209	210	211	212	213	214	215	216
Ch-B	169	170	171	172	173	174	175	176	177	178	179	180
ProT	489	490	491	492	493	494	495	496	497	498	499	500

Chym	I176	T177	D178	N179	M180	F181	C182	A183	G184	Y184a	K185	P186
Ch-A	217	218	219	220	221	222	223	224	225	226	227	228

Ch-B	181	182	183	184	185	186	187	188	189	190	191	192
ProT	501	502	503	504	505	506	507	508	509	510	511	512

Chym	D186a	E186b	G186c	K186d	R187	G188	D189	A190	C191	E192	G193	D194
Ch-A	229	230	231	232	233	234	235	236	237	238	239	240
Ch-B	193	194	195	196	197	198	199	200	201	202	203	204
ProT	513	514	515	516	517	518	519	520	521	522	523	524

Chym	S195	G196	G197	P198	F199	V200	M201	K202	S203	P204	F204a	N204b
Ch-A	241	242	243	244	245	246	247	248	249	250	251	252
Ch-B	205	206	207	208	209	210	211	212	213	214	215	216
ProT	525	526	527	528	529	530	531	532	533	534	535	536

Chym	N205	R206	W207	Y208	Q209	M210	G211	I212	V213	S214	W215	G216
Ch-A	253	254	255	256	257	258	259	260	261	262	263	264
Ch-B	217	218	219	220	221	222	223	224	225	226	227	228
ProT	537	538	539	540	541	542	543	544	545	546	547	548

Chym	E217	G219	C220	D221	R221a	D222	G223	K224	Y225	G226	F227	Y228
Ch-A	265	266	267	268	269	270	271	272	273	274	275	276
Ch-B	229	230	231	232	233	234	235	236	237	238	239	240
ProT	549	550	551	552	553	554	555	556	557	558	559	560

Chym	T229	H230	V231	F232	R233	L234	K235	K236	W237	I238	Q239	K240
Ch-A	277	278	279	280	281	282	283	284	285	286	287	288
Ch-B	241	242	243	244	245	246	247	248	249	250	251	252
ProT	561	562	563	564	565	566	567	568	569	570	571	572

Chym	V241	I242	D243	Q244	F245	G246	E247
Ch-A	289	290	291	292	293	294	295
Ch-B	253	254	255	256	257	258	259
ProT	573	574	575	576	577	578	579

In the first row the chymotrypsinogen numeration of thrombin is indicated; in the second row the numeration in which the first residue of the A-chain is designated as 1 is indicated.; in the third row the numeration in which the first residue of the B-chain is designated as 1 is indicated; finally, the last row show the numeration of prothrombin.

At the end of my PhD Thesis I would like to thank all those people who made this possible and an unforgettable experience for me.

First and foremost I would like to express my sincere gratitude to my supervisor Prof. Vincenzo De Filippis for the continuous support of my PhD study and research, for his patience, motivation, enthusiasm, and immense knowledge. Under his guidance I successfully overcame some difficulties and learned a lot: the joy and enthusiasm he has for his research is, for me, contagious and motivational.

My sincere thanks also go to
Prof. Raimondo De Cristofaro (Hemostasis Research Centre, Catholic University, Rome),
Prof. Alessandro Negro (Department of Biomedical Sciences, University of Padova),
Prof. Vadim Vasilyev (Institute of Experimental Medicine, Saint Petersburg, Russia),
Prof. Vittorio Pengo and Dr. Alessandra Banzato (Department of Cardiac, Thoracic, and Vascular Sciences, University of Padova),
for offer me internship opportunities in their groups and lading me working on diverse exciting projects.

and prof. James Huntington (University of Cambridge, UK) for give us the plasmid vector for wild-type human prethrombin-2.

Last but not the least, I would like to thank my family and all my friends.

Laura
January 2014